Studies on gut bacterial metabolisms of food-derived bioactive phytochemicals

Hiroko Watanabe

2020

CONTENTS

ABBREVIATIONS

ITC	isothiocyanate
GSL	glucosinolate
LAB	lactic acid bacteria
mGAM broth	modified Gifu anaerobic medium broth
HPLC	high performance liquid chromatography
LB medium	Luria-Bertani medium
OD_{600}	Optical densities at 600 nm
KPB	potassium phosphate buffer
DMA	*N*,*N*-dimethylacetamide
Tris	tris(hydroxymethyl)aminomethane
TEAB	tetraethyl ammonium bicarbonate
BCA	Bicinchoninic acid
LC-MS/MS	liquidchromatography-tandem mass spectrometry
ESI	electrospray ionization
NCBI	National Center for Biotechnology Information
PCR	polymerase chain reaction
ORFs	open reading frames
UroH-Histag	UroH tagged with six successive histidines
IPTG	isopropyl *β*-D-thiogalactopyranoside
FPLC	fast protein chromatography
SDS-PAGE	sodium dodecyl sulfate-polyacrylamide gel electrophoresis
ACMSD family	2-amino-3-carboxymuconate-6-semialdehyde decarboxylase family
CIs	confidence intervals
EDTA · 2Na	Ethylenediaminetetraacetic acid · 2Na
GEDTA	Glycoletherdiaminetetraacetic Acid
PMSs	peptide matches spectrum
Amp^R	ampicillin-resistant
Kan^R	kanamycin-resistant
US fraction	soluble enzyme fraction
UP fraction	membrane fraction
NADH	nicotinamide adenine dinucleotide

NADPH	nicotinamide adenine dinucleotide phosphate
FAD	flavin adenine dinucleotide
FMN	flavin mononucleotide
CV	column volumes
PVDF membrane	Polyvinylidene difluoride membrane
methylviologen	1,1'-dimethyl-4,4'-bipyridinium
MV^{2+}	methylviologen dication
$MV^{+\cdot}$	methylviologen cation radical
CoQ_0,	coenzyme Q_0
DCPIP	dichloroindophenol
PMS	phenazine methosulfate
DHNA	dihydroxynaphthoate
sinigrin	allylglucosidase
AITC	allylisothiocyanate
PTS	phosphotransferase system
MRS	De Man, Rogosa, Sharpe
mMRS	modified MRS
mM17	modified M17
TCA	trichloroacetic acid
TFA	trifluoroacetic acid
PCR	polymerase chain reaction
BLAST	Basic Local Alignment Search Tool
DDBJ	DNA Data Bank of Japan
GC- MS	gas chromatography- mass spectrometry
HEPES	4-(2-hydroxyethyl)-1-piperazineethanesulfonic acid
ATP	adenosine triphosphate
HPIC-HRMS/MS	high performance ion chromatography high resolution tandem mass spectrometry
AGC	automatic gain control
IT	injection time
PRM	parallel reaction monitoring
NCE	normalized collision energy
MES	2-(*N*-morpholino)ethanesulfonic acid
DDBJ	DNA Data Bank of Japan

OD_{550}	optical density at 550 nm
jPOST	Japan ProteOme Standard Repository/Database
GH	glucoside hydrolase
PEP	phosphoenolpyruvate
P-loop	phosphate-binding loop
NEM	*N*-Ethylmaleimide
PCMB	*p*-Choloromercuribenzoate
PMSF	Phenylmethylsulfonyl fluoride
INSDC	International Nucleotide Sequences Database Collaborators

INTRODUCTION

Phytochemicals are non-nutritive components derived from a plant-based diet such as vegetable, fruits, and nuts. Food-derived phytochemicals are precious for maintaining and improving human health due to the potential protective or disease-preventing effects (1,2). Actually in foods, many phytochemicals are accumulated as non-bioactive precursors. The precursors undergo conversion into the bioactive phytochemicals by gut microbiota (3,4). Thus, understanding physiology and enzymatic mechanism of phytochemical conversion by gut bacteria will be useful for further investigation for therapeutic application and proposing health-improving diet. However, detailed mechanisms of gut bacterial conversion of food-derived compounds into functional phytochemicals remain largely unknown. Here, the author aimed to accumulate knowledge on gut bacterial enzymes involved in generation of bioactive phytochemicals.

Urolithin is a collective term for multi-hydroxy benzo[c]chromen-6-one. Urolithins are derived from ellagitannins which are found in some dietary fruits and nuts such as pomegranate, although urolithins are not contained in them. Urolithins are formed through gut microbial metabolism of ellagic acid. Nine urolithins, namely, urolithin M5 (a pentahydroxy urolithin); urolithin M6, urolithin D and urolithin E (tetrahydroxy urolithins); urolithin C and urolithin M7 (trihydroxy urolithins); urolithin A and isourolithin A (dihydroxy urolithins); urolithin B (a monohydroxy urolithin) were found to be produced by human gut bacteria (9,10). Individual urolithins, such as urolithin A (3,8-dihydroxy-urolithin) and urolithin B (3-hydroxy-urolithin), have been found to have potentially beneficial effects. For example, urolithin A might exert a protective effect against colon cancer development through inhibition of cancer cell proliferation (5), inhibition of the Wnt signaling pathway (6), and inducing apoptosis in cancer cells and inhibition of CYP1 activity (7). Recently, urolithin A was reported to induce mitophagy, thereby preventing the accumulation of dysfunctional mitochondria with age and extending the lifespan of *Caenorhabditis elegans* (8).

Generation of urolithin M5 from ellagic acid leads to the production various

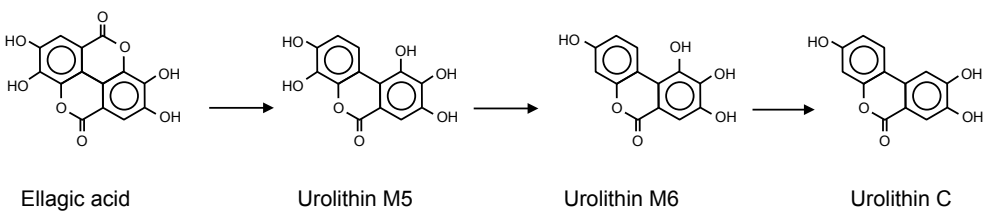

Fig. 1 Proposed pathway of ellagic acid metabolism in *G. urolithinfaciens* DSM 27213

urolithins via multiple dehydroxylation steps. Selma et al. were the first to describe ellagic acid transforming activity to produce urolithin C from ellagic acid, and urolithin M5 and urolithin M6 were assumed to be produced as intermediates in *Gordonibacter pamelaeae* and *G. urolithinfaciens* (11) (Fig. 1). Urolithin M5 production from ellagic acid is the fate-determining step of related compounds, because it is the initial step of whole pathway of the ellagic acid metabolism by gut microbiota.

Furthermore, the key reaction of ellagic acid metabolism involving the production of urolithins is the dehydroxylation of phenolic hydroxy groups. Although there are several reports on the dehydroxylation of phenolic compounds by gut bacteria and anaerobic bacteria, only a few investigations describing the enzymatic mechanism have been reported. To date, only two enzymes, 4-hydroxybenzoyl-CoA reductase (12−14) and dopamine dehydroxylase (Dadh) (15,16), have been described as phenolic dehydroxylation enzymes isolated from anaerobic bacteria.

To the best of the author's knowledge, there are no reports of an enzymatic system involved in urolithin production through ellagic acid metabolism in any bacteria.

Cruciferous vegetables such as broccoli are known to be providers of isothiocyanates (ITCs). ITCs are bioactive phytochemicals which exert anti-carcinogenic effects as well as induce host detoxifying defense system (17,18). ITCs are raised from

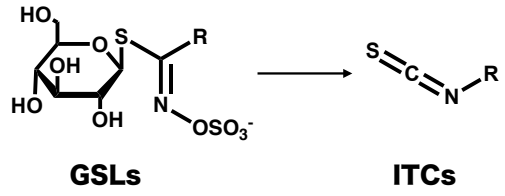

Fig. 2 Glucosinolates (GSLs) metabolism into isothiocyanate (ITCs) by gut bacteria

non-bioactive thioglucosides, glucosinolate (GSLs) contained in these cruciferous vegetables via hydrolysis of the *S*-glycosidic linkage by bacteria present in human gut (19) (Fig. 2) as found in other glycoside metabolism (20). Thus, gut bacteria mainly responsible for the exertion of beneficial physiological effects of ITCs upon intake of GSLs, there is a great interest in determining how human gut bacteria can degrade GSLs. Previously, some GSLs-degrading enzymes called myrosinases derived from plants (21), aphid (22), and a soil bacterium (23) were isolated and characterized. In contrast, although several gut bacteria are known to metabolize GSLs (24−28), the purification of active GSL-degrading enzymes has not been accomplished since no enzyme activity was reported in cell-free extracts of GSLs-metabolizing gut bacteria including lactic acid bacteria (LAB) to date.

In this study, the author analyzed the bacterial metabolisms of food-derived compounds generating phytochemicals, urolithins and ITCs, in *Gordonibacter urolithinfaciens* DSM 27213 and *Lactobacillus farciminis* KB1089, respectively, and identified novel enzyme systems involved in the metabolisms.

REFENRENCES

1. **Liu, R. H.:** Potential synergy of phytochemicals in cancer prevention: mechanism of action, J. Nutr.,**134**(12 Suppl), 3479S−3485S (2004).
2. **Liu, R. H.:** Health benefits of fruit and vegetables are from additive and synergistic combinations of phytochemicals, Am. J. Clin. Nutr., **78**(3 Suppl), 517S−520S (2003).
3. **Rowland, I., Gibson, G., Heinken, A., Scott, K., Swann, J., Thiele, I., Tuohy, K.:** Gut microbiota functions: metabolism of nutrients and other food components, Eur. J. Nutr., **57**, 1–24 (2018).
4. **Gerhauser, C.:** Impact of dietary gut microbial metabolites on the epigenome, Phil. Trans. R. Soc., **B373**, 20170359 (2018).
5. **Espín, J. C., Larrosa, M., García-Conesa, M. T., and Tomás-Baeberán, F.:** Biological significance of urolithins, the gut microbial ellagic Acid-derived metabolites: the evidence so far, Evid. Based Complement, Alternat. Med., **2013**, 270418 (2013).
6. **García-Villalba, R., Beltrán, D., Espín, J. C., Selma, M. V., and Tomás-Barberán, F. A.:** Time course production of urolithins from ellagic acid by human gut microbiota, J. Agric. Food Chem., **61**, 8797–8806 (2013).
7. **Gonzáles-Sarrías, A., Espín, J. C., Tomás-Barberán, F. A., and García-Conesa, M. T.:** Gene expression, cell cycle arrest and MAPK signalling regulation in Caco-2 cells exposed to ellagic acid and its metabolites, urolithins, Mol. Nutr. Food Res., **53**, 686–698 (2009).
8. **Sharma, M., Li, L., Celver, J., Killian, C., Kovoor, A., and Seeram, N. P.:** Effects of fruit ellagitannin extracts, ellagic acid, and their colonic metabolite, urolithin A, on Wnt signaling, J. Agric. Food Chem., **58**, 3965–3969 (2010).
9. **Kasimsetty, S. G., Bialonska, D., Reddy, M. K., Ma, G., Khan, S. I., and Ferreira, D.:** Colon cancer chemopreventive activities of pomegranate ellagitannins and urolithins, J. Agric. Food Chem., **58**, 2180–2187 (2010).
10. 4. **Ryu, D., Mouchiroud, L., Andreux, P. A., Katsyuba, E., Moullan, N., Nicolet-dit-Felix, A. A., Williams, E. G., Jha, P., Sasso, G. L., Huzard, D., and other 4 authors:** Urolithin A induces mitophagy and prolongs lifespan in *C. elegans* and increases muscle function in rodents, Nat. Med., **22**, 879–888 (2016).
11. **Selma, M. V., Beltrán, D., García-Villalba, R., Espín, J. C., Tomás-Barberán, F. A.:** Description of urolithin production capacity from ellagic acid of two human intestinal *Gordonibacter* species, Food Funct., **5**, 1779–1784 (2014).

12. **Brackmann, R. and Fuchs, G.:** Enzymes of anaerobic metabolism of phenolic compounds. 4-Hydroxybenzoyl-CoA reductase (dehydroxylating) from a denitrifying *Pseudomonas* species, Eur. J. Biochem., **213**, 563–571 (1993).
13. **Breese, K. and Fuchs, G.:** 4-Hydroxybenzoyl-CoA reductase (dehydroxylating) from the denitrifying bacterium *Thauera aromatica*. Prosthetic group, electron donor, and genes of a member of the molybdenum-flavin-iron-sulfur proteins, Eur. J. Biochem., **251**, 916–923 (1998).
14. **Unciuleac, M., Warkentin, E., Page, C. C., and Boll, M., and Ermler, U.:** Structure of a xanthine oxidase-related 4-hydroxybenzoyl-CoA reductase with an additional [4Fe-4S] cluster and an inverted electron flow, Structure, **12**, 2249–2256 (2004).
15. **Rekdal, V. M., Bess, E. N., Bisanz, J. E., Turnbaugh, P. J., and Balskus, E. P.:** Discovery and inhibition of an interspecies gut bacterial pathway for Levodopa metabolism, Science, **364**, pii:eaau6323 (2019).
16. **Rekdal, V. M., Bernardino, P. N., Luescher, M. U., Kiamehr, S., Turnbaugh, P. J., Bess, E. N., and Balskus, E. P.:** A widely distributed metalloenzyme class enables gut microbial metabolism of host- and diet-derived catechols, E. bioRxiv. Preprint, https://doi.org/10.1101/725358 (available online 5 Aug 2019).
17. **Higdon, J. V., Delage, B., Williams, D. E., Dashwood, R. H.:** Cruciferous vegetables and human cancer risk: epidemiologic evidence and mechanistic basis, Pharmacol. Res., **55**(3), 224−236 (2007).
18. **Elbarbry, F., Elrody, N.:** Potential health benefits of sulforaphane: a review of the experimental, clinical and epidemiological evidences and underlying mechanisms, J. Med. Plants Res., **5**(4), 473−484 (2011)
19. **Elfoul, L., Rabot, S., Khelifa, N., Quinsac, A., Duguay, A., Rimbault, A.:** Formation of allyl isothiocyanate from sinigrin in the digestive tract of rats monoassociated with a human colonic strain of *Bacteroides thetaiotaomicron*, FEMS Microbiol. Lett., **197**(1), 99−103 (2001).
20. **Sakurama, H., Kishino, S., Uchibori, Y., Yonejima, Y., Ashida, H., Kita, K., Takahashi, S., Ogawa, J.:** *β*-Glucuronidase from *Lactobacillus brevis* useful for baicalin hydrolysis belongs to glycoside hydrolase family 30, Appl. Microbiol. Biotechnol., **98**(9), 4021−4032 (2014).
21. **Bones, A. M., Rossiter, J. T.:** The enzymic and chemically induced decomposition of glucosinolates, Phytochemistry, **67**(11), 1053−1067 (2006).
22. **Pontoppidan, B., Ekbom, B., Eriksson, S., Meijer, J.:** Purification and characterization of myrosinase from the cabbage aphid (Brevicoryne brassicae), a brassica herbivore, Eur. J. Biochem., **268**(4), 1041−1048 (2001).

23. **Albaser, A., Kazana, E., Bennett, M., Cebeci, F., Luang-In, V., Spanu, P., Rossiter, J.:** Discovery of a bacterial glycoside hydrolase family 3 (GH3) β-glucosidase with myrosinase activity from a *Citrobacter* strain isolated from soil, J. Agric. Food Chem., **64**(7), 1520−1527 (2016).
24. **Cheng, D., Hashimoto, K., Uda, Y.:** In vitro digestion of sinigrin and glucotropaeolin by single strains of *Bifidobacterium* and identification of the digestive products, Food. chem. Toxicol., **42**(3), 351−357 (2004).
25. **Luciano, F. B., Belland, J., Holley, R. A.:** Microbial and chemical origins of the bactericidal activity of thermally treated yellow mustard powder toward E*scherichia coli* O157:H7 during dry sausage ripening, Int. J. Food Microbiol*.,* **145**(1), 69−76 (2011).
26. **Mullaney, J. A., Kelly, W. J., McGhie, T. K., Ansell, J., Heyes, J. A.:** Lactic acid bacteria convert glucosinolates to nitriles efficiently yet differently from enterobacteriaceae, J. Agric. Food Chem., **61**(12), 3039−3046 (2013).
27. **Luang-In, V., Narbad, A., Nueno-Palop, C., Mithen, R., Bennett, M., Rossiter, J. T.:** The metabolism of methylsulfinylalkyl- and methylthioalkyl-glucosinolates by a selection of human gut bacteria, Mol. Nutr. Food Res,. **58**(4), 875−883 (2014).
28. **Narbad, A., Rossiter, T. J.:** Gut glucosinolate metabolism and isothiocyanate production, Mol. Nutr. Food Res., **62**(1700991), 1−10 (2018).

CHAPTER I

Analysis on ellagic acid metabolism and related proteins in *Gordonibacter urolithinfaciens* DSM 27213

SECTION 1
Identification and the functional analysis of the proteins involved in ellagic acid metabolisms in *Gordonibacter urolithinfaciens* DSM 27213

In the present study, the author evaluated three reactions, i.e., ellagic acid to urolithin M5, urolithin M5 to urolithin M6, and urolithin M6 to urolithin C, using growing cells and resting cells of *G. urolithinfaciens* DSM 27213. As a result, the author revealed that the activities catalyzing the three reactions were induced by ellagic acid or urolithin M5. And then, by comparison of expressed proteins between in induced cells and non-induced cells, the author selected seven proteins as putative components of enzymes involved in ellagic acid metabolism in *G. urolithinfaciens* DSM 27213.

MATERIALS AND METHODS

Chemicals and bacterial strains Ellagic acid, urolithin M5, urolithin M6 and urolithin C were obtained from Daicel Corp. (Tokyo, Japan). All other chemicals were of analytical grade and commercially available. *G. urolithinfaciens* DSM 27213 was purchased from Leibniz Institute DSMZ-German Collection of Microorganisms and Cell Cultures (Braunschweig, Germany). The other bacterial strains used in this study are shown in Table S1.

Anaerobic conditions Three different conditions were applied for the following experiments. Anaerobic condition (x): operated in an anaerobic chamber (Coy Laboratory products Inc., Michigan, USA) of which atmosphere was N_2 with 1−2 % H_2. Anaerobic condition (y): operated in a sealed container (1.8 L) with O_2 absorbers (Aneropack Kenki; Mitsubishi Gas Chemical Co. Inc., Tokyo, Japan). Anaerobic condition (z): operated in a sealed container (1.8 L) with O_2 absorbers (Aneropack Kenki; Mitsubishi Gas Chemical Co. Inc., Tokyo, Japan) of which atmosphere was added with an adequate amount of H_2 gas.

Microorganism cultivation and preparation of washed cells *G. urolithinfaciens* DSM 27213 was cultivated in 10 mL of modified Gifu

anaerobic medium broth (mGAM broth, Nissui Pharmaceutical Co., Ltd., Tokyo, Japan) to which added 0.01 % (0.33 mM) ellagic acid, 0.01 % (0.36 mM) urolithin M5, 0.01 % (0.38 mM) urolithin M6, 0.01 % (0.40 mM) urolithin C, or not added any rerated compounds in a 50-mL Erlenmeyer flask at 37 °C for 2 days under anaerobic condition (x) with shaking (120 strokes min^{-1}), which was used as seed culture in the following procedures.

For evaluation of related compound metabolisms during cultivation and using washed cells, 1 mL of the seed culture was transferred to 100 mL of fresh mGAM medium to which added 0.01 % (0.33 mM) ellagic acid, 0.01 % (0.36 mM) urolithin M5, 0.01 % (0.38 mM) urolithin M6, 0.01 % (0.40 mM) urolithin C, or not added any rerated compounds in a 200-mL Erlenmeyer flask and incubated at 37 °C for 7 days under anaerobic condition (x) with shaking (120 strokes min^{-1}). At various time points, 50 µL of the culture was sampled for high performance liquid chromatography (HPLC) analysis. And then, 10 mL of the culture was sampled and centrifuged at 8,000 rpm for 10 min to collect the cells. The pellets were washed three times with 50 mM Na_2CO_3-$NaHCO_3$ buffer (pH 9.5) and the obtained cells were used for reactions with the washed cells. The experiments were performed in triplicate.

Escherichia coli strains were cultivated using Luria-Bertani (LB) medium containing 1.0 % tryptone, 0.50 % yeast extracts, and 1.0 % NaCl under aerobic condition with shaking at 300 rpm at 37 °C.

Growth For checking growing status of *G. urolithinfaciens* DSM 27213 during cultivation in mGAM medium under anaerobic condition (x) at 37 °C, 150 µL of the culture was sampled at various time points and placed into a 200 µL-well of a 96-well microplate. Optical densities at 600 nm (OD_{600}) of the samples were analyzed with a microplate reader (Spectra Max Plus, Moleculardevices, San Jose, California, USA).

Reactions using washed cells The reaction mixtures were prepared in an aerobic atmosphere and the reactions were performed under anaerobic conditions described above.

A reaction mixture containing the washed cells-obtained from 10 mL of culture and 0.1 % (w/v) (3.3 mM) ellagic acid in 50 mM potassium phosphate buffer (KPB; pH 6.5) (50 µL) in a 200-µL plastic tube was used. The reactions were carried out under anaerobic condition (z) at 37 °C for 16 h. The experiments were performed in triplicate.

Ellagic acid and urolithin analyses Ellagic acid and urolithins in 100 µL or 50 µL of the reaction mixture were dissolved by adding 200 µL or 100 µL of *N*,*N*-dimethylacetamide (DMA) containing 1 % formic acid, respectively, vortexed, and centrifuged at 15,300 ×*g* for 3 min. Then, 10 µL of the obtained supernatant was analyzed by HPLC using a Shimadzu LC System

(Shimadzu Corp., Kyoto, Japan) equipped with a 4.6 ID × 150 mm Cosmosil 5C18-AR-II column (Nacalai Tesque Inc., Kyoto, Japan) at 40 °C. The mobile phase gradient elution was performed using Milli-Q water containing 1 % formic acid (Eluent A) and acetonitrile containing 1 % formic acid (Eluent B). The flow rate was 1.0 mL min^{-1}. The gradient scheme of the analysis was as follows: 0–6 min: 20 % of Eluent B; 6–9 min: linear gradient from 20–90 % of Eluent B; 9–12 min: 90 % of Eluent B; and 12–18 min: 20 % of Eluent B. The effluents were monitored with an SPD-M20A photodiode array detector (Shimadzu Corp., Kyoto, Japan).

For quantification of ellagic acid, urolithin M5, urolithin M6, and urolithin C in the prepared samples, we used calibration curves obtained from the relationships between standard samples and the peak area at each optimal wavelength of ultraviolet absorbance (ellagic acid, 367 nm; urolithin M5, 349 nm; urolithin M6, 348 nm; and urolithin C, 337 nm).

Sample preparation for quantitative proteomic analysis The washed cells of *G. urolithinfaciens* (0.5 g), cultivated in the mGAM medium with or without ellagic acid, were suspended in with 500 μL of lysis buffer [2 % (w/v) 3-(3-cholamidopropyl) dimethylammonio -1-propanesulfonate, 10 mM dithiothreitol, 1 % (*v*/*v*) protease inhibitor cocktail for bacterial cell lysis (Sigma Aldrich, St. Louis, Missouri, USA), 7 M urea, and 2 M thiourea in 50 mM tris(hydroxymethyl)amino -methane [Tris]-HCl (Wako Pure Chemical Industries, Ltd., Osaka, Japan)]. The cells were disrupted with a Power Sonic model 50 (Yamamoto Scientific Co. Ltd., Tokyo, Japan) at 100 V, 15 s on-and-off cycles for 10 min on ice. The resulting solution was centrifuged at 13,000 ×*g* for 20 min. The supernatants were used as protein solutions for following preparation. To exchange the buffer, the protein solutions were filtrated by Vivaspin Turbo 4 Ultrafiltration Units with molecular weight-3,000 cutoff membranes (Sartorius AG, Göttingen, Germany). Then, 50 μL of the resulting desalted solutions were diluted with 950 μL of 0.20 M tetraethyl ammonium bicarbonate (TEAB; Wako Pure Chemical Industries, Ltd., Osaka, Japan). These filtration and dilution were repeated further two times. The resulting protein solutions buffer-exchanged to 0.20 M TEAB to which added 0.2 mM tris(2-carboxyethyl)phosphine and incubated at room temperature for 3 h to reduce disulfide bonds of the peptides. Then, 5 μL of iodoacetamide (375 mM) was added and the reaction continued for 30 min at room temperature in the dark. Proteins were precipitated by adding 1 mL of ice-cold acetone and incubating the solution overnight at −20 °C. The precipitated proteins were suspended with 100 μL of 200 mM TEAB, 2 μg of trypsin from bovine panceas, suitable for protein sequencing (Sigma-Aldrich Co., St. Louis, Missouri, USA) was added and incubated overnight at 37 °C. The protein concentration was determined by Bicinchoninic acid (BCA) protein assay kit

(Takara Bio Inc., Shiga, Japan) with bovine serum albumin used as a standard.

Quantitative proteomic analysis (liquid -chromatography-tandem mass spectrometry [LC-MS/MS] and data analysis) LC-MS/MS analysis was performed using an LC (Ultimate 3000; Thermo Scientific, Inc., Massachusetts, USA)-MS/MS (LTQ Orbitrap Velos Mass Spectrometer, Thermo Scientific, Inc., Massachusetts, USA) system equipped with a long monolithic capillary column. Tryptic digests were separated by reverse-phase chromatography using a monolithic silica capillary column (500 cm long, 0.1 mm ID) (1), at a flow rate of the two eluents: eluent A, 0.1 % (*v*/*v*) formic acid; eluent B, 80 % acetonitrile containing 0.1 % (*v*/*v*) formic acid. The gradient started with 5 % eluent B, increased to 45 % eluent B for 600 min, further increased to 95 % eluent B to wash the column for 140 min, returned to the initial condition, and was held for re-equilibration of the column. The separated analytes were detected using a mass spectrometer with a full scan range of 350–1,500 *m*/*z*. For data-dependent acquisition, analysis program was set to automatically analyze the top 10 most intense ions observed in the MS scan. An electrospray ionization (ESI) voltage of 2.4 kV was applied directly to the LC buffer end of the chromatography column by using a MicroTee (Upchurch Scientific Inc.). The ion transfer tube temperature was set to 300 °C. Data analysis was performed using Proteome Discoverer 1.4 (Thermo Fisher Scientific, Inc., Massachusetts, USA). Protein identification was performed using Mascot algorithm against the protein database of *G. pamelaeae* 7-10-1-b (NC_021021.1) from NCBI (National Center for Biotechnology Information).

Preparation of genomic DNA, extraction of plasmid DNA, amplification of DNA fragments (polymerase chain reaction, PCR), and purification of the PCR products *G. urolithinfaciens* DSM 27213 genomic DNA was extracted using DNeasy Blood & Tissue kit (Qiagen Inc., Hilden, Germany), according to manufacturer's instructions. All plasmids constructed in this study were extracted using QIAprep Spin Miniprep Kit (Qiagen Inc., Hilden, Germany), and were confirmed by sequence analysis (Eurofins Scientific SE). PCR amplification for cloning purposes was performed with PrimeSTAR Max DNA polymerase (Takara Bio Inc., Shiga, Japan) and colony PCR was performed with TAKARA Ex Taq (Takara Bio Inc., Shiga, Japan). All primers for PCR (listed in Table S3) were purchased from Hokkaido System Science Co. Ltd. (Sapporo, Japan) All PCR products were gel-purified using QIAgen gel extraction kit (Qiagen Inc., Hilden, Germany).

Genome sequencing The genome of *G. urolithinfaciens* DSM 27213 sequencing analysis was performed with PacBio RS II (Pacific Biosciences, USA) and assembled using

CRITICA and Glimmer 2 with totals of 929,538,597 base pairs. The annotation was performed using NCBI BioNCIB non-redundant amino acid database (nr) or COG database. Analysis of its genome, consisting showed that the G+C content was 66.0 % and the sequence contains 2,439 open reading frames (ORFs).

Cloning of *uroA123H*, *uroB123*, and *uroH* in *E. coli* Plasmids and primers used in this study are shown in Table S2 and S1. To construct pET21-*uroA123H*, pET-21-*uroH*, and pCold-*uroB123* the *uroA123H* and *uroH*, and *uroB123* genes were amplified from the genomic DNA of *G. urolithinfaciens* DSM27213 by PCR using primers uroa1_f_BamHI/urot_r_EcoRI, uroh-f_BamHI/uroh_r_EcoRI, and urob1_f_SalI/urob3_r_PstI, respectively. The PCR products were gel-purified and digested with the restriction enzymes (for *uroA123H* and *uroH*, BamHI and EcoRI; for *uroB123*, SalI and PstI). The digested fragments were gel-purified, and were ligated into the similarly digested and purified pET21b(+) or pCold(I) vector. The products of ligation were transformed into competent *E. coli* DH5α cells using Inoue's method (2), and ampicillin-resistant transformants were selected. Plasmids were purified from the selected transformants.

To construct *E. coli* pET21-*uroA123H*, pET21-*uroH*, and *E. coli* pCold-*uroB123*, the constructed vectors pET21-*uroA123H, pET21-uroH,* and pCold-*uroB123* were, respectively, transformed into *E. coli* Rosetta 2(DE3) competent cells using Inoue's method as described above, and ampicillin- and chloramphenicol-resistant transformants were selected.

To construct pET28-*uroH*, the *uroH* gene was amplified from the genomic DNA of *G. urolithinfaciens* DSM27213 by PCR using primers uroh_f_BamHI/uroh_r_EcoRI. The PCR products were gel-purified and digested with the restriction enzymes (BamHI and EcoRI). The digested fragments were gel-purified, and were ligated into the similarly digested and purified pET28a(+) vector. The products of ligation were transformed into competent *E. coli* DH5α cells using Inoue's method as described above, and kanamycin-resistant transformants were selected. Plasmids were purified from the selected transformants.

To construct *E. coli* pET28-*uroH*, the constructed vectors, pET28-*uroH* was transformed in *E. coli* Rosetta 2(DE3), as described above, and kanamycin- and chloramphenicol-resistant transformants were selected.

Heterologous expression of the candidate genes and preparation of cell lysates To evaluate whether the *E. coli* transformants showed the ellagic acid transforming activity, the *E. coli* strains were inoculated in 5 mL LB medium containing suitable antibiotics (100 μg mL^{-1} ampicillin or 34 μg mL^{-1} chloramphenicol) and incubated at 37 °C for 2.5 h with shaking at 300 strokes min^{-1}. Then, for *E. coli*

pET21-*uroA123H* and pET21-*uroH*, 1.0 mM isopropyl *β*-D-thiogalactopyranoside (IPTG) was added to the culture and incubated at 37 °C, under aerobic condition or anaerobic condition (y), and with shaking at 120 rpm for 3 h. For *E. coli* pCold-*uroB123*, the culture was incubated at 15 °C for 30 min, added 0.1 mM IPTG, then incubated 15 °C for 24 h under anaerobic condition (y). The cells were harvested by centrifugation at 8,000 rpm and washed with 0.85 % NaCl twice. The washed cells obtained from 5 mL culture were suspended in 300 μL 100 mM KPB (pH 6.5). The suspension was treated with an ultrasonic cell-disrupter Power Sonic model 50 (Yamamoto Scientific Co. Ltd., Tokyo, Japan) at 100 V, 5 s on-and-off cycles for 10 min on ice. 100 μL of the resulting solution was used as catalysts. The lysates obtained from 1.3 mL culture were incubated with 0.1 % ellagic acid (3.3 mM), urolithin M5 (3.6 mM), or urolithin M6 (3.8 mM) in 50 mM KPB (pH 6.5) at 37°C for 12 h under anaerobic condition (z). And then, amounts of ellagic acid and urolithins were determined as described above.

To obtain purified UroH tagged with six successive histidines (UroH-Histag), *E. coli* pET28-*uroH* was cultivated in 400 mL LB medium containing 30 μg mL^{-1} kanamycin in 2-L Sakaguchi flask at 37 °C for 2.5 h with shaking at 100 strokes min^{-1}. IPTG was added at 0.1 mM (final concentration) to the culture and further incubated at 30 °C for 4 h with shaking at 100 strokes min^{-1}. The cells were collected by centrifugation at 8,000 rpm for 10 min and washed twice with 0.85 % NaCl.

Enzyme purification of UroH-Histag All operations were performed below 4 °C. The washed cells of *E. coli* pET28-*uroH* (10 g, wet weight) were added to 20 mL of 50 mM KPB (pH 6.5), suspended, and treated with an ultrasonic oscillator (5 min, four times). The cellular debris was removed by centrifugation at 10,000 ×g for 20 min, and the crude enzymes separated using fast protein liquid chromatography (FPLC) equipped with a Ni-Sepharase affinity column (HisTrap HP 5 mL, GE healthcare Biosciences UP, Ltd., Chicago, Illinois, USA). After equibiliration of the column with 20 mM KPB (pH 7.4) containing 0.5 M NaCl and 20 mM imidazole, the proteins in the cell-free extracts were eluted with a linear gradient of 0.02−0.5 M imidazole. The fractions containing purified UroH were combined and the buffer was exchanged to 20 mM KPB (pH 6.5) through ultra-filtration with molecular weight-10,000 cutoff membrane and used further evaluation. The enzyme fractions before purification (cell-free extracts) and after purification (purified fraction) were analyzed using 12.5 % (w/v) sodium dodecyl sulfate-polyacrylamide gel electrophoresis (SDS-PAGE) with Tris-glycine buffer system. Protein concentration was determined using Takara bradford protein assay kit (Takara Bio Inc., Shiga, Japan), and bovine serum albumin was used as the standard. The activity of enzyme fractions of ellagic acid conversion into urolithin

M5 was clarified through the reaction using 3.3 mM ellagic acid with the cell-free extracts (25.6 μg mL^{-1} as protein concentration) or the purified fraction (7.6 μg mL^{-1} as protein concentration) in 50 mM KPB (pH 6.5) at 37 °C under anaerobic condition (y) for 3 h.

Determination of native molecular weight of UroH To determine the native molecular weight of UroH-Histag, the purified enzyme solution was analyzed through size-exclusion chromatography using a FPLC system equipped with Superdex 200 Increase 10/300 GL column (GE Healthcare Bio-Sciences AB, Uppsala, Sweden). Elution buffer was 0.15 M NaCl in 50 mM KPB (pH 6.5). The native molecular weight was calculated using a calibration curve of a protein standard containing ferritin (440,000), aldolase (158,000), phophorylose b (97,000), albumin (66,000), ovalbumin (45,000), carbonic anhydrase (30,000), trypsine inhibitor (20,100), and α-lactalbmin (14,400).

Enzymatic characterization (pH, temperature, and effects of metal ions) Lactonase activity was determined by production of urolithin M5 from ellagic acid.

To evaluate effects of temperature, the substrate solution contained ellagic acid were pre-incubated at varied temperature (10−70 °C) for 5 min, the reaction was initiated by adding 12.5 μL of the enzyme solution to the 37.5 μL substrate solution, and the mixture (the final concentrations of ellagic acid and UroH were 0.33 mM and 0.18 μM, respectively) was then incubated under aerobic condition at the temperature for 5 min. The reactions were stopped by adding 100 μL 1 % formic acid containing DMA.

To evaluate effects of pH, the substrate solution contained ellagic acid in varied 50 mM buffer (citric acid-sodium citrate, pH 2.5−3.5; acetic acid-sodium acetate, pH 3.5−5.5; KPB, pH 6.0−8.0; Tris-HCl, pH 7.5−9.0; sodium carbonate-sodium bicarbonate, pH 9.5−11.0; sodium phosphate-sodium hydrogen phosphate, pH 11.5−12.0) were pre-incubated at 37 °C for 5 min, the reaction was initiated by adding 12.5 μL of the enzyme solution to the 37.5 μL substrate solution. The mixture (the final concentrations of ellagic acid and UroH were 0.33 mM and 0.18 μM, respectively) was then incubated under aerobic condition at 37 °C for 5 min. The reactions were stopped by adding 100 μL 1 % formic acid containing DMA.

To evaluate effects of addition of metal ions and chelating agents, the substrate solution contained ellagic acid with various metal ion solution (0.1 mM $FeCl_2$, $PbCl_2$, or 1 mM other metal ion solutions) or 1 mM chelating agent solutions were pre-incubated at 37 °C for 5 min, the reaction was initiated by adding the enzyme solution to the substrate solution of which total volume was 50 μL. The mixture (the final concentrations of ellagic acid and UroH were 0.33 mM and 0.18 μM, respectively) was then incubated under anaerobic condition (z) at 37 °C for 3 h. The reactions were

stopped by adding 100 μL 1 % formic acid containing DMA.

Kinetic parameters In order to determine the kinetic parameters of UroH, 0.38 μM UroH-Histag was incubated with 0.0025 % to 0.020 % ellagic acid in 50 mM Tris-HCl (pH 9.0) at 37 °C for 1, 3, 5, 10 min under aerobic condition. The enzyme reaction was stopped by mixing with 60 μL of 1 % formic acid-containing DMA. The hydrolysis activity was determined by analyzing produced urolithin M5 using HPLC. The kinetic parameters were calculated by curve fitting the experimental data to the Michaelis-Menten equation, using KaleidaGraph 4.0 (Synergy Software Inc., PA, USA).

RESULTS

Bacterial growth and ellagic acid metabolism of *G. urolithinfaciens* DSM 27213 It was difficult to monitor the cell growth in the medium containing ellagic acid metabolites because of their own turbidities (the structures of ellagic acid and the metabolites are shown in Fig. 2A). The author, however, evaluated the growth profile of *G. urolithinfaciens* DSM 27213 in mGAM broth (Fig. 1A) to obtain the basis for the analysis of ellagic acid and its metabolites transformation during cultivation. This strain did not show considerably high cell growth throughout cultivation. During early period of cultivation, cell density was not increased for 1.5 day. During1.5 day to 2 day, OD_{600} was immediately increased from 0.074 to 0.16, and then the OD_{600} had been kept at about 0.15 until

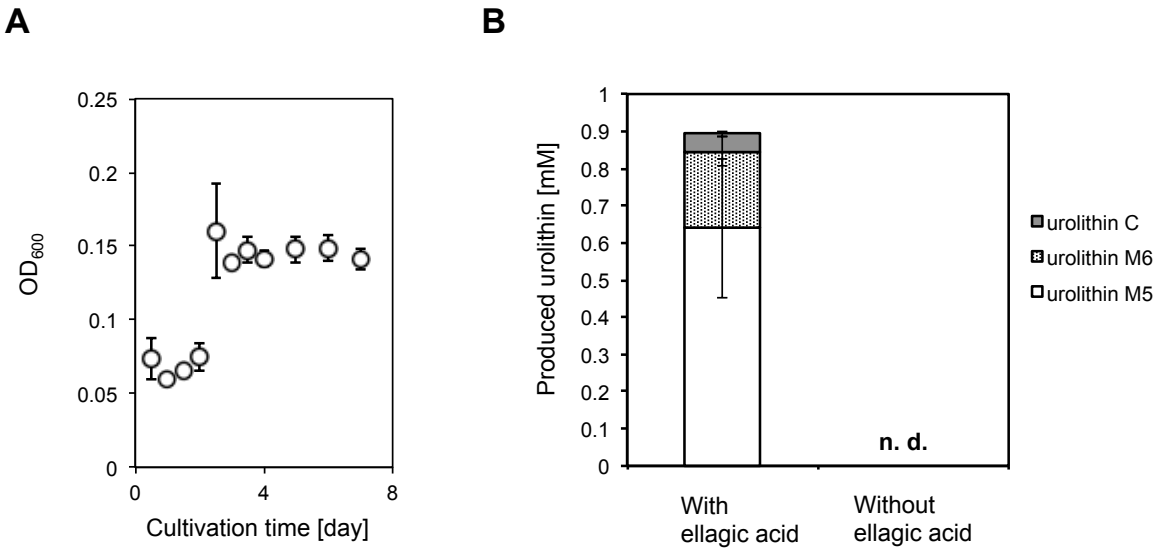

Fig. 1 Growth of *G. urolithinfaciens* DSM 27213 and ellagic acid conversion by washed cells
A, Growth curve of *G. urolithinfaciens* DSM 27213 in mGAM medium at 37 °C for 7 days under anaerobic condition (x). B, Washed cells grown in mGAM medium with or without ellagic acid were used as catalysts. 3.3 mM ellagic acid was added as a substrate in 0.1 M KPB (pH 6.5). Reactions were performed under anaerobic condition (z) at 37 °C for 16 h with shaking at 200 rpm. Error bars shows 95 % indicate CIs.

7day.

The author next evaluated the activity of washed cells obtained from the culture broth with or without ellagic acid. The cells cultivated in the medium containing ellagic acid were shown to degrade ellagic acid and produce urolithin M5, urolithin M6, and urolithin C (Fig. 1B). On the other hand, no ellagic acid conversion activity was observed in cells cultivated in the medium without ellagic acid (Fig. 1B). This indicated that the ellagic acid conversion activity of *G. urolithinfaciens* DSM 27213 was induced by ellagic acid. Furthermore, as described below, ellagic acid metabolites transforming activities were induced by ellagic acid and its metabolites.

G. urolithinfaciens DSM 27213 was grown in mGAM medium supplemented 0.01 % ellagic acid, 0.01 % urolithin M5, 0.01 % urolithin M6, or 0.01 % urolithin C, respectively. The ellagic acid and urolithin metabolizing profiles during 7 days cultivation were analyzed. When added ellagic acid to the culture, urolithin M5 was gradually increased until 24 h with decreasing ellagic acid (Fig. 2B[i]). After accumulation of urolithin M5 was reached maximum (0.10±0.01 mM) at 1 day, urolithin M5 was decreased until 2 day. Urolithin M6 and urolithin C were detected at 1.5 day at first and increased until 7 day (Fig. 2B[i]). Amounts of urolithin M6 and urolithin C at 7 day were 0.08±0.06 mM and 0.162±0.006 mM, respectively.

When added urolithin M5 to the

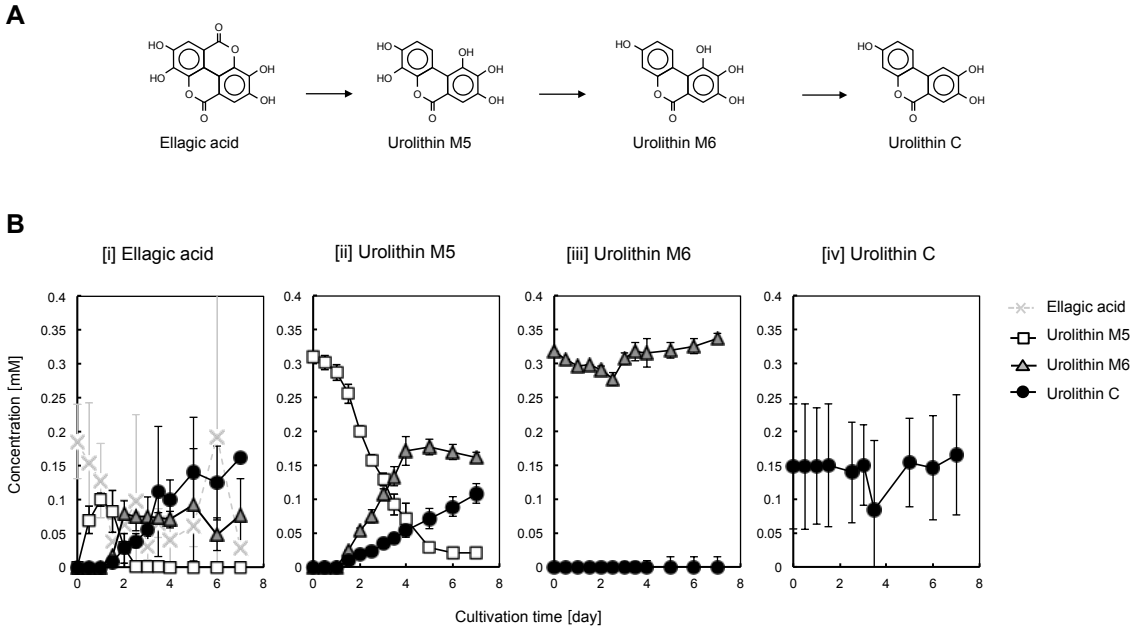

Fig. 2 Ellagic acid metabolism in *Gordonibacter urolithinfaciens* DSM 27213 with growing
A, Structures of ellagic acid and urolithins as the metabolic products and summary of the conversion pathway. B, Ellagic acid and urolithins transformation profiles during cultivation of *G. urolithinfaciens*. Initial concentration of each substrate was 0.01 % in mGAM medium: [i], 0.33 mM ellagic acid; [ii], 0.36 mM urolithin M5; [iii], 0.38 mM urolithin M6; and [iv], 0.40 mM urolithin C. Error bars shows 95 % indicate confidence intervals (CIs).

culture, urolithin M5 was decreased with production of urolithin M6 and urolithin C (Fig. 2B[ii]). Decrease of urolithin M5 was started in early phase of the cell growth (until 1 day). On the other hand, production of urolithin M6 and urolithin C was observed after 1.5-day incubation. After 1.5 day, urolithin M6 was linearly increased (5×10±6 μM day^{-1}) until 4 day then decreased gradually (7.9±0.3 μM day^{-1}) until 7 day. Urolithin C was increased linearly (18±2 μM day^{-1}) until 7 day. During 1.5 day to 4 day, urolithin M6-production rate was apparently about three times by urolithin C-production rate.

When added urolithin M6 to the culture, urolithin M6 was not converted to urolithin C throughout 7-day cultivation (Fig.

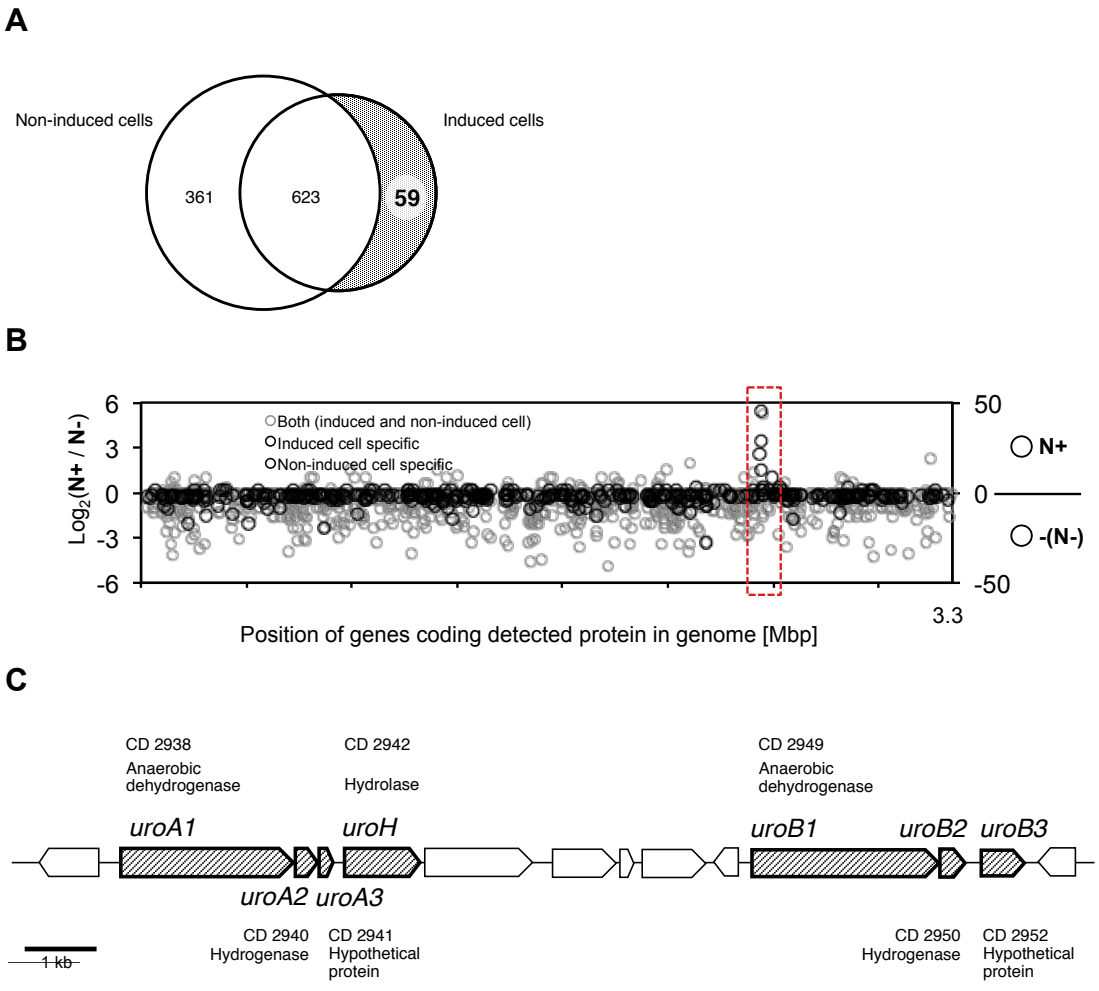

Fig. 3 Protein profiles identified in induced and non-induced cells
A, A Venn diagram describing number of proteins identified from the induced and non-induced cells through proteome analysis. B, Mapping the coding genes identified proteins through proteome analysis. One plot indicates one gene. N+, peptide matches spectrum (PMSs) value calculated according to the result of the induced cells. N-, PMSs value calculated according to the result of the non-induced cells. C, A gene map around the candidate genes in genome of *G. urolithinfaciens* DSM 27213, which indicated as a dashed square in C. The descriptions of the genes (*uroA1*, *uroA2*, *uroA3*, *uroH*, *uroB1*, *uroB2*, and *uroB3*) are shown in Table S4.

2B[iii]). Urolithin C was not further metabolized (Fig. B[i−iv]).

Comparative proteomic analysis We next compared the protein expression profiles of the ellagic acid-induced *G. urolithinfaciens* DSM 27213 (cultivated in 0.01 % ellagic acid containing mGAM medium) and the non-induced cells (cultivated in mGAM medium) by using proteomics technique. Among 682 proteins identified in the induced-cells, 59 proteins were specifically expressed in the induced cells (Fig. 3A, Table 1). Furthermore, among 623 proteins identified as commonly expressed in induced and non-induced cells, most proteins were less expressed in induced cells than in non-induced cells (Fig. 3B). On the other hand, as shown in Fig. 3B, a gene cluster notably expressed in induced cells was found. Among the 59 identified proteins in induced cells, seven proteins of which coding genes contained in a gene cluster in the genome of *G. urolithinfaciens* DSM 27213 were further chosen as the candidate proteins (Fig. 3B, C, Table 1). These proteins were assumed to compose three enzymes catalyzing three steps of ellagic acid metabolism. A hydrolase (CD 2942, namely UroH) was assumed to catalyze hydrolysis toward a lactone structure of ellagic acid, which is followed by spontaneous decarboxylation and results in generation of urolithin M5. Each one of two oxidoreductases (UroA and UroB) was assumed to consist of three subunits (Uro A1 [CD 2938], UroA2 [CD 2940], and UroA3 [CD 2941], and UroB1 [CD 2949], UroB2 [CD 2950], and UroB3 [CD 2952]). The author hypothesized that UroA or UroB was uroltihin M5 or urolithin M6 dehydroxylation enzyme.

Sequence analyses of candidate proteins By Interpro (https://www.ebi.ac.uk/interpro/) searching, domains contained in the selected proteins (UroA1, UroA2, UroA3, UroH, UroB1, UroB2, UroB3) were analyzed. As a result, both UroA1 and UroB1 were indicated to contain molybdopterin binding domain and a 4Fe-4S cluster-binding domain. UroA2 and UroB2 were indicated to contain two 4S-4Fe clusters. On the other hand, functions of neither UroA3 nor UroB3 were unknown. UroH was predicted as a metal-dependent hydrolase and probably belonged to 2-amino-3-carboxymuconate-6-semialdehyde

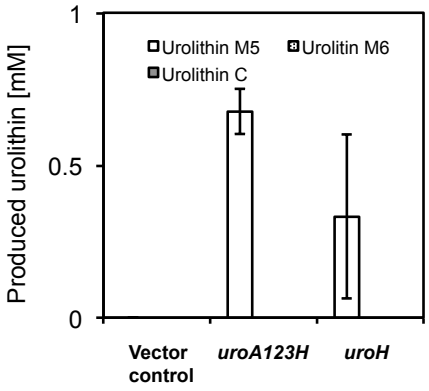

Fig. 4 Ellagic acid conversion using cell lysates of *E. coli* transformants
The reaction mixture contained 3.3 mM ellagic acid and the cell lysates of *E. coli* cells obtained from 1.3 mL culture, which were induced gene expression by adding IPTG under aerobic condition (y). Vector control, *E. coli*-pET21b. *uroA123H*, *E. coli* pET21 -*uroA123H*. *uroH*, *E. coli* pET21-*uroH*. Error bars shows 95 % indicate CIs.

decarboxylase (ACMSD) family.

Heterologously expression of UroA1, A2, A3, UroB1, B2, B3, and UroH in *E. coli* To evaluate whether the candidate proteins (UroH, UroA123, and UroB123) were involved in the transformation of ellagic acid, urolithin M5, and urolithin M6, the author constructed three expression vectors for *E. coli*: pET21-*uroA123H*, pCold-*uroB123*, and pET21-*uroH*. Then, each transformant harboring each vector was obtained. The cell lysates of the induced cells of *E. coli* pET21-*uroA123H* and *E. coli* pET21-*uroH* catalyzed ellagic acid conversion resulting in urolithin M5 production (Fig. 4). On the other hand, *E. coli* pET21-*uroA123H* nor *E. coli* pCold-*uroB123* did not show any urolithin dehydroxylation activity, namely, urolithin M5 conversion to urolithin M6 and urolithin M6 conversion to urolithin C (data not shown).

Purification of the ellagic acid lactonase (UroH-Histag) The recombinant UroH-Histag fused with 6 Histidine-tag at *N*-terminus was purified using FPLC equipped with Histrap HP 5 mL column. The purification of the enzyme was confirmed by SDS-PAGE analysis as a major band with a molecular weight of 44,700, which was in good agreement with the deduced molecular weight (43,400) of a putative UroH (Fig. 5A). The native molecular weight was calculated as 42,200. These results indicated that UroH was a monomer protein. The activities of enzyme solutions before and after the purification (cell-free extracts and purified UroH) were clarified as shown in Fig. 5B.

Effects of reaction conditions on the activity of UroH The purified UroH-Histag exhibited optimal activity at 50 °C (Fig. 6A). The purified UroH-Histag showed high urolithin M5 production from ellagic acid at pH 7.0 to 9.0 in KPB or Tris-HCl buffer (Fig. 6B).

To evaluate effects of metal ions and metal chelating agents on the lactonase activity of UroH-Histag, we added 0.1 mM $FeCl_2$ or $PbCl_2$, 1 mM other metal salts, or metal chelating agents to reaction using purified UroH

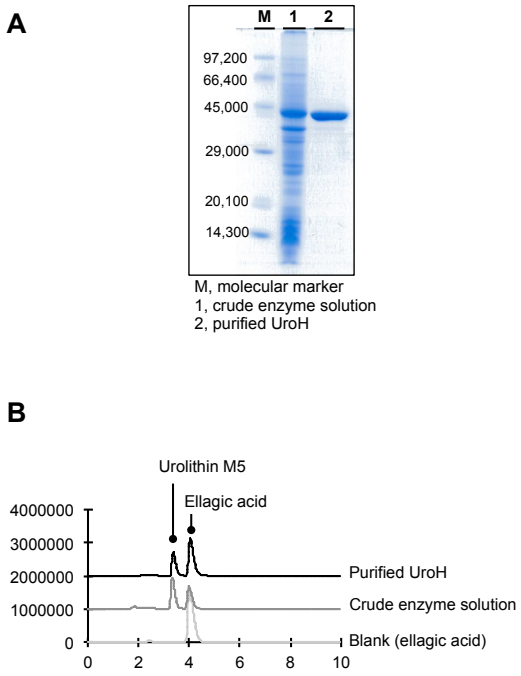

Fig. 5 Ellagic acid conversion into urolithin M5 using purified UroH A, SDS-PAGE analysis of UroH-Histag expressed in *E. coli*. M, Molecular marker; Lane 1, Crude enzyme solution which was cell-free extracts of *E. coli* pET28-*uroH* expressing UroH-Histag; Lane 2, Purified fraction of UroH-Histag. B, HPLC chromatograms indicating the results of ellagic acid conversion in reaction mixtures with 3.3 mM ellagic acid as a substrate and crude enzyme solution or purified UroH-Histag as a catalyst.

with 3.3 mM ellagic acid. As a result, addition of $MgSO_4$, $CaCl_2$, $MnCl_2$, $MnSO_4$, $CoCl_2$, and $NiCl_2$ significantly enhanced the activity and these relative activities were 153 %, 195 %, 151 %, 143 %, 165 %, and 195 %, respectively (Fig. 6C). $AgNO_3$, $FeSO_4$, $CuSO_4$, $HgSO_4$, $SnCl_2$, and $FeCl_2$ showed inhibitory effects on the activity of UroH (< 50 % relative activity) (Fig. 6C). There was no inhibitory agent for UroH activity among five chelating agents tested (α,α'-bioyridyl, 8-hydroxyquinoline, *o*-phenanthroline, ethylenediaminetetraacetic acid · 2Na (EDTA · 2Na) and glycoletherdiamin-etetraacetic acid (GEDTA), whereas addition of *o*-phenanthroline showed significantly enhancing effects and the relative activity was 221 % of the case of without any additives.

Kinetic analysis The k_{cat}, K_m, and k_{cat}/K_m values for ellagic acid hydrolysis of the recombinant UroH were as follows:, 1.0±0.1 sec^{-1}, 0.5±0.2 mM, 2±1 mM^{-1} sec^{-1}, respectively.

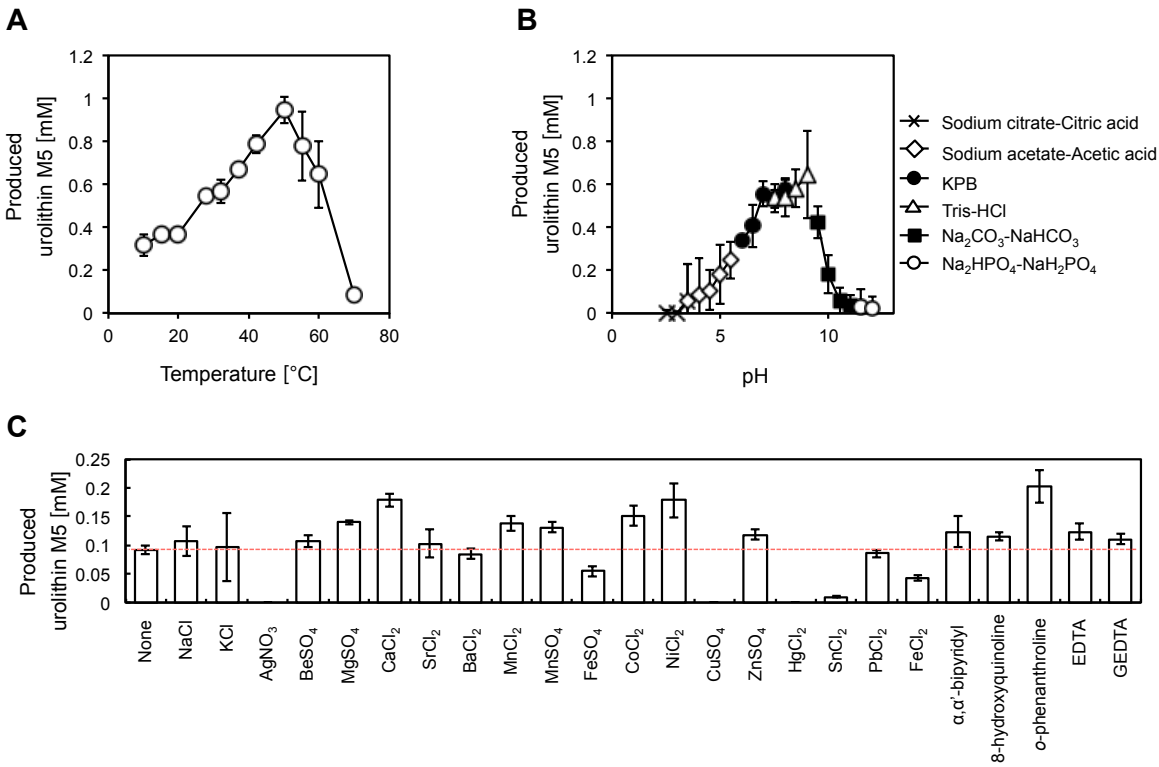

Fig. 6 Effects of reaction conditions on ellagic acid conversion by purified UroH A, Amounts of produced urolithin M5 using purified UroH-Histag at varied reaction temperature for 5 min. The reaction mixture contained 3.3 mM ellagic acid in 50 mM KPB (pH 6.5). B, Amounts of produced urolithin M5 using purified UroH-Histag at varied reaction temperature for 5 min. The reaction mixture contained 3.3 mM ellagic acid in 50 mM KPB (pH 6.5). C, Effects of addition of metals or chelating agents on ellagic acid converting activity of UroH-Histag. Activity was determined by amount of produced urolithin M5 after 180 min reaction in 50 mM KPB (pH 6.5) at 37 °C using 3.3 mM ellagic acid with 0.1 mM $FeCl_2$ or $PbCl_2$, 1 mM other metal solution, or 1 mM chelating agent except "None". Error bars shows 95 % indicate CIs.

DISCUSSION

G. urolithinfaciens DSM 27213 was reported to capable of growing in the presence of ellagic acid and its metabolites at the similar rate in the culture with or without these related polyphenols (3). As shown in Fig. 1A, when cultivated in mGAM broth, *G. urolithinfaciens* DSM 27213 showed 1−1.5 day lag phase, after that, less than a half day log phase, and then stationary phase of 2.5‑7 day. By checking these results with ellagic acid and urolithin M5 in the media, urolithin M5 production was occurred in the lag phase and urolithin M6 and urolithin C generation were started in the log phase, which continued in the stationary phase as well. It is suggested that ellagic acid converting reaction shows high efficiency. On the other hand, urolithin M5 and urolithin M6 dehydroxylation started in the log phase when amount of cells was increasing. In addition as shown in Fig. 2B [ii]), when added urolithin M5 to the culture medium, the production rate of urolithin M6 and urolithin C are apparently constant. These results indicate that the activities of the related enzymes are kept during stationary phase and the dehydroxylation of urolithin may be involved in energy generating or electron transferring metabolism of the bacterium.

The washed cells grown in the presence of ellagic acid converted ellagic acid to urolithin M5, urolithin M6, and urolithin C. The amount of urolithin M5 production was observed clearly. On the other hand, production of dehydroxylated urolithins (urolithin M6 and urolithin C) was not so high. Based on these results, it is suggested that electron donation to these dehydroxylation reaction may couple with other metabolic systems such as anaerobic respiration in living cells.

By comparison the number of detected proteins in induced cells and non-induced cells, much less variety of proteins expressed in induced cells than non-induced cells. There were 948 proteins were identified in the non-induced cells, whereas 682 proteins were identified in the induced cells (Fig. 3A). Furthermore, among 623 proteins detected in both induced and non-induced cells, there are many significantly less expressed proteins in induced cells than in non-induced cells (Fig. 3B). Many genes coding proteins involved in cell growth such as translation and cell division were apparently downregulated, which indicates that the cells are stressed in the presence of these polyphenols. Ellagic acid metabolism in *G. urolithinfaciens* DSM 27213 may function for cell protection against antibacterial compounds.

G. urolithinfaciens DSM 27213, three enzymes are assumed to catalyze the reactions of ellagic acid metabolism. From the results of proteomic analysis, the author hypothesizes a protein, namely UroH, may catalyze conversion of ellagic acid into urolithin M5. Two complex enzymes consisting of three subunits, namely UroA123 and UroB123, may catalyze conversion of urolithin M5 and urolithin

M6 into urolithin M6 and urolithin C. To evaluate the putative activities of the hypothesized enzymes, *E. coli* transformants harboring the genes coding candidate proteins were constructed. UroH was successfully expressed in *E. coli* Rosetta2(DE3) and the cell lysates showed ellagic acid conversion to urolithin M5 clearly. Therefore, the author identified an ellagic acid lactonase as a novel enzyme.

On the other hand, any transformants harboring *uroA* or *uroB* genes induced to express UroA or UroB showed no expected activity. The expected proteins were not successfully obtained in the soluble fraction as properly folded enzymes according to the results of SDS-PAGE analysis (data not shown). The urolithin M5 and urolithin M6 dehydroxylation enzymes assumed to be not suitable for heterologous expression in *E. coli*. Further investigations for evaluation of the enzymes (UroA and UroB) expressed in other bacterial hosts are on-going.

As predicted UoH as a metal-dependent hydrolase by sequence analysis, the author evaluated the effects of addition of metal ions and chelating agents on ellagic acid conversion activity of UroH. Any chelating agent tested did not inhibit the ellagic acid hydrolysis by UroH. On the other hand, by addition of *o*-phenanthroline, urolithin M5 production was highly enhanced, of which relative activity was 221 % of without any additives. *O*-phenanthroline is a chelating agent for Fe^{2+}, Cu^{2+}, Ni^{2+}, Co^{2+}, Cd^{2+}, and Zn^{2+}. These results suggest that Fe^{2+}, or Cu^{2+} have a negative effect on UroH enzymatic activity and *o*-phenanthroline remove inhibitor metals such as Fe^{2+}, Cu^{2+}, and Ag^{+} from the enzyme system, which is resulting in increasing urolithin M5 production. In addition, dicationic metal ions such as Ca^{2+}, Mg^{2+}, Mn^{2+}, and Ni^{2+} showed a significant activity enhancing effect. The property was similar to that of human1,4-lactonase (EC.3.1.1.25), which is Ca^{2+} dependent and investigated as a serum paraoxonase (PON1) based on analysis of crystal structures (4).

UroH shared approximately 24 % sequence identity with 2-amino-3-carboxymuconate-6-semialdehyde decarboxylase (ACMSD) of Homo sapiens, which catalyzes decarboxylation rather than hydrolase (5). The human ACMSD was reported to be enhanced in the presence of Co^{2+} and Fe^{2+} whereas inhibited in the presence of Zn^{2+} (5). On the other hand, some esterases or lactonases such as tannase catalyzing hydrolysis of ester in digallate (6) and dihydrocoumarin hydrolase (7) showed low homologies with UroH. Therefore, to the best of the author's knowledge, UroH is a novel enzyme belonging to ACMSD family with unique enzymatic properties toward metal ions compared with known ACMSD family enzymes.

Table 1 Proteins identified specifically in induced cells.

Accession No. ; CD	Description	Unique peptides	PSMs
64	chorismate synthase	1	1
258	hypothetical protein	1	1
298	MATE family efflux transporter	1	1
374	hypothetical protein	1	1
390	4Fe-4S ferredoxin	1	1
405	hypothetical protein	1	1
558	2-succynyl-5-enolpyruvyl-6-hydroxy-3-cyclohexene-1-carboxyate synthase	1	1
721	exonuclease DNA polymerase II ε-subunit family	1	1
789	pilus assembly protein	1	1
800	1-oxo acid:ferredoxin oxidereductase subunit γ	1	1
1086	molybdopterin dinucleotide binding protein	2	2
1102	PAS domain S-box /diguanylate cyclase (GGDEF) domain	1	1
1153	DNA binding response regulator	1	1
1266	radical SAM/SPAS domain containing protein	1	2
1269	formate dependent nitrite reductase	2	4
1289	recombination protein Rec	1	1
1440	5,10-methylene tetrahydrofolate reductase	1	1
1472	dihydroxyacetone kinase	1	1
1545	multidrug ABC transporter ATPase/permease	1	1

PSMs, Peptide spectrum matches. The PMSs value approximately reflected amount of detected protein.

Table 1 Proteins identified specifically in induced cells (continued).

Accession No. ; CD	Description	Unique peptides	PSMs
1566	hypothetical protein	1	1
1570	fructose-1,6-bisphosphatase	1	2
1661	DEAD/DEAH box helicase	1	1
1745	serine dehydtratase	1	1
1936	lipid II flippase	1	2
1995	MerR family transcription regulator	5	8
2017	amide hydrolase	1	1
2169	hypothetical protein	1	1
2214	HemK family methyltransferase	1	1
2259	MSF transporter	1	1
2454	carbamoyl phosphate synthase large subunit	1	1
1995	MerR family transcription regulator	5	8
2017	amide hydrolase	1	1
2169	hypothetical protein	1	1
2214	HemK family methyltransferase	1	1
2259	MSF transporter	1	1
2454	carbamoyl phosphate synthase large subunit	1	1
2492	RNA methyltransferase	1	1
2541	ATPase components of ABC transporters with duplicated ATPase domain	1	1
2636	hypothetical protein	1	3
2715	DNA binding protein	1	1

PSMs, Peptide spectrum matches. The PMSs value approximately reflected amount of detected protein.

Table 1 Proteins identified specifically in induced cells (continued).

Accession No. ; CD	Description	Unique peptides	PSMs
2745	permease of the drug/metabolite transporter (DMT) superfamily	1	1
2772	HTH type transcriptional repressor KstR	1	1
2938	Anaerobic dehydrogenases, typically selenocysteine-containing	6	22
2940	hypothetical protein	5	13
2941	hypothetical protein	5	29
2942	metal dependent hydrolase	10	45
2943	MFS transporter	1	1
2950	hypothetical protein	2	3
2952	hypothetical protein	1	1
2981	4Fe-4S ferredoxin	1	1
2996	transcription repair coupling factor	6	8
3018	GGDEF domain containing protein	1	1
3032	prephenate dehydratase	2	3
3040	multidrug ABC transporter ATPase/permease	1	1
3359	histidinol-phasphate transaminase	2	3
3423	DNA polymerase III subunit α	1	1
3464	ABC transporter	1	1
3471	metal binding protein	1	1

PSMs, Peptide spectrum matches. The PMSs value approximately reflected amount of detected protein.

Table S1 Bacterial strains used in this study

Strain	Description	Source or reference
Gordonibacter urolithinfaciens DSM 27213	Able to metabolize ellagic acid	DSM
Escherichia coli DH5α	Commercial transformation host for all plasmids	TOYOBO Co., Ltd.
E. coli Rosetta 2(DE3)	Commercial expression host	Novagen®
E. coli pET-21b	*E. coli* Rosetta 2(DE3) harboring pET-21b(+)	This study
E. coli pCold (I)	*E. coli* Rosetta 2(DE3) harboring pCold(I)	This study
E. coli pET21-*uroA123H*	*E. coli* Rosetta 2(DE3) harboring pET21-*uroH*	This study
E. coli pET21-*uroH*	*E. coli* Rosetta 2(DE3) harboring pET21-*uroH*	This study
E. coli pCold-*uroB123*	*E. coli* Rosetta 2(DE3) harboring pCold-*uroB123*	This study
E. coli pET-28a(+)	*E. coli* Rosetta 2(DE3) harboring pET-28a(+)	This study
E. coli pET28-*uroH*	*E. coli* Rosetta 2(DE3) harboring pET28-*uroH*	This study

Table S2 Plasmids used in this stud

Plasmid	Description	Source
pET-21b(+)	Amp^R, T7 promoter, pBR322ori, expression vector	Novagen
pCold (I)	Amp^R, *cspA* promoter, *lac* operator, ColE1 ori, expression vector	Takara Bio, Inc.
pET-28a(+)	Kan^R, T7 promoter, pBR322ori, expression vector	Novagen
pET21-*uroA123H*	Derivative of pET-21b(+) in which *uroA123H* gene region was cloned in BamHI and EcoRI sites	Novagen
pET21-*uroH*	Derivative of pET-21b(+) in which *uroH* gene region was cloned in BamHI and EcoRI sites	This study
pCold-*uroB123*	Derivative of pCold(I) in which *uroB123* gene region was cloned in SalI and PstI sites	This study
pET28-*uroH*	Derivative of pET-28a(+) in which *uroH* gene was cloned in BamHI and EcoRI sites	Novagen

Amp^R**,** ampicillin-resistant. Kan^R, kanamycin-resistant.

Table S3 Primers used in this study

Primer	Sequence
uroa1_f_BamHI	5'-CCTGGATCCATGAGAAGCAACGAGAAGGAGGAACGTATGGCC-3'
urot_r_EcoRI	5'-TCAGAATTCTTAGTGCTGTGCGGCTGCCTCGTCTGCGGGTTT-3'
uroh_f_BamHI	5'-GCCGGATCCATGGCAGACAACAAGGTCATCGACATCAACATG-3'
uroh_r_EcoRI	5'-TATGAATTCCTACAGGTTGAACAGCTTCGCCGCGTTGCCGCC-3'
urob1_f_SalI	5'-CGACATATGGTGATCGAAGTCATGGCCTGTCTCCTTACCTCG-3'
urob3_r_PstI	5'-AATCTGCAGCTAGCCCTTCTTCGCTGGCACGGGGTCCCGCTC-3'

Restriction site was underlined.

Table S4 Candidate genes probably involved in ellagic acid metabolism in *G. urolithinfaciens* DSM 27213

ID ; CD	Coding gene	Amino acids	Proposed function	Homology protein	Identity [%]
2938	*uroA1*	809	Anaerobic dehydrogenase	Anaerobic dehydrogenases, typically selenocysteine-containing | CBL04590.1 [*Gordonibacter pamelaeae* 7-10-1-b]	98
2940	*uroA2*	117	Hydrogenase	Hypothetical protein | WP_041239530.1 [*G. pamelaeae* 7-10-1-b]	92
2941	*uroA3*	65	Hypothetical protein	Hypothetical protein | WP_015539933.1 [*G. pamelaeae* 7-10-1-b]	100
2942	*uroH*	352	Hydrolase	Metal-dependent hydrolase | WP_015539932.1 [*G. pamelaeae* 7-10-1-b]	98
2949	*uroB1*	886	Anaerobic dehydrogenase	Anaerobic dehydrogenases, typically selenocysteine-containing | WP_015539923.1 [*G. pamelaeae* 7-10-1-b]	99
2950	*uroB2*	119	Hydrogenase	Hypothetical protein | WP_015539922.1 [*G. pamelaeae* 7-10-1-b]	97
2952	*uroB3*	186	Hypothetical protein	Hypothetical protein | WP_015539920.1 [*G. pamelaeae* 7-10-1-b]	90

SUMMARY

G. urolithinfaciens DSM 27213, a gut bacterium isolated from human feces, metabolizes ellagic acid into urolithin M5, urolithin M6 and urolithin C. Enzymes involved in the ellagic acid metabolisms in any gut bacteria have been remained unknown. In this study, the author evaluated effects of culture conditions on ellagic acid and related compounds metabolizing profiles in *G. urolithinfaciens* DSM 27213 and showed that the activities were induced by ellagic acid or urolithin M5. To identify the enzymes the author compared the proteins expressed in induced cells and non-induced cells. As a result, three enzymes (UroH, UroA1,A2,A3, and UroB1,B2,B3) specifically expressed in induced cells were focused on as putative enzymes involved in three reactions (ellagic acid to urolithin M5, urolithin M5 to urolithin M6, and urolithin M6 to urolithin C). The author successfully established a high-level expression system of recombinant UroH in *E. coli* and found the UroH as a novel enzyme catalyzing ellagic acid conversion into urolithin M5. Further analyses on enzymatic properties of UroH revealed that the optimal reaction condition was in pH 7.0−9.0 at 50 °C and some metal ions, such as Ca^{2+} enhanced the activity. On the other hand, the functions of UroA1,A2,A3 and UroB1,B2,B3 have been remained to be elucidated.

REFERENCES

1. **Morisaka, H., Matsui, K., Tatsukami, Y., Kuroda, K., Miyake, H., Tamaru, Y., Ueda, M.:** Profile of native cellulosomal proteins of *Clostridium cellulovorans* adapted to various carbon sources, AMB Express, **2**(1), 37 (2012).
2. **Inoue, H., Nojima, H., Okayama, H.:** High efficiency transformation of *Escherichia coli* with plasmids, Gene, **96**(1), 23-28 (1990).
3. **Selma, M. V., Beltrán, D., García-Villalba, R., Espín, J. C., Tomás-Barberán, F. A.:** Description of urolithin production capacity from ellagic acid of two human intestinal *Gordonibacter* species, Food Funct., **5**, 1779–1784 (2014).
4. **Khersonsky, O., Tawfik, D. S.:** Structure-reactivity studies of serum paraoxonase PON1 suggest that its native activity is lactonase, Biochemistry, **44**, 6371−6382 (2005).
5. **Li, T., Iwaki, H., Fu, R., Hasegawa, Y., Zhang, H., Liu, A.:** Alpha-amino-beta-carboxymuconic-epsilon-semialdehyde decarboxylase (ACMSD) is a new member of the amidohydrolase superfamily, Biochemistry, **45**, 6628−6634 (2006).
6. **Aharwar, A., Parihar, D. K.:** Tannases: Production, properties, applications, Biocatal. Agric. Biotechnol., **15**, 322−334 (2018).
7. **Kataoka, M., Honda, K., Shimizu S.:** 3,4-Dihydrocoumarin hydrolase with haloperoxidase activity from *Acinetobacter calcoaceticus* F46, Eur. J. Biochem. **267**, 3−10 (2000).

SECTION 2

Evaluation of electron-transferring cofactor mediating enzyme systems involved in urolithin dehydroxlation in *Gordonibacter urolithinfaciens* DSM 27213

This study describes the enzymatic conversion of urolithin M5 to urolithin C via urolithin M6 by cell-free extracts of *G. urolithinfaciens* DSM 27213 and explains the involvement of cofactors for electron transfer for the first time. Furthermore, the author shows that molybdopterin containing reductases are involved in the urolithin dehydroxylation through protein purification.

MATERIALS AND METHODS

Chemicals and bacterial strains Ellagic acid, urolithin M5, urolithin M6 and urolithin C were obtained from Daicel Corp. (Tokyo, Japan). All other chemicals were of analytical grade and commercially available. *G. urolithinfaciens* DSM 27213 was purchased from Leibniz Institute DSMZ-German Collection of Microorganisms and Cell Cultures (Braunschweig, Germany).

Anaerobic conditions Three different conditions were applied for the following experiments. Anaerobic condition (x): operated in an anaerobic chamber (Coy Laboratory products Inc., Michigan, USA) of which atmosphere was N_2 with 1−2 % H_2. Anaerobic condition (y): operated in a sealed container (1.8 L) with O_2 absorbers (Aneropack Kenki; Mitsubishi Gas Chemical Co. Inc., Tokyo, Japan). Anaerobic condition (z): operated in a sealed container (1.8 L) with O_2 absorbers (Aneropack Kenki; Mitsubishi Gas Chemical Co. Inc., Tokyo, Japan) of which atmosphere was added with an adequate amount of H_2 gas.

Microorganism cultivation and preparation of washed cells *G. urolithinfaciens* DSM 27213 was cultivated in 10 mL of mGAM broth (Nissui Pharmaceutical Co., Ltd., Tokyo, Japan) to which added 0.01 % (0.33 mM) ellagic acid in a 50-mL Erlenmeyer flask at 37 °C for 2 days under anaerobic condition (x) with shaking (120 strokes min^{-1}). Then, 10 mL of the seed culture was transferred to 800 mL of fresh same medium in a 2-L Erlenmeyer flask and incubated at 37 °C for 7 days under anaerobic condition (x) with shaking (120 strokes min^{-1}). The cultured cells were harvested by centrifugation (12,000 ×*g*, 10 min), washed twice with 0.85 % NaCl and stored at −80 °C until use.

Preparation of cell-free extracts and

fractionation All operations were performed below 4 °C. Frozen cells (10 g, wet weight) were added to 20 mL of 50 mM potassium phosphate buffer (KPB; pH 6.5), suspended, and treated with an ultrasonic oscillator (10 min, four times). The solution was centrifuged at 20,000 ×*g* for 20 min. The resulting supernatant solutions were used as cell-free extracts. The pellet was suspended in 30 mL of 50 mM KPB (pH 6.5) and used as cell debris suspension. The cell-free extracts (3 mL) were fractioned by ultracentrifugation at 100,000 ×*g* for 60 min, and the supernatant solutions and precipitates were obtained. The supernatants obtained after ultracentrifugation (the soluble fraction) were made up to 3 mL with 50 mM KPB (pH 6.5) and used as soluble enzyme fraction (US). The precipitates obtained after ultracentrifugation (the membrane fraction) were suspended in 3 mL of 50 mM KPB (pH 6.5), and the suspension was used as membrane fraction (UP). To remove the low molecular compounds, US fraction (3 mL) was filtrated by a Vivaspin Turbo 4 Ultrafiltration Unit with a molecular weight-10,000 cutoff membrane (Sartorius AG, Göttingen, Germany). Then, 60 µL of the resulting desalted solution was diluted with 2.94 ml of 50 mM KPB (pH 6.5). This operation (filtration and dilution) was repeated further two times to tightly remove the low molecular compounds. The resultant desalted solution (3 mL) was named as US/HM fraction.

Reaction conditions The reaction mixtures were prepared in an aerobic atmosphere and the reactions were performed under anaerobic conditions described above.

For reaction time-course analysis, a reaction mixture containing the washed cells or the cell-free extracts obtained from 10 mL of culture and 0.1 % (w/v) (3.3 mM) ellagic acid or 0.1 % (w/v) (3.6 mM) urolithin M5 as the substrate, in 50 mM KPB (pH 6.5) (2 mL) in a test tube (16.5 × 125 mm) was used. The reactions were carried out under anaerobic condition (z) at 37 °C for 72 h. At various time points, 100 µL of the reaction mixture was sampled. The experiments were performed in triplicate, and the averages of three separate experiments that were reproducible within 10 % are presented in the Fig. 2.

To evaluate the effects of cofactors, the reactions with cell-free extracts were performed under the anaerobic condition (z). The reaction mixture containing 0.1 % (w/v) (3.6 mM) urolithin M5 or 0.1 % (w/v) (3.8 mM) urolithin M6 as the substrate, 12.5 µL of cell-free extracts, and a cofactor, in 50 mM KPB (pH 6.5) (50 µL) in a 200-µL plastic tube was used. The cofactors used were; nicotinamide adenine dinucleotide (NADH) and nicotinamide adenine dinucleotide phosphate (NADPH), 10 mM; flavin adenine dinucleotide (FAD) and flavin mononucleotide (FMN), 0.2 mM; and other electron-transferring mediators, 0.1 % [w/v]. The reactions were carried out under anaerobic condition (z) and gently shaken (200 strokes min^{-1}) at 37 °C for 24 h. The

experiments were carried out in triplicate and the averages of three separate experiments that were reproducible within 10 % are presented in Tables 1 and 2.

To investigate the reaction using each fractionated enzyme solution with methylviologen and H_2 (Fig. 2B), a reaction mixture containing 10 mM methylviologen dichloride, 0.1 % (w/v) (3.6 mM) urolithin M5 or 0.1 % (w/v) (3.8 mM) urolithin M6 as the substrate, and 12.5 µL of enzyme solutions with varied fraction combinations, in 50 mM KPB (pH 6.5) (50 µL), in a 200-µL plastic tube was used. The reactions were performed under the anaerobic condition (z) and gently shaken (200 strokes min^{-1}) at 37 °C for 8 h.

To evaluate the effects of electron mediating compounds on the reaction with US/HM fraction (Fig. 3C), a reaction mixture containing electron meditating compounds in varied combinations, 0.1 % (w/v) (3.6 mM) urolithin M5 as the substrate, and 12.5 µL of the US/HM fraction, in 50 mM KPB (pH 6.5) (50 µL) in a 200-µL plastic tube was used. The electron mediating compounds used were 10 mM methylviologen dichloride, 0.2 mM FAD, and 10 mM NADPH. The reactions were performed under the anaerobic condition (y) or condition (z) and gently shaken (200 strokes min^{-1}) at 37 °C for 8 h.

Enzyme purification All enzyme purification procedures were carried out at 0–4 °C, and 50 mM KPB (pH 6.5) was used as a standard buffer. The US fraction was prepared as described above and filtered using a 0.45-µm pore size membrane filter (Merck Millipore, Burlington, Massachusetts, USA). Purification was performed as follows using a FPLC system (GE Healthcare Biosciences UK Ltd., Buckinghamshire, UK). The activity in each fraction obtained after each step of column chromatography was evaluated as amount of produced urolithin M6 from 0.1 % (3.6 mM) urolithin M5 reaction. The reaction mixture contained 10 mM methylvologen dichloride, 10 mM NADPH, 0.2 mM FAD, and 50 % (v/v) each fraction in 50 mM KPB (pH 6.5), of which total volume was 30 µL. The reaction was performed under anaerobic condition (z) at 37 °C with shaking at 200 rpm for 90 min.

Step 1: Mono Q 5/50 GL column chromatography

The US fraction were loaded onto an 1-mL column of Mono Q 5/50 GL column (GE Healthcare Biosciences UK Ltd., Buckinghamshire, UK) equilibrated with the standard buffer. Then, the enzyme was eluted with a following gradient program; 0 M NaCl, 0−10 column volumes (CV); 0−0.29 M NaCl, 10−12 CV; 0.29 M NaCl, 12−24 CV; 0.29−0.5 M NaCl, 24−44 CV; 0.5−1.0 M NaCl, 44−47 CV; 1 M NaCl, 47−52 CV. The active fractions were combined and concentrated through ultrafiltration using a Vivaspin Turbo 4 Ultrafiltration Units with molecular weight-10,000 cutoff membranes (Sartorius AG, Göttingen,

Germany).

Step 2: Superdex 200 Increase 10/300 GL column chromatography

The concentrated fraction was loaded onto an 24-mL column of Superdex 200 Increase 10/300 GL column (GE Healthcare Biosciences UK Ltd., Buckinghamshire, UK) equilibrated with 0.15 M NaCl in 50 mM KPB (pH 6.5).

Step 3: Mono Q 5/50 GL column chromatography

The concentrated fraction was loaded onto an 1-mL column of Mono Q 5/50 GL column (GE Healthcare Biosciences UK Ltd., Buckinghamshire, UK) equilibrated with the standard buffer. Then, the enzyme was eluted with a following gradient program; 0 M NaCl, 0−7 CV; 0−0.22 M NaCl, 7−8 CV; 0.22 −0.37 M NaCl, 8−28 CV; 0.37−1.0 M NaCl, 28−30 CV; 1.0 M NaCl, 30−35 CV. The active fractions were concentrated through ultrafiltration using a Vivaspin Turbo 4 Ultrafiltration Units with molecular weight-10,000 cutoff membranes (Sartorius AG, Göttingen, Germany) and exchanged the buffer to 50 mM KPB (pH 6.5).

PAGE analyses The enzyme solutions were analyzed by SDS-PAGE and Native-PAGE. SDS-PAGE was performed on a 5 − 20 % gradient polyacrylamide gel (e·Pagel, Atto Co., Tokyo, Japan) using Tris-glycine buffer system. To estimate molecular weight of proteins, Protein Molecular Marker (Broad) (Takara Bio Inc., Shiga, Japan) was used as the protein standard. Native-PAGE was performed on a 5−20 % gradient polyacrylamide gel (Pagel, Atto Co., Tokyo, Japan) using Tris-glycine buffer system. The gels were stained using EzStain Aqua (Atto Co., Tokyo, Japan).

N-terminal amino acid sequence analysis The proteins in the polyacrylamide gel were blotted to Polyvinylidene difluoride (PVDF) membrane (Merck Millipore, Burlington, Massachusetts, USA) through semidry blotting according to the procedures previously reported (1). The N-terminal amino acid sequence of the immobilized protein was analyzed by automated Edman degradation with a PPSQ-33A protein sequencer (Shimadzu Co., Ltd., Kyoto, Japan).

RESULTS

Profiles of ellagic acid or urolithin M5 conversion using resting cells and cell-free extracts Urolithin production using *G. urolithinfaciens* DSM 27213 resting cells or cell-free extracts was monitored under the anaerobic condition (z) for 72 h. With ellagic acid as the substrate and the washed cells as the catalyst, urolithin M5 increased to 0.73mM until 24 h and then gradually decreased with the production of dehydroxylated urolithin (urolithin M6 and urolithin C) productions (Fig. 1A). When urolithin M5 was used as the substrate

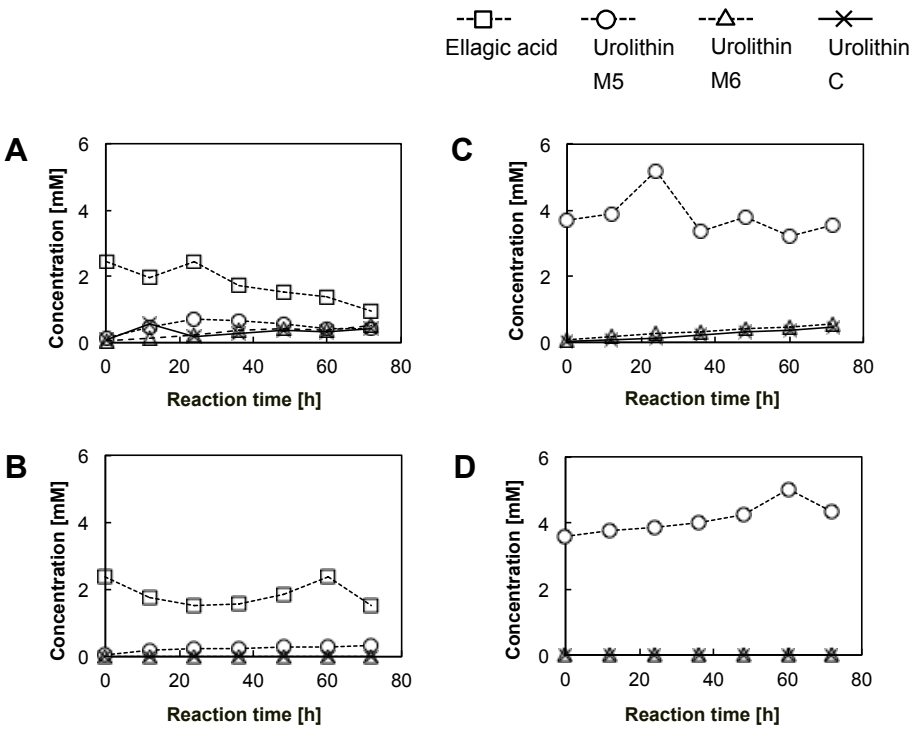

Fig. 1 Profiles of ellagic acid and urolithin M5 conversion by the resting cells and the cell-free extracts of *Gordonibacter urolithinfaciens* A, The reaction mixture contained 0.1 % (w/v) (3.3 mM) ellagic acid and the washed cells obtained from 10 mL of the cell culture. B, The reaction mixture contained 0.1 % (w/v) (3.3 mM) ellagic acid and the cell-free extracts obtained from 10 mL of the cell culture cells. C, The reaction mixture contained 0.1 % (w/v) (3.6 mM) urolithin M5 and the washed cells obtained from 10 mL of the cell culture. D, The reaction mixture contained 0.1 % (w/v) (3.6 mM) urolithin M5 and the cell-free extracts obtained from 10 mL of the cell culture cells. The detail conditions were described in the materials and methods section.

with washed cells, urolithin M6 and urolithin C gradually increased until 72 h. The production rate of urolithin M6 and urolithin C were almost equal (Fig. 1C). On the other hand, with ellagic acid as the substrate and cell-free extracts as the catalyst, urolithin M5 increased until 24 h without dehydroxylated urolithin production (Fig. 1B). In the reaction using urolithin M5 as the substrate and cell-free extracts as the catalysts, urolithin M5 conversion to urolithin M6 was not observed (Fig. 1D). The addition of the cell debris to the reaction mixture did not show significant effects (Table 1).

Effects of redox coenzymes and electron -transferring mediators on urolithins dehydroxylation Urolithin M5- and urolithin M6-converting reactions were carried out using the cell-free extracts with 10 mM of nicotinamide adenine dinucleotide coenzymes (NADH and NADPH) and 0.2 mM of flavins (FAD and FMN) under the anaerobic condition (z). When urolithin M5 was used as the substrate, dehydroxylated urolithin (urolithin M6 and urolithin C) production was not detected with any coenzymes (Table 1). Similarly, urolithin M6 was not converted to urolithin C by the cell-free extracts with any coenzymes (Table 1).

Next, the effects of other electron-transferring mediators (0.1 % [w/v]) on urolithin M5 and urolithin M6 dehydroxylation by the cell-free extracts under the anaerobic condition (z) were investigated. The tested mediators were coenzyme Q_0 (2,3-dimethoxy -5-methyl-1,4-benzoquinone), dichloro-indo -phenol, 1-methoxy-phenazine methosulfate, phenazine methosulfate, 3,7-diaminopheno -thiazin-5-ium chloride (thionine), 1,4-naphtho -quinone, dihydroxynaphthoate, menadione (vitamin K_3), anthraquinone-β-sulfate, anthraquinone, 6-methyl-1,3,8-trihydroxy -anthraquinone (emodine), 3-amino-7-dimethyl -amino-2-methylphenazine hydro -chloride (neutral red), riboflavin (vitamin B_2), and 1,1'-dimethyl-4,4'-bipyridinium (methyl -viologen) dichloride. Two mediators (anthraquinone and methylviologen) were found to be effective on expression of activity of the cell-free extracts to dehydroxylate urolithin M5. When 0.1 % (w/v) anthraquinone was added to the urolithin M5-containing reaction mixture, urolithin M6 was produced by the cell-free extracts, and the conversion yield was 4.42 % of the total urolithins observed after the 12 h reaction (Table 2). On the other hand, urolithin C was not detected when urolithin M5 and urolithin M6 were used as the substrates (Table 2). When 0.1 % (w/v) methylviologen was added

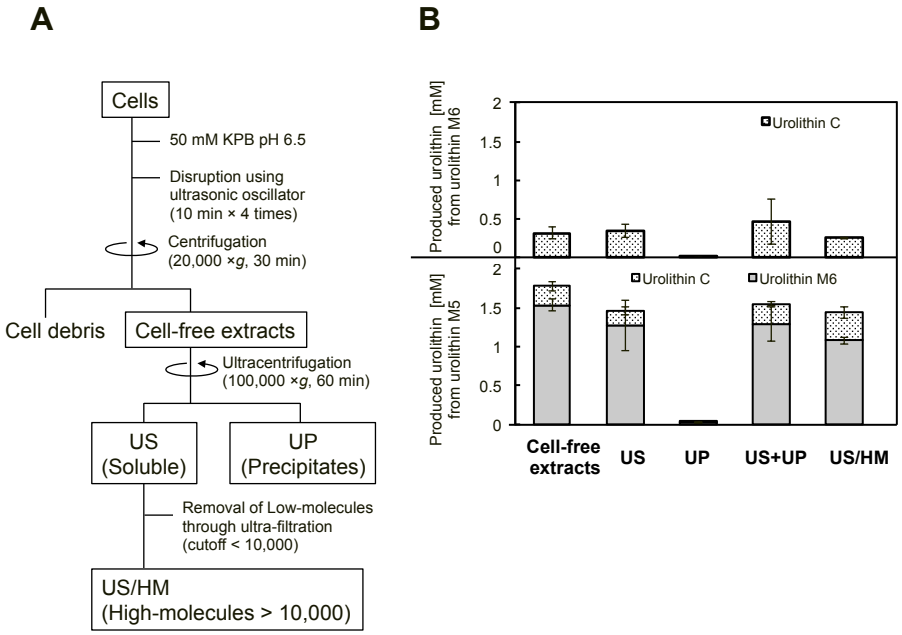

Fig. 2. Profiles of urolithin M5 and urolithin M6 conversion by the enzyme fractions. A, Preparation scheme of enzyme fractions from cell-free extracts of *Gordonibacter urolithinfaciens* DSM 27213. B, Amount of produced urolithins. The lower graph shows the reaction results of using urolithin M5 as substrate. The upper graph shows the reaction results using urolithin M6 as the substrate. The reaction mixture contained 0.1 % (w/v) substrate (3.6 mM urolithin M5 or 3.8 mM urolithin M6) and 25 % (v/v) of enzyme solutions in various combinations of fractions with 10 mM methylviologen dichloride, which was incubated for 8 h with shaking at 200 strokes min^{-1} under H_2-added anaerobic conditions. The detail conditions were described in the Materials and Methods. Error bars shows 95 % indicate CIs.

to the urolithin M5-containing reaction mixture, dehydroxylated urolithins (urolithin M6 and urolithin C) were produced by the cell-free extracts after 12 h. The molar conversion yields reached 58.3 % (urolithin M6, 34.0 % and urolithin C, 24.3 %). Urolithin C was also detected when methylviologen was added to the reaction mixture with urolithin M6 as the substrate, and the produced urolithin C comprised 5.78 % of the total urolithins observed after the reaction (Table 2). Although the cell-free extracts did not demonstrate any significant catalytic activity by themselves, the addition of methylviologen in the presence H_2 resulted in expression of the activation of urolithin M6 and urolithin C production from urolithin M5 as well as urolithin C production from urolithin M6. Based on these results, the author concluded that the enzyme system was effectively supported by methylviologen to dehydroxylate urolithin M5 and urolithin M6, and slightly by anthraquinone.

Urolithin M5 and urolithin M6 dehydroxylation activity of enzyme fractions Enzyme fractions were prepared by the procedures summarized in Fig. 2A. The cell-free extracts produced 1.78 mM of dehydroxylated urolithin mixture (1.54 mM urolithin M6 and 0.24 mM of urolithin C) from 3.6 mM urolithin M5 in the presence of methylviologen dication (MV^{2+}) under the anaerobic condition (z) (Fig. 2B). Fraction US only and UP only produced 1.46 mM dehydroxylated urolithin mixture (1.27 mM urolithin M6 and 0.19 mM urolithin C) and 0.02 mM dehydroxylated urolithin mixture (0.02 mM urolithin M6 and 0.003 mM urolithin C), respectively (Fig. 2B). Urolithin M5 was transformed to 1.55 mM dehydroxylated urolithin mixture (1.29 mM urolithin M6 and 0.26 mM urolithin C) by a combination of US and UP fractions to a similar extent as that of the cell-free extracts and as that of US fraction only in the presence of MV^{2+} (Fig. 2B). When urolithin M6 was used as the substrate, the cell-free extracts and the US faction only produced 0.32 mM or 0.35 mM urolithin C respectively, in the presence of MV^{2+}. On the other hand, the UP fraction only produced a trace amount of urolithin C (Fig. 2B). A combination of the US and the UP fractions produced 0.46 mM urolithin C to a similar extent as that of the cell-free extracts and as that of the US fraction (Fig. 2B). Based on these results, the enzymes involved in the production of two urolithins (urolithin M6 and urolithin C) from urolithin M5 in *G. urolithinfaciens* DSM 27213 were found to exist in the US fraction.

Factors affecting dehydroxylated urolithin production The US fraction was desalted with the same fresh buffer (50 mM KPB, pH 6.5) by ultrafiltration. The resultant solution, of which high molecular (>10,000) components were remained while small molecules were removed, was named as the US/HM fraction. The US/HM fraction produced 1.44 mM dehydroxylated urolithin mixture (1.08 mM urolithin M6 and

0.36 mM urolithin C) from urolithin M5 and 0.25 mM urolithin C from urolithin M6 in the presence of MV^{2+} to a similar extent as that of the US fraction (Fig. 2B).

With the US/HM fraction, the effects of native electron-donors and -mediators (H_2, NAD[P]H, and FAD) on urolithin M5 dehydroxylation were investigated. As NADPH addition was much more effective than NADH addition on urolithin M5 dehydroxylation by US fraction, we used NADPH for the following analysis. FAD, which was reported as an electron transferring-element of some molybdenum cofactor dependent reductases such as 4-hydroxybenzoyl-CoA reductase (2,3), was added throughout the reactions.

As shown in Fig. 3, no activity was observed without MV^{2+} under conditions 1 and 2. The comparison of conditions 3 and 4 indicates that MV^{2+} should be reduced with H_2 as an electron donor for the activity expression. The result condition 5 showed that MV^{2+} could be reduced by NADPH to a similar extent as H_2 by enzymes in US/HM fraction. The additive effect of H_2 and NADPH was observed under condition 6. These results indicated that NADPH involved in the electron transfer system of the dehydroxylation enzyme.

Purification and identification of the enzyme converting urolithin M5 to urolithin M6 from *G. urolithinfaciens* DSM 27213 As shown in Fig. 3, the urolithin M5 dehydroxylation enzyme activity was activated and enhanced in the presence of MV^{2+}, NADPH, FAD, and H_2. Therefore, the author analyzed the enzyme activity by monitoring urolithin M5 conversion in the presence of MV^{2+}, NADPH, FAD, and H_2

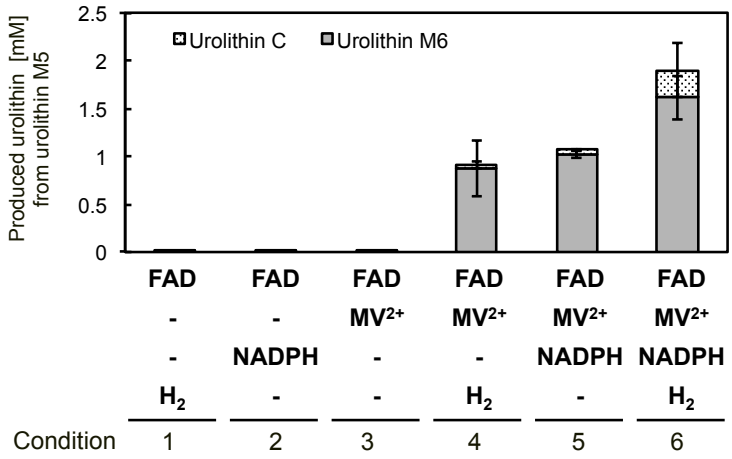

Fig. 3. Profiles of urolithin M5 conversion by US/HM fractions with cofactors Amount of produced urolithins. The graph shows the reaction results using urolithin M5 as the substrate. The reaction mixture contained 0.1 % (w/v) (3.6 mM) urolithin M5 as substrate, 0.2 mM FAD, and 25 % (v/v) of the US/HM fraction with various combinations of factors (10 mM methylviologen dichloride, 10 mM NADPH, and H_2). For conditions 1, 4, and, 6, the reactions were performed under the anaerobic condition (z) (with H_2) at 37 °C for 8 h. For conditions 2, 3, and 5, the reactions were performed under the anaerobic condition (y) (without H_2) at 37 °C for 8 h. Error bars shows 95 % indicate CIs.

throughout enzyme purification. The urolithin M5 converting enzyme was purified from the US fraction of *G. urolithinfaciens* DSM 27213 with three successive column chromatography steps for protein separation. The results of purification processes were summarized in Table 3. The purification process increased the specific activity by 1.83-fold. The SDS-PAGE, the Native-PAGE, and N-terminal amino acid sequence analyses of purified fraction showed the possibility that the molybdopterin containing oxidereductases, UroA1, A2, and UroB1, B2, which were described in SECTION 1, were involved in urolithin M5 dehydroxylation. The SDS-PAGE analysis indicated that there were two bands in the purified solution and the molecular weights were estimated to be 90,000 and 87,000, respectively. Moreover, the Native-PAGE analysis also showed mainly two bands in the purified fraction. The author carried out N-terminal amino acid sequence analysis on separated bands obtained from SDS-PAGE and Native-PAGE. As a result, from two bands of SDS-PAGE (90,000 and 87,000), two peptides were detected as shown in Fig. 4C. These sequences well correlated with N-terminal amino acid sequences of UroA1 and UroB1, respectively. Two proteins which respectively showed single bands in Native-PAGE were analyzed their N-terminal amino acid sequences (Fig. 4B, bands [1] and [2]). From the single band [1], two peptides of which N-terminal

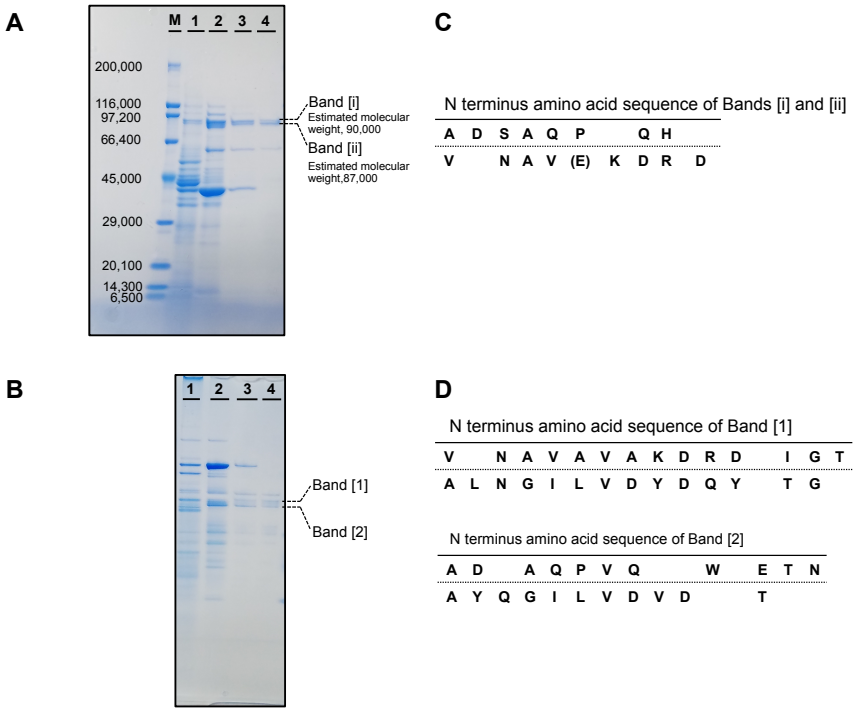

Fig. 4. Protein analysis of a purified enzyme fraction. A, SDS-PAGE analysis of proteins contained in the enzyme solutions through the purification steps. B, Native-PAGE analysis of proteins contained in the enzyme solutions through the purification steps. M, Molecular marker; Lane 1, US fraction; Lane 2, the first Mono Q 5/50 GL fraction; Lane 3, Superdex 200 Increase 10/300 GL fraction; Lane 4, the second Mono Q 5/50 fraction (purified fraction). C, Result of N-terminal amino acid sequencing of bands [i] and [ii] mixture isolated through SDS-PAGE. D, Result of N terminal amino acid sequencing of the single bands [1] and [2] isolated through Native-PAGE.

amino acid sequences correlated with UroB1 and UroB2 were detected (Fig. 4D). From the single band [2], two peptides of which N-terminal amino acid sequences correlated with UroA1 and UroA2 were detected (Fig. 4D).

DISCUSSION

The author observed that the resting cells converted ellagic acid to urolithin M5, urolithin M6, and urolithin C (Fig. 1A, C). The cell-free extracts could convert ellagic acid into urolithin M5 (Fig. 1B), although the cell-free extracts did not show the dehydroxylation activity without any electron-transferring cofactor (Fig. 1B, D). Addition of the cell debris did not restore the urolithin M5 and urolithin M6 dehydroxylation activity of the cell-free extracts under the tested conditions (Table 1). The redox coenzymes NADH, NADPH, FAD, and FMN, had no effect on the dehydroxylation activity of urolithin M5, even though the addition of a combination of all the four coenzymes (Table 1).

By testing the effects of various electron-transferring mediators on the dehydroxylation activity, the author found that anthraquinone and methylviologen affected the urolithin M5 and urolithin M6 dehydroxylation activity of the enzymes in vitro in the presence of H_2 (Table 2). Neither anthraquinone nor methylviologen served as an electron donor without H_2. Anthraquinone was reported as a non-dissolved redox mediator that increased the decolorization rate of azo dye under anaerobic conditions (4) and was also reported to be involved in the reductive reaction by azoreducatase (5). Furthermore, it was reported that anthraquinone raised the denitrification rate of heterotrophic denitrification bacteria (6).

In the present study, with the addition of MV^{2+} to the reaction performed under an H_2-containing anaerobic atmosphere, urolithin M5 was converted into urolithin M6 and urolithin C and urolithin M6 was converted into urolithin C. Methylviologen has been reported as an electron-transferring mediator for various oxidation/reduction reactions catalyzed by enzymes, such as a soluble nitrate reductase (7), formate dehydrogenase (8,9), 4-hydroxybenzoyl-CoA reductase (10), and Dadh (dopamine dehydroxylase) (11,12). The reactions by these redox enzymes containing tungsten or molybdenum have been reported to couple with redox transformation of methylviologen between a dication form (MV^{2+}) and a cation radical form ($MV^{+\cdot}$) (13–16).

Enzyme fractionation revealed that the enzyme was located in the soluble fraction. Further investigation of cofactors in the presence of MV^{2+} suggested that MV^{2+} reduction catalyzed by the enzyme in the soluble fraction with H_2 and NADPH was required for the dehydroxylation. The author evaluated reduction activities in the US/HM fraction with MV^{2+} and H_2 (*i.e.,* hydrogenase activity) and with MV^{2+} and NADPH (*i.e.,* NADPH-dehydrogenase activity) under anaerobic condition through

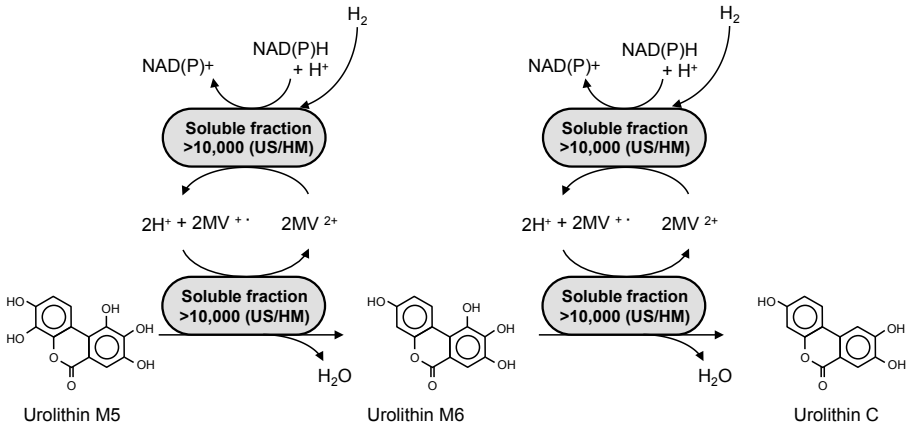

Fig. 5. Proposed mechanisms of urolithin dehydroxylation catalyzed by the enzyme system in *Gordonibacter urolithinfaciens* DSM 27213

observing color change of the reaction mixture from colorless (MV^{2+}) to blue ($MV^{+\cdot}$). Hydrogenase would not catalyze NADPH-dependent reduction of MV^{2+}. These results support the possible electron transfer pathway involved in the dehydroxylation summarized in Fig. 5. As to the involvement of FAD, the author compared the effect of FAD supplementation on urolithin M5 dehydroxylation activity of the US/HM in the presence of MV^{2+}, NADPH, and H_2. The reaction without FAD, the dehydroxylated urolithin yield was 78.2 % of the case with 0.2 mM FAD (data not shown). FAD is suggested to be involved in the enzyme system. Thus, these results shows the involvement of some physiological electron-transferring elements, H_2, NAD(P)H, and FAD, in the complex enzyme system.

As methylviologen is an artificial compound, the author speculate that electron carrier proteins such as ferredoxins and cytochromes may function as physiological electron mediators involved in the enzyme system, as in the case of 4-hydroxybenzoyl-CoA reductase and bacterial nitrate reductases. As for dehydroxylation activity of 4-hydroxybenzoyl-CoA reductase, a reduced ferredoxin with two [4Fe-4S] clusters functions as the natural electron donor (2,3). In the case of nitrate reductases, a respiratory nitrate reductase NarG catalyze nitrate reduction to nitrite using electrons mediated from menaquinol and membrane bound *b*-type hemes containing cytochrome in vivo (17).

Further investigation through enzyme purification showed that UroA1,A2 and UroB1,B2 may be involved in urolithin M5 dehydroxylation. As described in SECTION 1, these four proteins were strongly expressed in ellagic acid metabolizing activity-induced cells. The SDS- and Native-PAGE analyses indicated that UroA1 and UroA2 form a complex, and UroB1 and UroB2 form another complex. On the

other hand, UroA complex and UroB complex seemed to exist separately, since these proteins showed separated by Native-PAGE.

Based on these facts, urolithin M5 dehydroxylation enzyme seems to consist of a large component containing a molybdopterin and an Fe-S cluster and a small component containing two Fe-S clusters and use $MV^{+\cdot}$ as an electron donor. As far as the author knows, this is the first report describing specific enzymes involved in urolithin dehydroxylation. Further analyses of the urolithin dehydroxylation enzyme system through heterologous expression analysis of UroA1, A2, and UroB1, B2 to reveal the detailed mechanism is ongoing.

Table 1. Effects of redox coenzymes on urolithin M5 and urolithin M6 dehydroxylation by the cell-free extracts

	Urolithin M5 conversion yield (%)			Urolithin M6 conversion yield (%)
	Urolithin M6[a]	Urolithin C[b]	Urolithin M6 + urolithin C[c]	Urolithin C[d]
None	−	−	−	−
Cell debris	−	−	−	−
NADH	−	−	−	−
NADPH	−	−	−	−
FAD	−	−	−	−
FMN	−	−	−	−
NADH+NAPH+FAD+FMN	−	−	−	−

The reaction mixture contained 0.1 % (w/v) urolithin M5 (3.6 mM) or urolithin M6 (3.8 mM) as the substrate, 20 % (v/v) of the cell-free extracts, and 20 % (v/v) of the cell debris suspension or the electron-transferring cofactors (10 mM, NADH and NADPH; 0.2 mM, FAD and FMN; 0.1 % (w/v), other mediators), except for "None". The detail conditions were described in the materials and methods section. The conversion yield (%) was calculated using following formula:

[a], 100×[urolithin M6]/([urolithin M5]+[urolithin M6]+[urolithin C]);

[b], 100×[urolithin C]/([uroltihin M5]+[urolithin M6]+[urolithin C]);

[c], 100×([urolithin M6]+[urolithin C])/([urolithin M5]+[urolithin M6]+[urolithin C]);

[d],100×([urolithin C]/([urolithin M6]+[urolithin C]).

−, not converted.

Table 2. Effects of electron-transferring mediators on urolithin M5 and urolithin M6 dehydroxylation by the cell-free extracts

	Urolithin M5 conversion yield (%)			Urolithin M6 conversion yield (%)
	Urolithin M6[a]	Urolithin C[b]	Urolithin M6 + urolithin C[c]	Urolithin C[d]
None	−	−	−	−
DCPIP	−	−	−	−
1-Methoxy-PMS	−	−	−	−
PMS	−	−	−	−
Thionine	−	−	−	−
1,4-Naphtoquinone	−	−	−	−
DHNA	−	−	−	−
Methylene blue	−	−	−	−

The reaction mixture contained 0.1 % (w/v) urolithin M5 (3.6 mM) or urolithin M6 (3.8 mM) as the substrate, 20 % (v/v) of the cell-free extracts, and 0.1 % (w/v) mediators, except for "None". The detail conditions were described in the materials and methods section. The conversion yield (%) was calculated using following formula:

[a], 100×[urolithin M6]/([urolithin M5]+[urolithin M6]+[urolithin C]);

[b], 100×[urolithin C]/([uroltihin M5]+[urolithin M6]+[urolithin C]);

[c], 100×([urolithin M6]+[urolithin C])/([urolithin M5]+[urolithin M6]+[urolithin C]);

[d],100×([urolithin C]/([urolithin M6]+[urolithin C]).

−, not converted. CoQ_0, coenzyme Q_0; DCPIP, dichloroindophenol; PMS, phenazine methosulfate; DHNA, dihydroxynaphthoate.

Table 2. Effects of electron-transferring mediators on urolithin M5 and urolithin M6 dehydroxylation by the cell-free extracts (continued)

	Urolithin M5 conversion yield (%)			Urolithin M6 conversion yield (%)
	Urolithin M6[a]	Urolithin C[b]	Urolithin M6 + urolithin C[c]	Urolithin C[d]
Vitamin K_3	−	−	−	−
Anthraquinone-β-sulfonate	−	−	−	−
Anthraquinone	4.42	−	4.42	−
Emodine	−	−	−	−
Alizarin	−	−	−	−
Neutral red	−	−	−	−
Riboflavin	−	−	−	−
Methylviologen	34.0	24.3	58.3	5.78

The reaction mixture contained 0.1 % (w/v) urolithin M5 (3.6 mM) or urolithin M6 (3.8 mM) as the substrate, 20 % (v/v) of the cell-free extracts, and 0.1 % (w/v) mediators, except for "None". The detail conditions were described in the materials and methods section. The conversion yield (%) was calculated using following formula:

[a], 100×[urolithin M6]/([urolithin M5]+[urolithin M6]+[urolithin C]);

[b], 100×[urolithin C]/([uroltihin M5]+[urolithin M6]+[urolithin C]);

[c], 100×([urolithin M6]+[urolithin C])/([urolithin M5]+[urolithin M6]+[urolithin C]);

[d],100×([urolithin C]/([urolithin M6]+[urolithin C]).

−, not converted. CoQ_0, coenzyme Q_0; DCPIP, dichloroindophenol; PMS, phenazine methosulfate; DHNA, dihydroxynaphthoate.

Table 3. Summary of purification of urolithin M5 dehydroxylation enzyme

Purification step		Total Protein [mg]	Total unit [mU]	Specific unit mU/mg	Fold	Yield %
	US	8.52	6.02	7.07	1	100
(1)	Mono Q 5/50 GL	0.768	0.944	1.23	1.74	15.7
(2)	Superdex 200 Increase 10/300 GL	0.0480	0.0601	1.25	1.77	0.998
(3)	Mono Q 5/50 GL	0.00192	0.00248	1.29	1.83	0.0412

Purification was carried out through monitoring urolithin M5 dehydroxlation activity, as described in the Materials and Methods. One unit (1 U) was defined as amount of enzyme which could produce 1 μmol urolithin M6 from urolithin M5 through 1 min reaction. The reaction mixture contained 3.6 mM urolithin M5, 10 mM methylviologen dichloride, 10 mM NADPH, and 0.2 mM FAD in 50 mM KPB (pH 6.5) and incubated at 37 °C under anaerobic condition (z).

SUMMARY

The key reactions of the ellagic acid metabolism pathway are the dehydroxylation of the phenolic hydroxy group, i.e., conversion of urolithin M5 to urolithin M6, and successive conversion of urolithin M6 to urolithin C. By testing the effects of various electron-transferring compounds on the dehydroxylation reactions, methylviologen was found to effectively support the dehydroxylation catalyzed by the cell free extracts of *G. urolithinfaciens* DSM 27213. The urolithin dehydroxylation enzymes were found in the soluble fraction of the cell-free extracts. The urolithin dehydroxylation was found to be coupled with reduction of MV^{2+} to $MV^{+\cdot}$ catalyzed by enzymes with hydrogen as an electron donor, which was also found with the soluble fraction. Further investigation of the reaction in the presence of natural cofactors with or without methylviologen and hydrogen revealed the involvement of NADPH and FAD in the electron transportation systems of the urolithin dehydroxylation. Moreover, through enzyme purification, the author showed that UroA1,A2 and UroB1,B2 were probably involved in urolithin dehydroxylation.

REFERENCES

1. **Kyhse-Andersen, J.:** Electroblotting of multiple gels: a simple apparatus without buffer tank for rapid transfer of proteins from polyacrylamide to nitrocellulose, J. Biochem. Biophvsic. Methods, **10**, 203–209 (1984).
2. **Breese, K. and Fuchs, G.:** 4-Hydroxybenzoyl-CoA reductase (dehydroxylating) from the denitrifying bacterium *Thauera aromatica*. Prosthetic group, electron donor, and genes of a member of the molybdenum-flavin-iron-sulfur proteins, Eur. J. Biochem., **251**, 916–923 (1998).
3. **Unciuleac, M., Warkentin, E., Page, C. C., and Boll, M., and Ermler, U.:** Structure of a xanthine oxidase-related 4-hydroxybenzoyl-CoA reductase with an additional [4Fe-4S] cluster and an inverted electron flow, Structure, **12**, 2249–2256 (2004).
4. **Guo, J., Zhou, J., Wang, D., Tian, C., Wang, P., Uddin, M. S., and Yu, H.:** Biocalalyst effects of immobilized anthraquinone on the anaerobic reduction of azo dyes by the salt-tolerant bacteria, Water Res., **41**, 426-432 (2007).
5. **Saratale, R. G., Saratale, G. D., Chang, J. S., and Govindwar, S. P.;** Bacterial decolorization and degradation of azo dyes: A review, J. Taiwan Inst. Chem. Eng., **42**, 138-157 (2011).
6. **Guo, J., Kang, Li., Yang, J., Wang, X., Lian, J., Li, H., Guo, Y., and Wang, Y.:** Study on a novel non-dissolved redox mediator catalyzing biological denitrification (RMBDN) technology, Bioresour. Technol., **101**, 4238-4241 (2010).
7. **Lowe, R. H., and Evans, H. J.:** Preparation and some properties of a soluble nitrate reductase from *Rhizobium japonicum,* Biochim. Biophys. Acta, **85**, 377–389 (1964).
8. **Andreesen, J. R., Ghazzawi, E. E., and Gottschalk, G.:** The effect of ferrous ions, tungstate and selenite on the level of formate dehydrogenase in *Clostridium formicoaceticum* and formate synthesis from CO_2 during pyruvate fermentation, Arch. Microbiol., **96**, 103–118 (1974).
9. **Ljungdahl, L. G., and Andreesen, J. R.:** Formate dehydrogenase, a selenium-tungsten enzyme from *Clostridium thermoaceticum*, Methods Enzymol., **53**, 360–372 (1978).
10. **Brackmann, R. and Fuchs, G.:** Enzymes of anaerobic metabolism of phenolic compounds. 4-Hydroxybenzoyl-CoA reductase (dehydroxylating) from a denitrifying *Pseudomonas* species, Eur. J. Biochem., **213**, 563–571 (1993).
11. **Rekdal, V. M., Bess, E. N., Bisanz, J. E., Turnbaugh, P. J., and Balskus, E. P.:** Discovery and inhibition of an interspecies gut bacterial pathway for Levodopa metabolism, Science, **364**, pii:eaau6323 (2019).
12. **Rekdal, V. M., Bernardino, P. N., Luescher, M. U., Kiamehr, S., Turnbaugh, P. J., Bess, E. N., and Balskus, E. P.:** A widely distributed metalloenzyme class enables gut microbial metabolism

of host- and diet-derived catechols, E. bioRxiv. Preprint., https://doi.org/10.1101/725358 (available online 5 Aug 2019).

13. **Mukund, S. and Adams, W. W.:** The novel tungsten-iron-sulfur protein of the hyperthermophilic archaebacterium, *Pyrococcus furiosus*, is an aldehyde ferredoxin oxidoreductase. Evidence for its participation in a unique glycolytic pathway, J. Biol. Chem., **266**, 14208–14216 (1991).
14. **Williams, K., Lowe, P. N., and Leadlay, P. F.:** Purification and characterization of pyruvate: ferredoxin oxidoreductase from the anaerobic protozoon *Trichomonas vaginalis*, Biochem. J., **246**, 529–536 (1987).
15. **White, H., Strobl, G., Feicht, R., and Simon, H.:** Carboxylic acid reductase: a new tungsten enzyme catalyses the reduction of non-activated carboxylic acids to aldehydes, Eur. J. Biochem., **184**, 89–96 (1989).
16. **Adams, M. W. W., Holden, J. F., Menon, A. L., Schut, G. J., Grunden, A. M., Hou, C., Hutchins, A. M., Jenney, F. E. J. Jr., Kim, C., Ma, K., and other 5 authors:** Key role for sulfur in peptide metabolism and in regulation of three hydrogenases in the hyperthermophilic archaeon *Pyrococcus furiosus*, J. Bacteriol., **183**, 716–724 (2001).
17. **González, P. J., Correia, C., Moura, I., Brondino, C. D., Moura, and J. J. G.:** Bacterial nitrate reductases: Molecular and biological aspects of nitrate reduction, J. Inorg., Biochem., **100**, 1015–1023 (2006)

CHAPTER II

Enzyme system involved in glucosinolate metabolism in lactic acid bacteria

To date, the purification of an active GSL-degrading enzyme has not been accomplished since no enzyme activity was reported in cell-free extracts of GSLs-metabolizing LAB and other gut bacteria, although several but bacteria are known to metabolize GSLs (1−7). In the present study, the author elucidates the enzyme system involved in GSL-metabolism in LAB by using *Lactobacillus farciminis* KB1089, which exhibits notable allylglucosinolate (sinigrin)-degrading and allyisothiocyanate (AITC)-generating activity. The author identified proteins specifically expressed in sinigrin-induced cells by quantitative proteomics. Among the identified proteins, the author focused on three candidate proteins expected to be involved in GSL-metabolism. Functional analysis of candidate proteins by heterologous expression in *E. coli* and LAB revealed the involvement of phosphotransferase system (PTS) sugar transporter (*Lf*PttS) and aryl-phospho-*β*-D-glucosidase (*Lf*PbgS) in sinigrin-degradation.

MATERIALS AND METHODS

Chemicals Sinigrin was purchased from Sigma Aldrich Co. (St. Louis, Missouri, USA). AITC was purchased from FUJIFILM Wako Pure Chemical Co. (Osaka, Japan). All other chemicals were of analytical grade and commercially available.

Culture media De Man, Rogosa, Sharpe (MRS) broth (Difco, BD) containing 2 % dextrose and basal solution (1 % proteose peptone No. 3; 1 % beef extract; 0.5 % yeast extract; 0.1 % polysorbate 80; 0.2 % ammonium citrate; 0.5 % sodium acetate; 0.01 % magnesium sulfate; 0.005 % manganese sulfate; 2 % dipotassium phosphate) and that was adjusted to pH 6.5 with HCl was used for LAB cultivation. For analyzing the activity of LAB on sinigrin degradation, four modified MRS (mMRS) media (G10S6-mMRS, S3-mMRS, G3S3-mMRS, and G3-mMRS) were used. G10S6-mMRS contained 10 mM glucose, 6 mM sinigrin, and the basal solution. S3-mMRS contained 3 mM sinigrin and the basal solution. G3S3-mMRS contained 3 mM glucose, 3 mM sinigrin, and the basal solution. G3-mMRS contained 10 mM glucose and the basal solution. For cultivation of *E. coli* transformants, LB medium containing 1.0 %

tryptone, 0.50 % yeast extract, and 1.0 % NaCl was used. For cultivation of *Lc. lactis* transformants, modified M17 (mM17) medium obtained by supplementation of 30 mM glucose and 0.1 mg mL^{-1} catalase (from bovine liver) to M17 broth (Difco, BD), and M17 broth was used.

Bacterial strains, plasmids, and primers. Bacterial strains, plasmids, and primers used in this chapter are listed in Tables S1–S3

Screening of GSL-metabolizing LAB. Glycerol stocks of laboratory stock LAB, isolated from human's feces, animal feces, or pickles were inoculated in 10 mL of MRS broth and were cultivated at 30 °C without shaking for 24 h. Culture medium at 100 μL was added to 10 mL of fresh MRS broth and was cultivated at 30 °C without shaking for 24 h. Of the culture medium, 50 μL was added to 5 mL of S3-mMRS medium and was cultivated further at 30 °C without shaking for 120 h. The culture medium was centrifuged at 12,000 ×*g* for 20 min, and 600 μL of the obtained supernatant was transferred to a 1.5-mL plastic tube. An identical volume of 30 % (w/v) trichloroacetic acid (TCA) solution was added to the tube, mixed by inversion, placed on ice for 30 min, and centrifuged at 12,000 ×*g* for 20 min. The obtained supernatant was filtered with a 0.22-μm pore size membrane filter and was analyzed by HPLC.

HPLC analysis. Of the treated mixtures, 10 μL was analyzed by HPLC, using Shimadzu LC 10A system (Shimadzu Corp., Kyoto, Japan) equipped with a Cosmosil column ($5C_{18}$-MS-II; 3.0 mm ID × 250 mm; Nacalai Tesque Inc., Kyoto, Japan). The mobile phase for HPLC analysis of culture supernatants was methanol-H_2O (20:80, by volume, supplemented with 0.05 % [w/v] trifluoroacetic acid [TFA]). The mobile phase for HPLC analysis of supernatants of the resting cell reaction mixtures was acetonitrile-H_2O (7:93, by volume, supplemented with 0.05 % [w/v] TFA). The column temperature was maintained at 35 °C. The flow rate was 1.0 mL min^{-1} and the effluent was monitored with SPD-10A (Shimadzu Corp., Kyoto, Japan) at a wavelength of 235 nm.

16S rRNA and phenylalanyl-tRNA synthetase (*pheS*) gene sequencing. All primers used for the 16S rRNA and *pheS* gene sequencing are listed in Table S3. The 16S rRNA gene was amplified by PCR using the primers 27f/1525r and Ampli Taq Gold PR Master Mix (Thermo Fisher Scientific, Inc., Massachusetts, USA). The PCR product was gel-purified and sequenced using 27F, 1525R, 516F, 1087F, 531R, 1104R, and 518R (Tsukuba Oligo Service, Co., Ltd., Tsukuba, Japan). The obtained sequences were assembled using BioEdit to create a contig, which was then searched using the Basic Local Alignment Search Tool (BLAST) program on the DNA Data Bank of Japan (DDBJ) database.

The *pheS* gene (8) was amplified by

PCR using the primers pheS-21F/pheS-22R (Eurofins Genomics, Inc., Tokyo, Japan). The PCR product was gel-purified and sequenced using the same primers. The obtained sequences were assembled and searched, as described in Materials and Methods.

Cultivation of *Lb. farciminis* KB1089. *Lb. farciminis* KB1089 was inoculated from a glycerol stock into 5 mL of MRS broth, cultivated for 24 h, and subcultured in fresh MRS broth. It was then cultivated further for 24 h as described above. Of the culture, 350 µL was inoculated in 35 mL of G10S6-mMRS medium and cultivated at 30 °C without shaking. Of the culture, 1.2 mL was sampled at different time points, out of which 100 µL aliquots were each used for measurement of optical density at 550 nm (OD_{550}) and for pH determination using a portable pH Meter (Model B212, Horiba Ltd., Kyoto, Japan). The remaining 1 mL culture aliquot was centrifuged and was treated with TCA solution, as described above, after which sinigrin and glucose concentrations were determined using HPLC and Biosensor BF-5i (Oji Scientific Instruments Co., Ltd., Hyogo, Japan), respectively.

Resting cell reactions using washed cells of *Lb. farciminis* KB1089. *Lb. farciminis* KB1089 was inoculated from a glycerol stock into 10 mL of MRS broth in glass test tubes (16.5 × 125 mm), and was cultivated at 28 °C with 120 strokes min^{-1} shaking for 16 h. Of the culture, 100 µL was added to 10 mL of either G3S3-mMRS or G3-mMRS medium and was cultivated at 28 °C with 120 strokes min^{-1} shaking for 7 h. After confirming the consumption of glucose in the culture medium using Glucose CII-Test Wako (FUJIFILM Wako Pure Chemicals Ind., Co., Osaka, Japan), cells were harvested by centrifugation at 1,500 ×*g* for 10 min, and pellets were washed twice with 0.85 % (w/v) NaCl. The washed cell pellets were resuspended in 1 mL of reaction solution containing 3 mM sinigrin in 20 mM KPB (pH 6.5) and were incubated at 28 °C with 120 strokes min^{-1} shaking for 16 h. The reaction mixtures were centrifuged at 1,500 ×*g* for 10 min. For the detection of sinigrin, the supernatants were analyzed using HPLC. For the detection of AITC, 0.6 mL of the supernatants were transferred to a glass test tube and an identical volume of hexane (including 25 nM benzylpropionate as the internal standard) was added to the sample, mixed by vortexing for 1 min, and centrifuged at 1,500 ×*g* for 10 min. The aliquot corresponding to the hexane layer was filtered with a 0.45-µm pore size membrane filter (Merck Millipore, Burlington, Massachusetts, USA) and was analyzed using gas chromatography-mass spectrometry (GC-MS).

GC-MS analysis. A treated sample (hexane solution) was analyzed by GC-MS using GC-MS QP2010 (Shimadzu Co., Kyoto, Japan) with a GC-2010 gas chromatograph equipped with a split injection system and a Supelco column (SPB-1; 0.25 mm ID × 30 m; Sigma-Aldrich Co.,

St. Louis, Missouri, USA). The column temperature was maintained at 80 °C for 35 min. The injector was operated at 250 °C. Helium was used as a carrier gas at 0.62 mL min^{-1}. MS was used in the electron impact mode at 70 eV with a source temperature of 250 °C.

Reactions using cell-free extracts of *Lb. farciminis* KB1089. Four kinds of cell lysates of *Lb. farciminis* KB1089 were prepared using different cell disruption methods: (i) with an Insonator 201M ultrasonic oscillator (Kubota Co., Osaka, Japan) for 10 min × 2 cycles; (ii) with glass beads (0.1 mm diameter) using a Multi-beads shocker MB701 (Yasui Kikai Co., Osaka, Japan) with 12 cycles of 60 s each on and off at 2,700 rpm; (iii) with a FRENCH press (Thermo Electron Co., Ltd., Waltham, Massachusetts, USA) at 1,000 psi four times; and (iv) with Bug-Buster reagents (Novagen, Merck Millipore, Burlington, Massachusetts, USA). Of washed cells of *Lb. farciminis* KB1089 grown in G3S3-mMRS medium, as described in the Materials and Methods, 0.5 g was suspended with 1 mL of 20 mM KPB (pH 6.5) for the cell disruption methods (i)-(iii), or was suspended with 2.5 mL of the Bug-Buster reagents for method (iv). Supernatants obtained after removal of cell debris in each lysate by centrifugation at 8,000 ×*g* for 20 min were used as cell-free extracts. Of each cell-free extracts, 50 μL was mixed with 850 μL of 0.1 M KPB (pH 6.5) and 100 μL of 30 mM sinigrin, incubated at 28 °C with shaking at 120 strokes min^{-1} for 12 h, and was analyzed by HPLC. To examine the effect of additional reagents, 50 μL of cell-free extracts prepared by the above-mentioned method (ii) was mixed with 750 μL of 0.1 M KPB (pH 6.5), 100 μL of 30 mM sinigrin, and reagent listed in Tables S4, S5, and incubated at 28 °C with shaking at 120 strokes min^{-1} for 12 h, and was analyzed by HPLC.

Draft genome sequencing. Draft genome sequences of *Lb. farciminis* KB1089, LMG9189, NRIC0416, and NRIC0417 were determined by the whole-genome shotgun strategy using 454 pyrosequencing by GS-junior bench top system (F. Hoffmann-La Roche, Ltd., Basel, Switzerland). The draft genome sequences of *Lb. farciminis* KB1089, LMG9189, NRIC0416, and NRIC0417, were obtained with 67, 67, 112 and 166 contigs, respectively.

Sample preparation for quantitative proteomic analysis. Cells in 500 mL cultures of *Lb. farciminis* KB1089, grown either in G3S3-mMRS or G3-mMRS medium, were harvested by centrifugation at 1,500 ×*g* for 10 min. Of cell pellets, 0.1 g were resuspended with 500 μL of lysis buffer (containing 50 mM Tris-HCl [pH 7.0], 7 M urea, 2 M thiourea, 2 % [w/v] 3-(3-cholamidopropyl)dimethylammonio-1-propanesulfonate, 10 mM dithiothreitol, and 1 % [*v*/*v*] protease inhibitor cocktail for cell lysis [Sigma-Aldrich Co., St. Louis, Missouri, USA]).

Cells were disrupted with sonication using Powersonic Model50 (Yamato Scientific Co., Ltd., Tokyo, Japan) and were later centrifuged at 14,000 ×g for 10 min. The resultant supernatant was filtrated using an Amicon Ultra-0.5 Centrifugal Filter Unit (with molecular weight-10,000 cutoff membrane, Merck Millipore, Burlington, Massachusetts, USA) and buffer-exchanged with 0.2 M TEAB. Of 0.2 M tris(2-calboxyethyl) phosphine, 50 μL was added to the solution and was incubated at 55 °C for 60 min to reduce proteins. Of 375 mM iodoacetoamide, 5 μL was added and was incubated at room temperature for 30 min in the dark. Proteins were precipitated by adding 2 mL of ice-cold acetone and by overnight incubation at −20 °C. The precipitated proteins were resuspended with 200 μL of 0.2 M TEAB supplemented with 20 μg of sequencing grade modified trypsin (Promega Co., Madison, Wisconsin, USA), and were incubated overnight at 37 °C. The digested samples were subjected to proteome analysis.

Quantitative proteomic analysis (LC-MS/MS and data analysis). LC-MS/MS analysis was performed using an LC (Ultimate 3000; Thermo Scientific, Inc., Massachusetts, USA)-MS/MS (LTQ Orbitrap Velos Mass Spectrometer, Thermo Scientific, Inc., Massachusetts, USA) system equipped with a long monolithic capillary column. Tryptic digests were separated by reverse-phase chromatography using a monolithic silica capillary column (500 cm long, 0.1 mm ID) (9), at a flow rate of the two eluents: eluent A, 0.1 % (*v*/*v*) formic acid; eluent B, 80 % acetonitrile containing 0.1 % (*v*/*v*) formic acid. The gradient started with 5 % eluent B, increased to 45 % eluent B for 600 min, further increased to 95 % eluent B to wash the column for 140 min, returned to the initial condition, and was held for re-equilibration of the column. The separated analytes were detected using a mass spectrometer with a full scan range of 350–1,500 *m*/*z*. For data-dependent acquisition, analysis program was set to automatically analyze the top 10 most intense ions observed in the MS scan. An ESI voltage of 2.4 kV was applied directly to the LC buffer end of the chromatography column by using a MicroTee (Upchurch Scientific Inc.). The ion transfer tube temperature was set to 300 °C. Data analysis was performed using Proteome Discoverer 1.4 (Thermo Scientific, Inc., Massachusetts, USA). Protein identification was performed using Mascot algorithm against the protein database of *Lb. farciminis* KCTC3681 (GCA_000184535.1) (10) from NCBI.

Preparation of genomic DNA, extraction of plasmid DNA, DNA sequence analysis, PCR amplification, and purification of PCR products. *Lb. farciminis* KB1089 genomic DNA was extracted using DNeasy Blood & Tissue kit (Qiagen Inc., Hilden, Germany), according to manufacturer's instructions. All plasmids constructed in this study were extracted using QIAprep Spin Miniprep Kit (Qiagen Inc., Hilden, Germany), and were confirmed by sequence

analysis using GenomeLab DTCS Quick Start kit and a Beckman-Coulter CEQ8000 (Beckman Coulter Co., Ltd., Brea, California, USA). PCR amplification for cloning purposes was performed with PrimeSTAR Max DNA polymerase (Takara Bio Inc., Shiga, Japan) and colony PCR was performed with TAKARA Ex Taq (Takara Bio Inc., Shiga, Japan). All oligonucleotides, used as primers for PCR (listed in Table S3), were purchased from Hokkaido System Science Co. Ltd. (Sapporo, Japan) All PCR products were gel-purified using QIAgen gel extraction kit (Qiagen Inc., Hilden, Germany).

Cloning of *nukS*, *pbgS,* and *pttS* in *E. coli*. To construct pET28-*nukS*, pET28-*pbgS,* and pET28-*pttS*, the *nukS*, *pbgS*, and *pttS* genes were amplified from the genomic DNA of *Lb. farciminis* KB1089 by PCR using primers oET-*nukS*-Fw/oET-*nukS*-Rv, oET-*pbgS*-Fw/oET-*pbgS*-Rv, and oET28-*pttS*-Fw/oET28-*pttS*-Rv, respectively. The PCR products were gel-purified and digested with the restriction enzymes SalI and NotI. The digested fragments were gel-purified, and were ligated into the similarly digested and purified pET-28a(+) vector. The products of ligation were transformed into competent *E. coli* DH5α cells using Inoue's method (11), and kanamycin-resistant transformants were selected. Plasmids were purified from the selected transformants. To construct pET21-*pbgS*, the *pbgS* gene was cloned into pET-21b(+), as described above, except for selection of ampicillin-resistant transformants. To construct pRSF-*pttS*, the *pttS* gene was cloned in SalI and NotI sites of pRSFDuet-1 as described above. To construct pRSF-*pttS*-*nukS*, the *nukS* gene was amplified from the genomic DNA of *Lb. farciminis* KB1089 by PCR using primers oRSF-*nukS*-Fw/oRSF-*nukS*-Rv. The PCR products were gel-purified and digested with restriction enzymes BglII and XhoI. The digested fragments were gel-purified and ligated into the similarly digested and purified pRSF-*pttS* vector. The following procedures are as described above.

To construct *E. coli* pET28-*nukS*, *E. coli* pET28-*pbgS*, *E. coli* pET28-*pttS*, and *E. coli* pRSF-*pttS*-*nukS*, the constructed vectors pET28-*nukS*, pET28-*pbgS*, pET28-*pttS*, and pRSF-*pttS*-*nukS* were, respectively, transformed into *E. coli* Rosetta 2(DE3) competent cells using Inoue's method (11), and kanamycin and chloramphenicol-resistant transformants were selected. A successful introduction of vectors in the selected transformants was confirmed by colony PCR using primers for T7-promoter/T7-terminator for *E. coli* pET28-*nukS*, *E. coli* pET28-*pbgS*, and *E. coli* pET28-*pttS*, and primers for ACYCDuetUP-1/T7-terminator for *E. coli* pRSF-*pttS*-*nukS*, respectively. To construct *E. coli* pET21-*pbgS*/pRSF-*pttS* and *E. coli* pET21-*pbgS*/pRSF-*pttS*-*nukS*, the constructed vectors pRSF-*pttS* and pRSF-*pttS*-*nukS* were simultaneously transformed with pET21-*pbgS* in

E. coli Rosetta 2(DE3), as described above, and ampicillin, kanamycin, and chloramphenicol-resistant transformants were selected. A successful introduction of vectors in selected transformants was confirmed by colony PCR using primers T7-promoter/T7-terminator and ACYCDuetUP-1/T7-terminator, respectively.

Cultivation of *E. coli* transformants and resting cell reaction using washed cells. All *E. coli* transformants were grown at 37 °C under shaking at 150 strokes min^{-1} in 5 mL of LB medium containing 34 μg mL^{-1} chloramphenicol and also other antibiotics corresponding to the resistance conferring genes present in the indicated harbored vectors (30 μg mL^{-1} kanamycin for *E. coli* pET28-*nukS*, *E. coli* pET28-*pbgS*, *E. coli* pET28-*pttS*, and *E. coli* pRSF-*pttS*-*nukS*, and 100 μg mL^{-1} ampicillin together with 30 μg mL^{-1} kanamycin for *E. coli* pET21-*pbgS*/pRSF-*pttS* and *E. coli* pET21-*pbgS*/pRSF-*pttS*-*nukS*, respectively.) in 12-mL culture tubes (Fisher Scientific, Inc., Massachusetts, USA). Of each overnight culture medium, 50 μL was added to 5 mL of LB medium containing the appropriate antibiotics. Upon incubation at 37 °C under shaking at 150 strokes min^{-1} for 2.5 h, IPTG was added to a final concentration of 0.1 mM and cells were cultivated at 20 °C with shaking at 120 strokes min^{-1} for 16 h. The cells were harvested by centrifugation at 1,500 ×*g* for 10 min, washed twice with 0.85 % (w/v) NaCl, resuspended with 1 mL of reaction solution containing 3 mM sinigrin in 20 mM KPB (pH 6.5), and incubated at 28 °C with 120 strokes min^{-1} for 20 h. Subsequently, the supernatants were obtained by centrifugation and were analyzed using HPLC and GC-MS, according to the same procedure described above.

Cloning of *nukS*, *pbgS,* and *pttS* in *Lc. lactis*. In order to construct pNZ7021-*nukS*, pNZ7021-*pbgS*, and pNZ7021-*pttS*, the *nukS*, *pbgS* and *pttS* genes together with approximately 100 bp upstream regions were amplified from the genomic DNA of *Lb. farciminis* KB1089 by PCR using primers oNZ-*nukS*-Fw/oNZ-*nukS*-Rv, oNZ-*pbgS*-Fw/oNZ-*pbgS*-Rv, and oNZ-*pttS*-Fw/oNZ-*pttS*-Rv, respectively. To construct pNZ7021-*pttS*-*pbgS*-*nukS*, the region that contained *pttS*, *pbgS*, and *nukS* genes together with approximately 100 bp upstream region of the start codon of *pttS* gene was amplified from the genomic DNA of *Lb. farciminis* KB1089 by PCR using primers oNZ-*nukS*-Fw/oNZ-*pttS*-Rv. The PCR products were gel-purified and digested with restriction enzymes SpeI and HindIII. The digested fragments were gel-purified and ligated into the similarly digested and purified vector pNZ7021. The ligation products were transformed into competent cells of transformed *E. coli* MC1061 using Inoue's method (11). Chloramphenicol-resistant transformants were selected, and plasmids were purified from the transformants.

Electrocompetent cells of *Lc. lactis* NZ9000 were prepared according to the manufacturer's protocol. To construct *Lc. lactis* pNZ7021-*nukS*, *Lc. lactis* pNZ7021-*pbgS*, *Lc. lactis* pNZ7021-*pttS*, and *Lc. lactis* pNZ7021-*pttS-pbgS-nukS,* the constructed vectors pNZ7021-*nukS*, pNZ7021-*pbgS*, pNZ7021-*pttS*, and pNZ7021-*pttS-pbgS-nukS* were transformed into electrocompetent cells of *Lc. lactis* NZ9000 by electroporation, according to the manufacturer's protocol and chloramphenicol-resistant transformants were selected. A successful introduction of vectors in the selected transformants was confirmed by colony PCR by using the primers pNZ7021-Fw/pNZ7021-Rv.

Cultivation of *Lc. lactis* transformants and resting cell reaction using the washed cells. All *Lc. lactis* transformants were grown under anaerobic conditions (using the Anaropack, Mitsubishi Gas Chemical Co., Inc.) at 30 °C for 18 h in 5 mL of mM17 medium supplemented with 10 μg mL^{-1} chloramphenicol in glass test tubes (16.5 × 150 mm). Of each culture medium, 250 μL was added to 10 mL of an identical fresh medium. After incubation (under anaerobic conditions at 30 °C for 7 h), the cells were harvested by centrifugation at 1,500 ×*g* for 20 min, washed twice with 0.85 % (w/v) NaCl, and resuspended in 1 mL of reaction solution containing 3 mM sinigrin in 20 mM KPB (pH 6.5) and were incubated at 28 °C with 120 strokes min^{-1} for 16 h. Subsequently, supernatants were obtained by centrifugation and were analyzed using HPLC and GC-MS, according to the same procedure described above.

Enzymatic synthesis of sinigrin-6-phosphate by BglK. The expression vector for BglK (*β*-glucoside kinase from *Klebisiella pneumoniae* ATCC 23357, AAK58463.1 (12), pET28-*bglK*, was constructed by GenScript Corp., and transformed into *E. coli* Rosetta 2(DE3), as described above. The transformed cells were grown with shaking at 150 strokes min^{-1} at 37 °C in 5 mL LB medium containing 34 μg mL^{-1} chloramphenicol and 30 μg mL^{-1} kanamycin. Of the overnight cultures, 50 μL were added to 5 mL of the same medium. After cultures were grown for 2.5 h with shaking 150 strokes min^{-1} at 37 °C, IPTG was added to a final concentration of 0.5 mM, and cells were cultured at 37 °C for 4 h with shaking at 150 strokes min^{-1}. Cells were then harvested by centrifugation at 1,500 ×*g* for 10 min, washed twice with 0.85 % (w/v) NaCl, and resuspended with 500 μL of 25 mM 4-(2-hydroxyethyl)-1-piperazineethanesulfonic acid buffer (HEPES; pH 7.5) containing 2 mM $MgSO_4 \cdot 7H_2O$. The cell suspensions were treated with an identical volume of glass beads (0.1 mm diameter) using a Multi-beads shocker MB701 (Yasui Kikai Co. Osaka, Japan) with 6 cycles of time at 60 s on at 2,700 rpm and 60 s off. Cell debris were removed by centrifugation at 8,000 ×*g* for 20 min. The supernatants thus obtained

were used as crude BglK.

To synthesize sinigrin-6-phosphate, 1 mL of reaction mixtures containing 350 μL of crude BglK, 3 mM sinigrin, and 1.5 mM adenosine triphosphate (ATP) (adjusted to pH 7.5 by addition of less than 10 μL of 1M NaOH) were incubated at 25 °C for 2 h. After the reaction, the sugar phosphates were extracted from the reaction mixtures according to the procedure described below.

Extraction of phosphorylated sugar compounds. Phosphorylated sugar compounds in the BglK reaction mixtures were isolated according to a previously described procedure (12), and with slight modifications. pH in 1 mL of the samples prepared as described above was adjusted to 8.2 with 1 M NaOH and 0.5 mL of 25 % (w/v) aqueous solution of barium acetate was added. The mixture was vortexed and chilled on ice for 30 min. Heavy white precipitates of water-insoluble Ba^{2+} salts were removed by centrifugation (1,500 ×*g* for 10 min). The obtained supernatants were filtrated with a 0.45-μm pore size membrane filter (Merck Millipore, Burlington, Massachusetts, USA), added to 6 mL of ethanol and chilled overnight at 4 °C. The flocculent precipitates of the ethanol-insoluble Ba^{2+} salts were collected by centrifugation (1,500 ×*g* for 10 min), and were dried overnight in a vacuum desiccator. The obtained pellets were stored at −20 °C.

Detection of phosphorylated sinigrin by high performance ion chromatography high resolution tandem mass spectrometry (HPIC-HRMS/MS) analysis. Of the Ba^{2+} salts containing phosphorylated sugar compounds, 50 mg were redissolved in 100 μL of H_2O, and 2 μL of the supernatant were analyzed by a HPIC-HRMS/MS. The HPIC was performed using a Dionex ICS-5000· system (Thermo Fisher Scientific, Inc., Massachusetts, USA) equipped with an anion electrolyte suppressor (Dionex AERS 500e 2 mm, Thermo Fisher Scientific, Inc., Massachusetts, USA), a guard column (Dionex IonPac AG11-HC-4 μm; 3.0 mm ID × 250 mm; 4 μm particle size; Thermo Fisher Scientific Inc.), and a separation column (Dionex IonPac AS11-HC-4 μm; 3.0 mm ID × 250 mm; 4 μm particle size; Thermo Fisher Scientific, Inc., Massachusetts, USA). The HPIC flow rate was 0.3 mL min^{-1} supplemented post column with 0.1 mL min^{-1} makeup flow of 1 mM ammonium acetate in MeOH. The gradient conditions for KOH eluent for HPIC separation were set as follows: 0.0–24.0 min, a linear gradient from 10 mM to 100 mM; 24.0–27.0 min, 100 mM; 27.0–27.1 min, a linear gradient from 100 mM to 10 mM; 27.1–30 min, 10 mM.

The HRMS/MS was performed using a Q Exactive, a high-performance benchtop quadrupole Orbitrap mass mass spectrometer (Thermo Fisher Scientific, Inc., Massachusetts, USA) equipped with a heated under an ESI source. The HRMS analysis conditions were as follows: polarity, negative ionization; sheath gas flow rate, 40 arb; auxiliary gas flow rate, 10 arb;

spray voltage, 2.0 kV; capillary temperature, 350 °C; S-lens level, 50; probe heater temperature, 300 °C; mass resolution, 70000; automatic gain control (AGC) target (the number of ions to fill the C-trap), 100000; maximum injection time (IT), 100 ms; and MS scan range, 70–1050 (*m/z*). The parallel reaction monitoring (PRM) conditions for each target compound were as follows: mass resolution, 70000; AGC target, 200000; maximum IT, 100 ms; isolation window, 4.0 (*m/z*); and stepped normalized collision energy (NCE), 10, 20, and 35.

Reaction using cell-free extracts of *Lc. lactis* transformants. Washed cells of *Lc. lactis* pNZ7021-*pbgS* were suspended with 1 mL of 100 mM MES (pH 6.5) and disrupted with an Insonator 201M ultrasonic oscillator (Kubota Co., Osaka, Japan) for 5 min × 4 cycles. The supernatants obtained after removal of cell debris by centrifugation at 8,000 ×*g* for 20 min were used as cell-free extracts. The cell-free extracts at 450 µL was mixed with 50 µL of 0.3 mg/mL Ba^{2+} salts containing phosphorylated sugar compounds, obtained as described above, in 100 mM 2-(*N*-morpholino)ethanesulfonic acid buffer (MES; pH 6.5) and incubated at 28 °C under shaking at 120 strokes min^{-1} for 1.5 h. Subsequently, produced AITC were extracted and analyzed as described above.

Sodium dodecyl sulfate-polyacrylamide gel electrophoresis (SDS-PAGE) analysis. Washed cells of transformed *E. coli* or *Lc. lactis* were suspended with 500 µL of 20 mM KPB (pH 6.5). Cell suspensions were treated with an identical volume of glass beads (0.1 mm diameter) using a Multi-beads shocker MB701 (Yasui Kikai Corp.) with six cycles of 60 s on at 2,700 rpm and 60 s off. The cell lysates of *E. coli* were analyzed by SDS-PAGE. The cell lysates of *Lc. lactis* were centrifuged at 8,000 ×*g* for 20 min and both precipitates and supernatants were suspended with 20 mM KPB (pH 6.5) and analyzed by SDS-PAGE.

SDS-PAGE was performed on a 12.5% polyacrylamide gel using Tris-glycine buffer system. To estimate protein molecular weights, EZ Standard AE1440 (Atto Co., Ltd.) was used as the protein standard. The gels were stained using EzStain Aqua (Atto Co., Ltd.).

Data availability The genome sequences were deposited in DNA Data Bank of Japan (DDBJ) and the accession numbers summarized in Supplementary Table S6. The proteomic data were deposited in Japan ProteOme Standard Repository/Database (jPOST) (13) with the accession number as PXD011820. The *pttS*. *pbgS* and *nukS* gene sequences were deposited in DDBJ under accession number LC422123, LC422124, and LC42125, respectively.

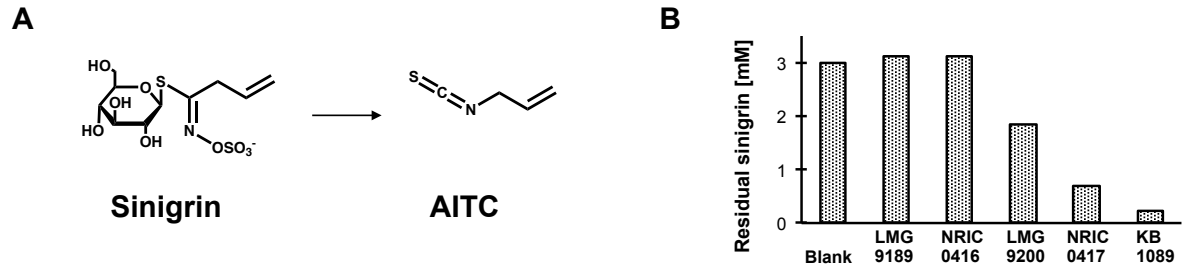

Fig. 1 Screening of GSL-degrading LAB A, Structures of substrate (sinigrin) and product (AITC). B, Amounts of residual sinigrin in the culture medium (initial sinigrin; 3.0 mM) after 24 h cultivation of each strain of *Lb. farciminis*. Blank indicates uninoculated sample.

RESULTS

Screening of GSL-degrading lactic acid bacteria Only four among the 279 strains screened using S3-mMRS, a sinigrin containing culture medium, showed target activity. The LAB strain KB1089, isolated from suguki, which are traditional Japanese pickles, showed the highest sinigrin-degrading activity. 16S rRNA and *pheS* gene sequencing identified this strain as *Lactobacillus farciminis*. Furthermore, the author evaluated sinigrin-degrading activity of six strains of *Lb. farciminis* that are available in public culture collections (Fig. 1). Four among the six tested strains exhibited sinigrin-degrading activity; the highest activity was observed in the KB1089 strain.

Analysis of sinigrin-degrading activity of *Lb. farciminis* KB1089 The author monitored sinigrin-degrading activity of *Lb. farciminis* KB1089 in glucose containing G10S6-mMRS medium. Degradation of sinigrin in the culture medium started in the logarithmic growth phase after consumption of glucose (Fig. 2A).

To examine whether sinigrin-degrading activity was induced by sinigrin itself, the author evaluated the activity of washed cells obtained after glucose consumption from the culture broth. The cells cultivated in G3S3-mMRS medium were shown to degrade sinigrin (Fig. 2B-(i)) and produce AITC (Fig. 2B-(ii), Fig. S1). No sinigrin-degradation was observed in cells cultivated in G3-mMRS medium. This indicated that the sinigrin-degradation activity of *Lb. farciminis* KB1089 was induced by sinigrin itself, and sinigrin was degraded into a corresponding isothiocyanate, AITC.

While *Lb. farciminis* KB1089 exhibited sinigrin-degrading activity in resting cell reactions, sinigrin-degrading activity could not be observed when using cell free extracts prepared by four kinds of cell disruption methods (i)-(iv) described in Materials and Methods. No activity was observed even in the reactions which had various added regents, such as cofactors and metal ions (Table S4, S5).

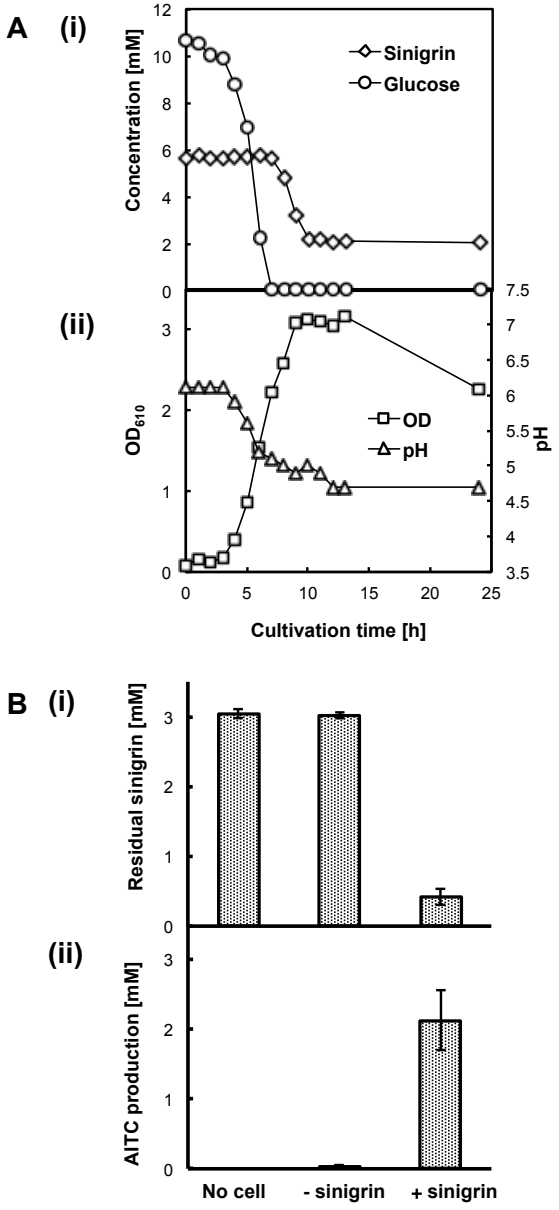

Fig. 2 Sinigrin-degrading activity of *Lb. farciminis* KB1089 A: Profiles of glucose and sinigrin concentrations (i), optical density (OD_{550}), and pH (ii) during cultivation of *Lb. farciminis* KB1089 in the G10S6-mMRS medium. B: Sinigrin-degrading activity of *Lb. farciminis* KB1089 in resting cell reactions using washed cells cultivated in G3-mMRS medium (−sinigrin) or G3S3-mMRS medium (+sinigrin). Amounts of residual sinigrin (i) and produced AITC (ii) in the reaction mixture. "No cell" indicates a reaction solution without cells. Error bars indicate 95 % CIs.

Comparative proteomic in sinigrin-induced and non-induced cells of *Lb. farciminis* KB1089 The author compared the protein expression profiles of *Lb. farciminis* KB1089 in sinigrin-induced cells (cultivated in G3S3-mMRS medium) and non-induced cells (cultivated in G3-mMRS medium). Twenty six proteins were specifically expressed in the induced-cells (Table 1).

Among the 26 identified proteins, three proteins, namely, PTS sugar transporter (*Lf*PttS), arl-phospho-*β*-D-glucosidase (*Lf*PbgS), and a hypothetical protein (*Lf*NnukS) were further chosen as candidate proteins that were expected to be involved in sinigrin-degradation, based on the three following reasons: (1) homologous genes were found in the genome of the other sinigrin-degrading strains of *Lb. farciminis* (the strains LMG9200, KCTC3681 [CP017702.1], and NRIC0417); (2) no homologous genes were found in the genome of the other strains of *Lb. farciminis* without sinigrin-degrading activity (the strains LMG9189 and NRIC0416); (3) the genes existed adjacent to each other in the genome of *Lb. farciminis* KB1089 (Fig. 3A).

Results obtained from InterPro (https://www.ebi.ac.uk/interpro/) analysis showed that *Lf*PttS contains three structurally distinct domains, namely, IIA, IIB, and IIC (14), which form a membrane-bound complex; *Lf*PbgS, belonging to the glucoside hydrolase (GH) family 1 (15); *Lf*NukS contains a phosphate-binding loop (P-loop) which is a

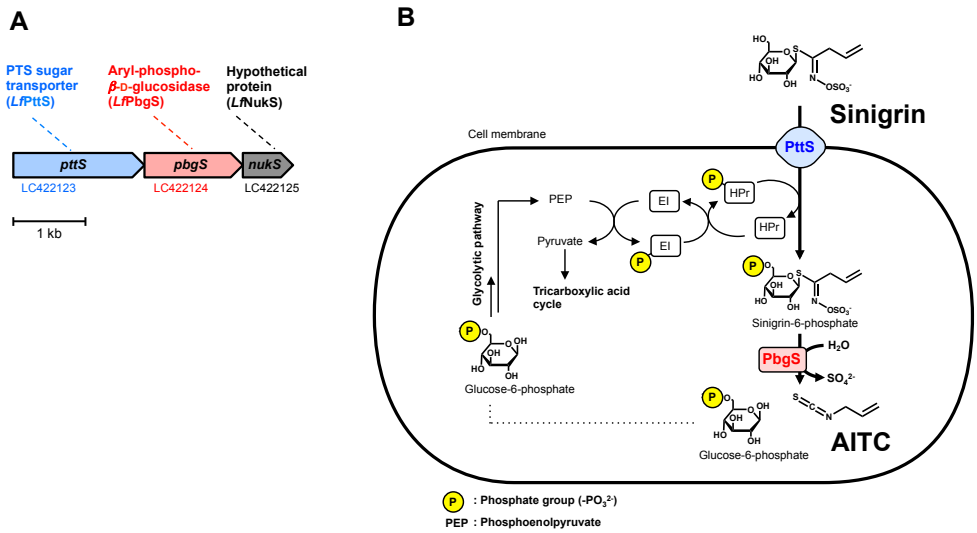

Fig. 3 The gene cluster encoding candidate proteins found in the genome of *Lb. farciminis* KB1089 (A) and the putative pathway of sinigrin-degradation (B)
The DDBJ accession number assigned to each gene is shown below its coding region (A).

common motif in ATP binding proteins (16).

Heterologous expression and functional analysis of candidate proteins. The author constructed heterologous expression systems of candidate genes (*pttS* [LC422123], *pbgS* [LC422124], and *nukS* [LC422125] encoding *Lf*PttS, *Lf*PbgS, and *Lf*NukS, respectively) in *E. coli* Rosetta 2(DE3) and in *Lactococcus lactis* NZ9000.

Transformed *E. coli* strains harboring individual genes among the three identified candidate genes, among a combination of two genes, or among all three genes were constructed, and sinigrin-degrading activities were evaluated in resting cell reactions using washed cells (Table S7). None of the strains harboring empty vectors (pET-28a(+), pET-21b(+)/pET-28s(+), pRSFDuet-1, and pET21b(+)/pRSFDuet-1) showed target activity. The strains harboring one candidate gene (pET28-*pttS*, pET28-*pbgS*, and pET28-*nukS*), or a combination of two genes, namely, *pttS* and *nukS* (pRSF-*pttS*-*nukS*), or of *pbgS* and *nukS* (pET21-*pbgS*/pRSF-*nukS*), showed no target activity. The strain harboring both *pbgS* and *pttS* genes (pET21-*pbgS*/pRSF-*pttS*) was able to degrade sinigrin into AITC. The strain harboring all three genes (pET21-*pbgS*/pRSF-*pttS*-*nukS*) also showed target activity to a similar extent as the strain pET21-*pbgS*/pRSF-*pttS* (Fig. 4A).

The transformed *Lc. lactis* strains that harbor each individual candidate gene or all three genes were analyzed for their sinigrin-degrading activities in resting cell reactions by using washed cells (Fig. 4B). The strain harboring the empty vector (pNZ7021) showed slight sinigrin-degradation. The strains harboring only the *nukS* gene (pNZ7021-*nukS*) and the *pbgS* gene (pNZ7021-*pbgS*) degraded

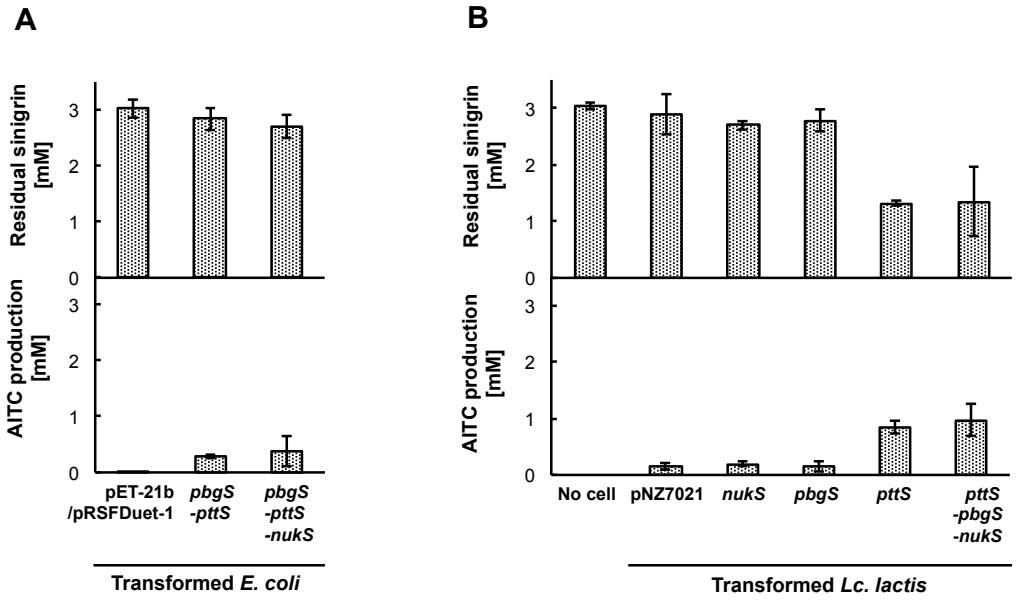

Fig. 4 Sinigrin-degrading activity of transformed *E. coli* or *Lc. lactis* in resting cell reactions using washed cells. Amounts of residual sinigrin and produced AITC in the reaction mixtures using transformed *E. coli* (A) or *Lc. lactis* (B) cells. "pET-21b/pRSFDuet-1" indicates the vector control strain; "*pbgS-pttS*" indicates the strain pET21-*pbgS*/pRSFDuet-*pttS*; "*pbgS-pttS-nukS*" indicates the pET21-*pbgS*/pRSFDuet-*pttS-nukS*. "No cell" indicates a reaction solution without cells, "pNZ7021" indicates the vector control strain, "*nukS*" indicates the strain pNZ7021-*nukS*, "*pbgS*" indicates the strain pNZ7021-*pbgS,* "*pttS*" indicates the strain pNZ7021-*pttS, "pttS-pbgS-nukS"* indicates the strain pNZ7021-*pttS-pbgS-nukS.* Error bars indicate 95 % CIs.

sinigrin to a similar extent as pNZ7021. However, the strains harboring only the *pttS* gene (pNZ7021-*pttS*) showed higher sinigrin-degradation activity. The strain harboring all three candidate genes (pNZ7021-*pttS-pbgS-nukS*) showed activity to a similar extent as did the strain pNZ7021-*pttS*.

Discussion

In this study, the author isolated *Lb. farciminis* KB1089, a GSL-degrading LAB that exhibited significant sinigrin-degrading activity. Since the *Lb. farciminis* KB1089 strain was isolated from a traditional Japanese food, it was considered safe as a component of food. It may also be applicable as a probiotic strain that confers GSL-degrading activity and ITC generation upon its hosts and thereby provides several beneficial health effects (17-21). A few strains of *Lb. farciminis* are known probiotic strains (22-25).

Comparative proteomic analysis of induced and non-induced cells of *Lb. farciminis* KB1089 led to identification of three proteins (*Lf*PttS, *Lf*PbgS, and *Lf*NukS), selected as candidate sinigrin degrading enzymes. *Lf*PttS and *Lf*PbgS appeared to be involved in sugar metabolism initiated by the PTS, a major pathway of sugar metabolism in bacteria (14). Based on the PTS-mediated pathway, the author hypothesized the existence of a sinigrin-degradation pathway in *Lb. farciminis*

KB1089 (Fig. 3B). In the hypothetical pathway, sinigrin is imported to the cytosol and its glucose moiety is phosphorylated by *Lf*PttS. The phosphate group may be transferred from phosphoenolpyruvate (PEP) via universal PTS components (EI and HPr) and a PTS sugar transporter (14) to sinigrin. Subsequently, the *S*-glycosidic bond of phosphorylated sinigrin is hydrolyzed by *Lf*PbgS and is followed by a non-enzymatic rearrangement and elimination of the sulfate group to yield AITC (26).

Functional analysis of candidate genes expressed in *E. coli* Rosetta 2(DE3) indicated sinigrin-degrading activity in the pET21-*pbgS*/pRSF-*pttS* and pET21-*pbgS*/pRSF-*pttS*-*nukS* strains. The host and the other transformed strains showed no such activity. Thus, *Lf*PttS and *Lf*PbgS are probably the enzymes that are responsible for sinigrin-degradation. The strain pET21-*pbgS*/pRSF-*pttS*-*nukS* showed GSL-degrading activity to a similar extent as did pET21-*pbgS*/pRSF-*pttS*. Thus, the function of the hypothetical protein (*Lf*NukS) remains to be elucidated. SDS-PAGE analysis could not detect any band corresponding to the expression product of *pttS* gene in the pET21-*pbgS*/pET28-*pttS* and pET21-*pbgS*/pRSF-*pttS*-*nukS* (Fig. S2). The low activities of sinigrin-degradation by the two strains may be due to the weak expression of *Lf*PttS or an inefficient relay of the phosphoryl group from the inherent PTS components (EI, HPr) to the exogenous PTS sugar transporter, *Lf*PttS.

InterPro analysis suggests that the PTS sugar transporter, a membrane bound complex, consists of three components (IIA, IIB, IIC), and enables the transfer of a phosphoryl group to sinigrin from soluble PTS components (EI, HPr). An appropriate arrangement of those components seemed to be important for a successful phosphoryl relay. Destruction of this arrangement by membrane disruption may have caused a loss of the sinigrin-degrading activity of cell-free extracts, as was observed in *Lb. farciminis* KB1089 in this study as well as in many other GSL-degrading bacteria (3,6,7,27).

*Lf*PbgS belongs to the GH1 family of proteins as well as to plant and aphid myrosinase (28) and 6-phospho-*β*-D-glucosidases (encoded in *bglA* and *ascB*) of *E. coli* O157:H7. Δ*bglA* and Δ*ascB* mutants showed decreased activity of sinigrin-degradation (29). The 6-phospho-*β*-D-glucosidases of *E. coli* O157:H7 have a high identity with *Lf*PbgS (Fig. S3). However, *Lf*PbgS has a low identity (< 20%) with a bacterial myrosinase from *Citrobacter* WYE1, which belongs to the GH3 family (30).

Functional analyses of candidate genes expressed in *Lc. lactis* NZ9000 and BLAST search indicated two genes encoding *Lf*PbgS homologues in *Lc. lactis* NZ9000. One homologue, which exists adjacent to a gene encoding a homologue of *Lf*PttS, is described in Fig. S3. The strain pNZ7021-*pttS* which expressed *Lf*PttS showed a notably higher

activity of sinigrin-degradation by compared with the slight sinigrin-degradation activity of the host strain. The expression of *Lf*PttS in *Lc. lactis* NZ9000 resulted in a significant increase of activity. However, the expression of *Lf*PbgS showed no effect on activity. These results are consistent with the putative pathway which assumes that sinigrin is degraded after transport into cells and undergoes simultaneous phosphorylation. The strain pNZ7021-*pttS*-*pbgS*-*nukS* showed sinigrin-degrading activity to a similar extent as did the strain pNZ7021-*pttS*. SDS-PAGE analysis could not detect any band corresponding to the expression products of *pbgS* and *nukS* genes in the strain pNZ7021-*pttS*-*pbgS*-*nukS* (Fig. S4). Thus, it appears that *pbgS* and *nukS* might not be expressed or might be only weakly expressed such that GSL-degrading activity is unaffected.

Furthermore, the author compared the glucosidase activity of *Lf*PbgS toward sinigrin and phosphorylated sinigrin in order to demonstrate the sinigrin-degradation pathway involving sinigrin phosphorylation. To this end, the author obtained phosphorylated sinigrin using *β*-glucoside kinase (BglK) from *K. pneumoniae* ATCC23357, the phosphorylation activity on the 6' carbon of few *β*-thioglucosides which has been reported (12) (Fig. S5). The author evaluated the sinigrin or phosphorylated sinigrin degradation activity using cell-free extracts of strains expressing *Lf*PbgS, *Lc. lactis* pNZ7021-*pbgS*. AITC production was detected in reactions only with phosphorylated sinigrin (Fig. S7). This was confirmation that *Lf*PbgS showed activity only toward phosphorylated sinigrin. The author thus concluded that the candidate genes (*pttS* and *pbgS*) encode a sinigrin-degrading enzyme system, as is summarized in Fig. 3B.

These results should be clue to understand unclear mechanisms of GSLs bioconversion by gut bacteria. The author found homologous gene clusters using BLAST search in gut bacterial metagenomic sequence data obtained by the Human Microbiome Project (31) (Fig. S8) and also found the gene clusters containing homologues of *pttS* and *pbgS* in genomes of other GSL-degrading bacteria (5-7) included the strains isolated from human feces (Fig. S3). For further understanding of GSL-metabolism in gut bacteria, a functional analysis of these homologous genes is currently underway. The conclusion from these results is that, to the best of the author's knowledge, this is the first study that has elucidated a novel GSL-degrading pathway in specific gut bacteria.

Table 1 Proteins expressed specifically in induced cells of *Lb. faciminis* KB1089.

GI number	Description	PSMs
497703868	membrane protein	28.50
497703951	copper-binding protein	50.62
497704178	hypothetical protein	238.86
497704179	NAD-dependent protein deacetylase	480.95
497704231	amino acid ABC transporter substrate-binding protein	25.72
497704455	hypothetical protein	37.71
497704462	phosphoglycerate mutase	92.68
497704588	cell surface glycerophosphoryl diester phosphodiesterase precursor	31.54
497704685	2,5-diketo-D-gluconic acid reductase	26.18
497704861	fructose-bisphosphate aldolase	22.70
497705001	dihydrodipicolinate synthase	95.96
497705162	dephospho-CoA kinase	21.97
497705186	amidase	24.95
497705218	putative ribosomal protein	36.66
497705412	PTS sugar transporter subunit IIB	38.92
497705415	PTS sugar transporter	25.30
497705416	aryl-phospho-β-D-glucosidase	106.94
497705417	hypothetical protein	419.72

Protein sequence GI numbers are shown in the left column. PSMs reflected approximately the amounts of proteins detected. The highlighted proteins indicate candidates for sinigrin degradation activity.

Table 1 Proteins expressed specifically in induced cells of *Lb. faciminis* KB1089 (continued).

GI number	Description	PSMs
497705600	DNA replication protein DnaD	29.86
497705688	ribonuclease HII	26.64
497705698	thymidylate synthase	119.15
497706403	transcriptional regulator	102.89
497706509	hypothetical protein	42.32
497706520	nucleotide-structuring protein H-NS	34.74
497706929	thiol-disulfide isomerase	28.65
497706931	hypothetical protein	38.63

Protein sequence GI numbers are shown in the left column. PSMs reflected approximately the amounts of proteins detected. The highlighted proteins indicate candidates for sinigrin degradation activity.

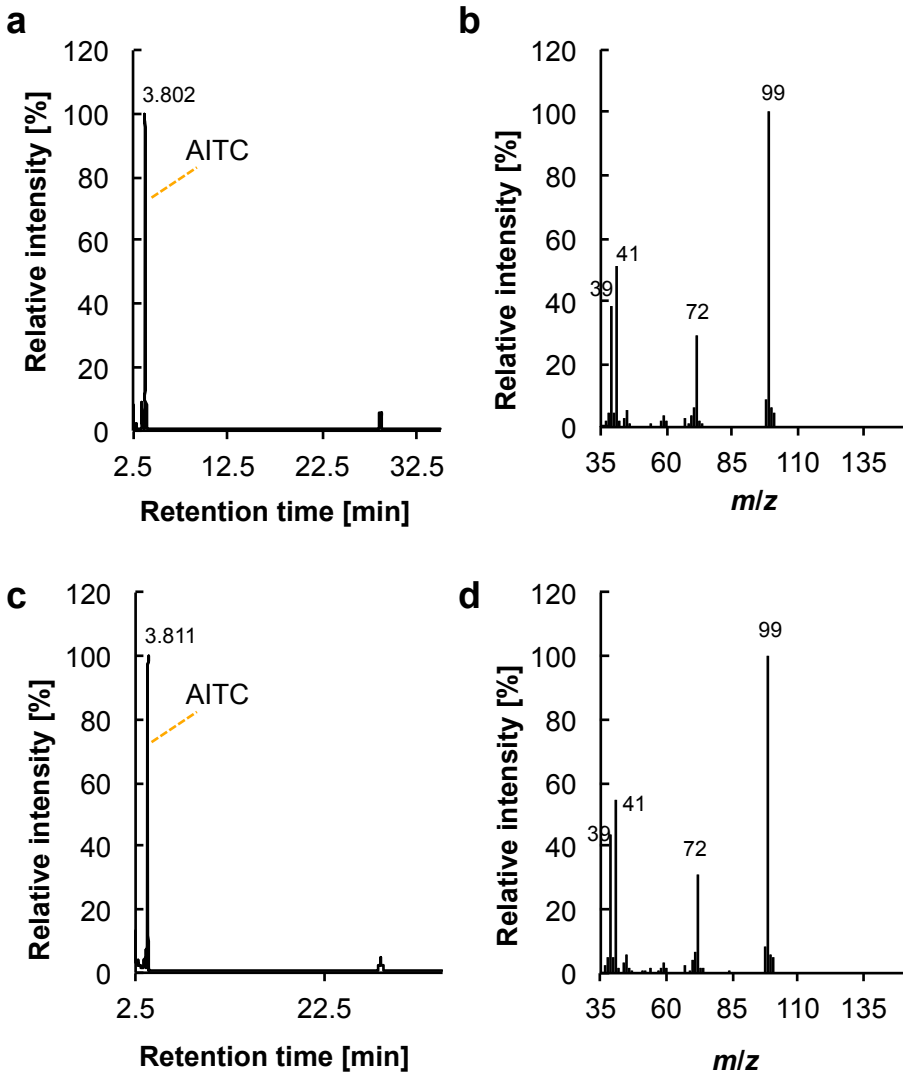

Fig. S1 GC-MS analysis of the sinigrin converted products by washed cells of *Lb. farciminis* KB1089. a, A GC-MS total ion current chromatogram of 3 mM AITC in 20 mM KPB (pH 6.5). **b**, The mass spectrum at the retention time 3.802 min in the GC-MS chromatogram **a**. **c**, A GC-MS total ion current chromatogram of the sinigrin converted products in the resting cell reaction using washed cells of *Lb. farciminis* KB1089. **d**, A mass spectrum at the retention time 3.811 min in the GC-MS chromatogram **c**.

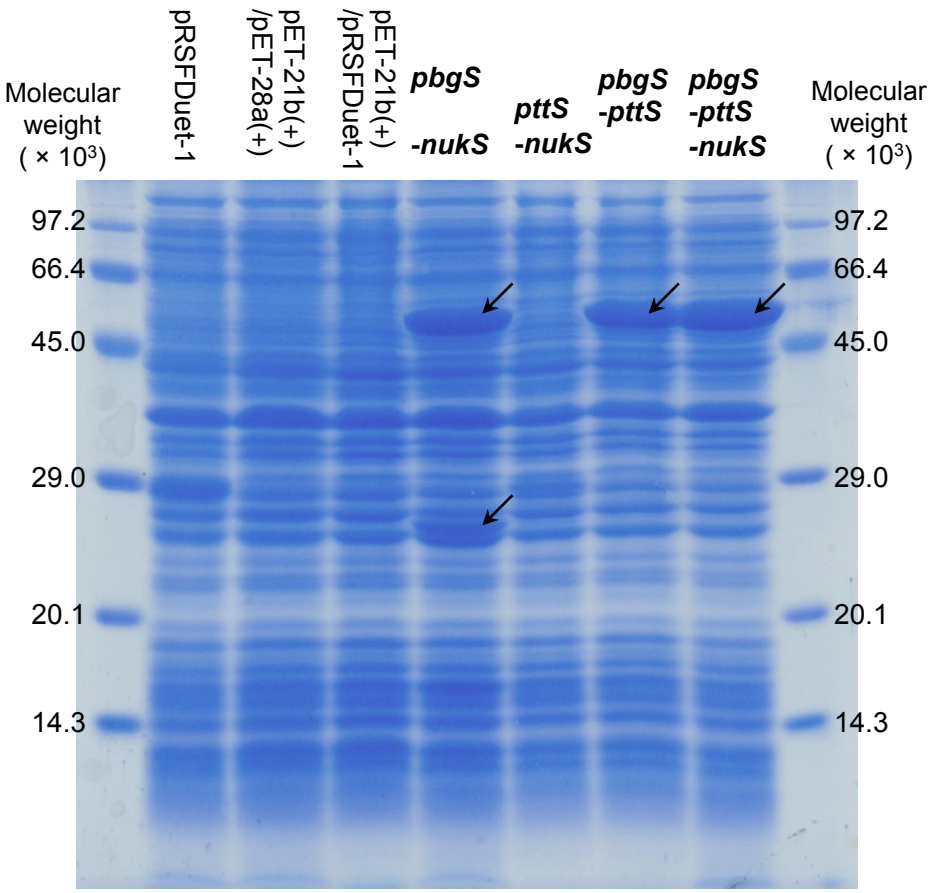

Fig. S2 SDS-PAGE analysis of cell lysates of transformed *E. coli* cells. The calculated molecular weights of *Lf*PttS, *Lf*PbgS, and *Lf*NukS were 67,200, 57,500, and 25,000, respectively. "*pbgS-nukS*" indicates the strain pET21-*pbgS*/pET28-*nukS*, "*pttS-nukS*" indicates the strain pRSF-*pttS-nukS*, "*pbgS-pttS*" indicates the strain pET21-*pbgS*/pRSF-*pttS*, and "*pbgS-pttS-nukS*" indicates the strain pET21-*pbgS*/pRSF-*pttS-nukS*. The allows indicate the expressed proteins.

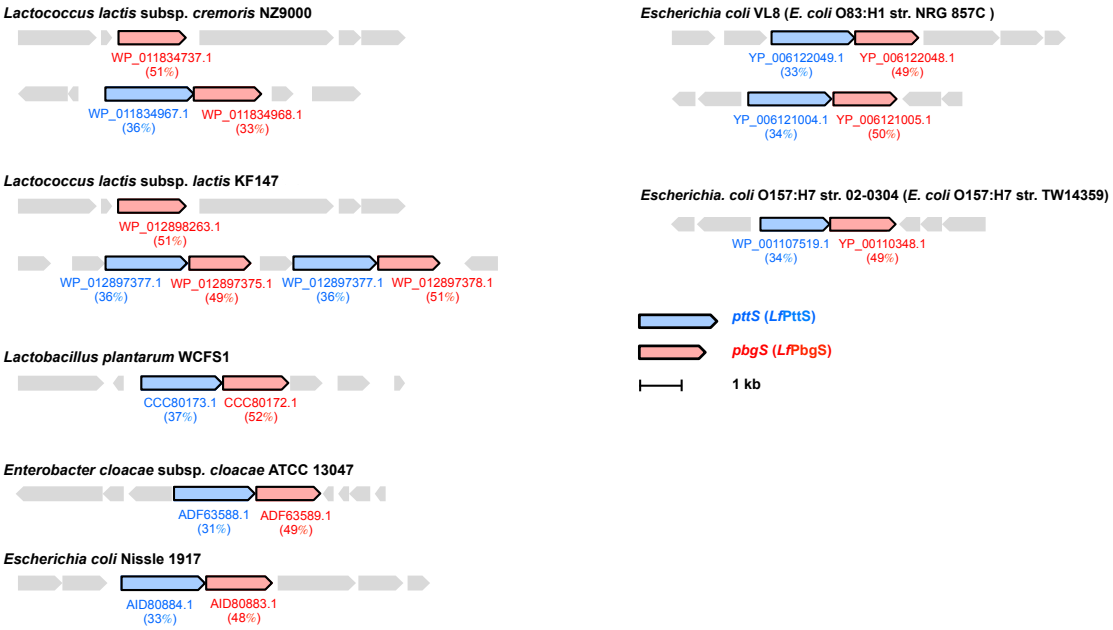

Fig. S3 Distribution of gene clusters containing *pttS* and *pbgS* homologues in GSL-degrading bacteria. Genes encoding homologues of *Lf*PttS and *Lf*PbgS are colored blue and red, respectively. The GenBank accession number assigned to each gene encoding a *Lf*PttS or *Lf*PbgS homologue and its sequence identity obtained by TBLASTN analysis is shown below its coding region. GSL-degrading activities of all bacteria listed above were confirmed in the present study or in previous studies (5−7). The strains shown in parenthesis were used as the genome reference in the previous study. The listed bacteria except for *Lc. lactis* and *E. coli* O157:H7 were isolated from human.

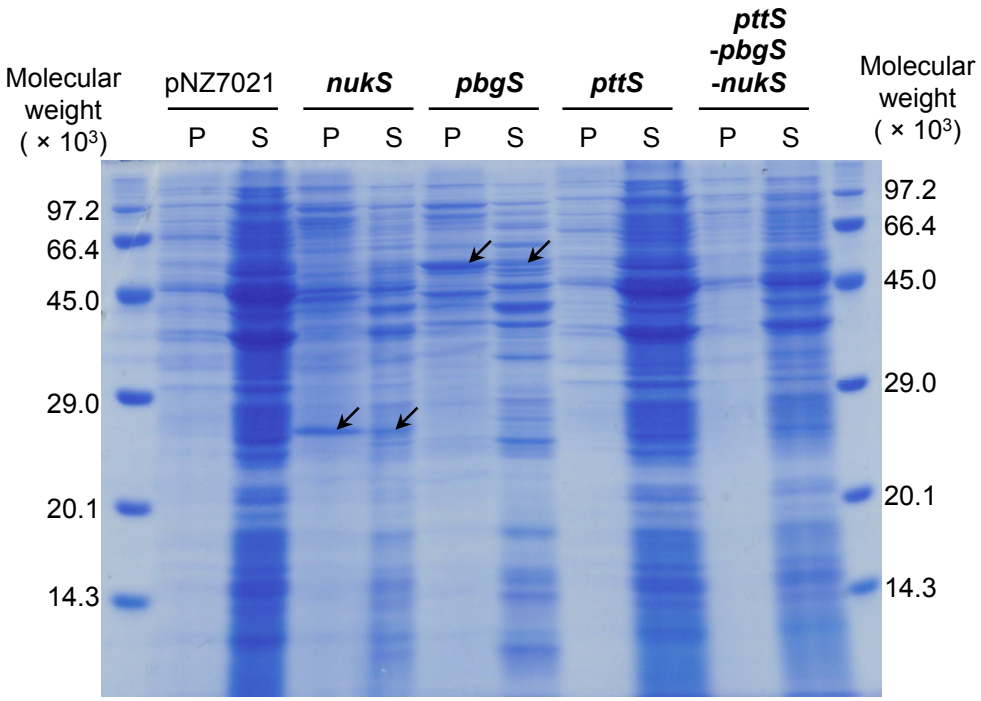

Fig. S4 SDS-PAGE analysis of cell lysate fractions of transformed *Lc. lactis*. The calculated molecular weights of *Lf*PttS, *Lf*PbgS, and *Lf*NukS were 67,200, 57,500, and 25,000, respectively. "pNZ7021" indicates the vector control strain, "*nukS*" indicates the strain pNZ7021-*nukS*, "*pbgS*" indicates the strain pNZ7021-*pbgS*, "*pttS*" indicates the strain pNZ7021-*pttS*, and *"pttS-pbgS-nukS"* indicates the strain pNZ7021-*pttS-pbgS-nukS*. Lane P and S indicate suspensions of the precipitates and supernatants, respectively, obtained after centrifugation of the cell lysate of each strain.

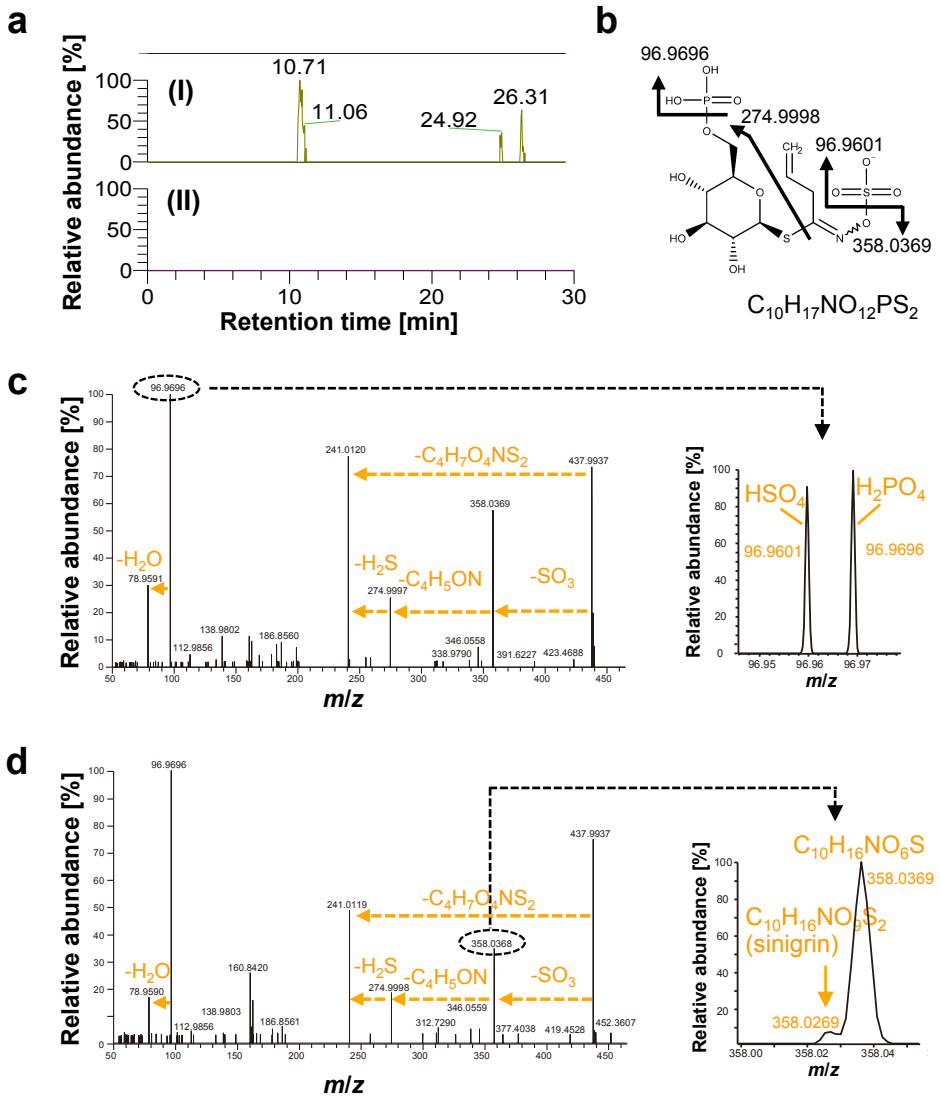

Fig. S6 HPIC-HRMS/MS analysis of sinigrin converted products (phosphorylated sinigrin) by cell-free extracts of *E. coli* pET28-*bglK*. a, HPIC-MS chromatograms at *m/z* 437.9935 of the sinigrin converted products by cell-free extracts of *E. coli* pET28-*bglK* (I) and the vector control strain, *E. coli* pET-28a(+) (II). **b**, Expected fragmentation patterns of sinigrin-6-phosphate as a representative of sinigrin monophosphate. **c**, HRMS/MS spectra at the retention time 24.92 min in HPIC-HRMS chromatograms **a**-(I). **d**, HRMS/MS spectra at the retention time 26.31 min in HPIC-HRMS chromatograms **a**-(I).

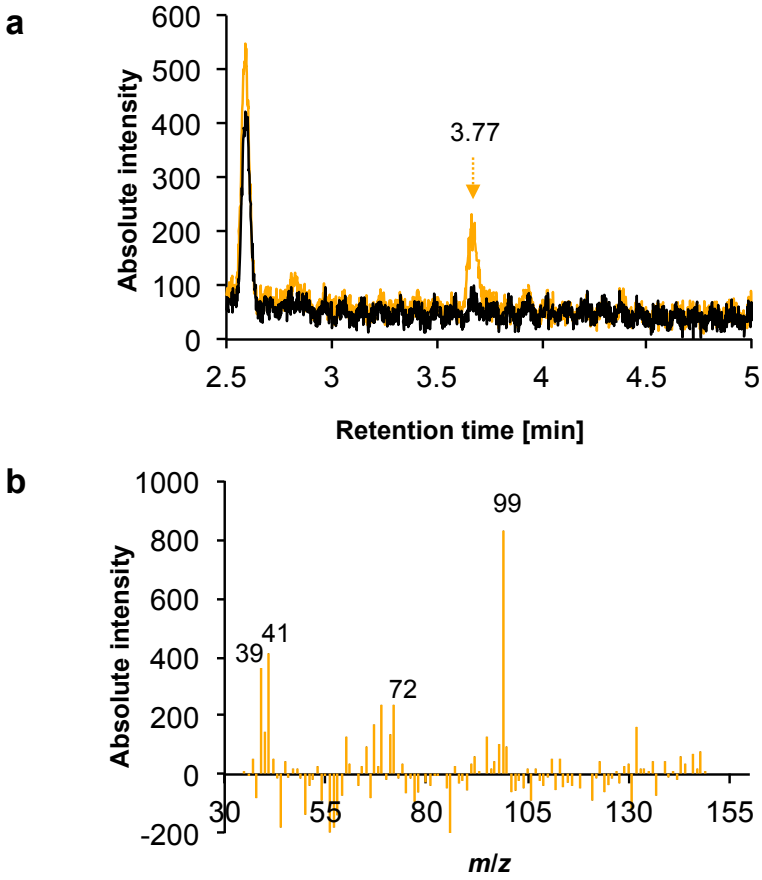

Fig. S7 GC-MS analysis of a sinigrin monophosphate converted product (AITC) by cell-free extracts of *Lc. lactis* pNZ7021-*pbgS*. a, GC-MS SIM chromatograms at *m/z* 99 of the reaction products by *Lc. lactis* pNZ7021-*pbgS* with the sinigrin converted products by cell-free extracts of *E. coli* pET28-*bglK* (yellow) and *E. coli* pET-28a(+) (black) as the reaction substrates. **b**, The difference mass spectrum at the retention time of 3.77 min obtained by subtracting the mass spectrum of the reaction products by *Lc. lactis* pNZ7021-*pbgS* with the sinigrin converted products by cell-free extracts of *E. coli* pET-28a(+) from the mass spectrum of the reaction products by *Lc. lactis* pNZ7021-*pbgS* with the sinigrin converted products by cell-free extracts of *E. coli* pET28-*bglK*. The molecular weight of AITC is 99.15.

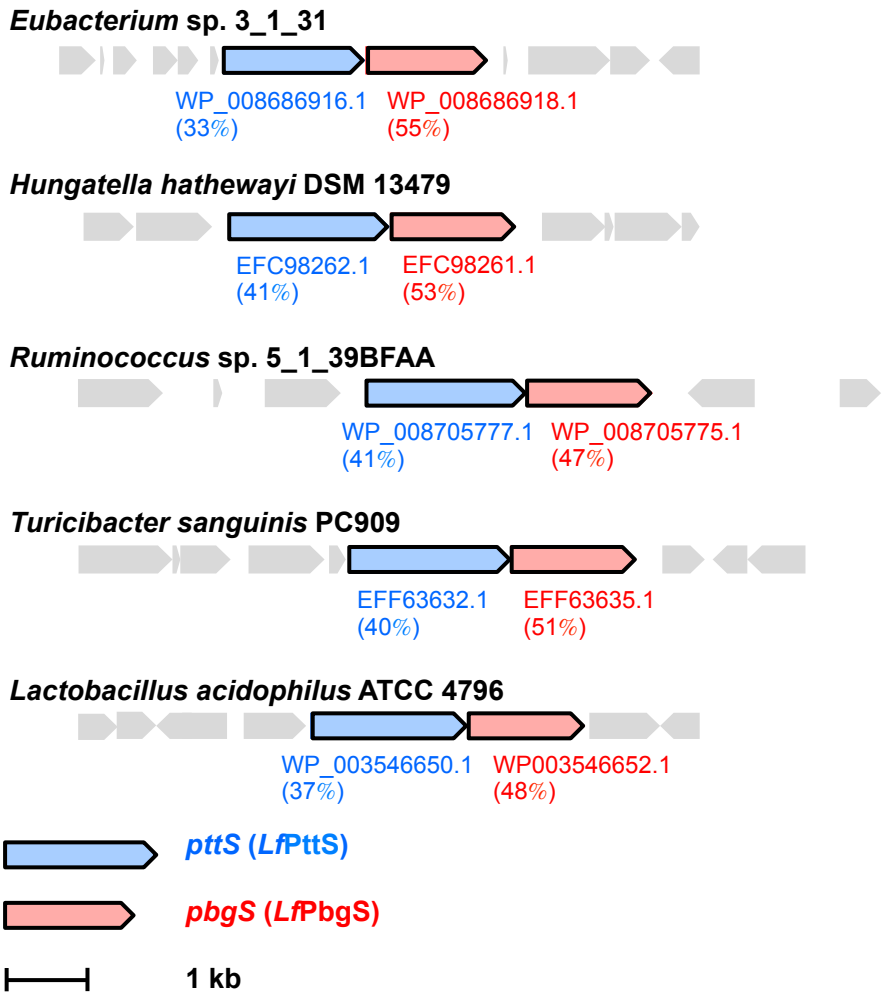

Fig. S8 Distribution of gene clusters containing *pttS* and *pbgS* homologues in gut bacteria. Genes encoding homologues of *Lf*PttS and *Lf*PbgS are colored blue and red, respectively. The GenBank accession number assigned to each gene encoding a *Lf*PttS or *Lf*PbgS homologue and its sequence identity obtained by TBLASTN analysis is shown below its coding region. All bacteria listed above are gut bacteria whose genomic sequences were obtained by metagenomic sequencing of gut microbiome in the Human Microbiome Project (31).

Table S1 Bacterial strains used in this study

Strain	Description	Source or reference
Lb. farciminis KB1089	Isolated from pickled suguki turnips	This study
Lb. farciminis KCTC3681 (= JCM1092 = DSM20184)	Able to metabolize sinigrin	JCM
Lb. farciminis LMG9200 (= DSM20184)	Able to metabolize sinigrin	LMG
Lb. farciminis NRIC0417	Able to metabolize sinigrin	NRIC
Lb. farciminis LMG9189	Unable to metabolize sinigrin	LMG
Lb. farciminis NRIC0416	Unable to metabolize sinigrin	NRIC
E. coli DH5α	Commercial transformation host for all plasmids except for pNZ7021 series	TOYOBO Co., Ltd.
E. coli MC1061	Commercial transformation host for pNZ7021 series	MoBiTec Co., Ltd.
E. coli Rosetta 2(DE3)	Commercial expression host	Novagen®
E. coli pET-28a(+)	*E. coli* Rosetta 2(DE3) harboring pET-28a(+)	This study
E. coli pET-21b(+)/pET-28a(+)	*E. coli* Rosetta 2(DE3) harboring pET-21b(+) and pET-28a(+)	This study
E. coli pRSFDuet-1	*E. coli* Rosetta 2(DE3) harboring pRSFDuet-1	This study
E. coli pET-21b(+)/pRSFDuet-1	*E. coli* Rosetta 2(DE3) harboring pET-21b(+) and pRSFDuet-1	This study
E. coli pET28-*nukS*	*E. coli* Rosetta 2(DE3) harboring pET-*nukS*	This study
E. coli pET28-*pbgS*	*E. coli* Rosetta 2(DE3) harboring pET-*pbgS*	This study
E. coli pET28-*pttS*	*E. coli* Rosetta 2(DE3) harboring pET-*pttS*	This study

Table S1 Bacterial strains used in this study (continued)

Strain	Description	Source or reference
E. coli pRSF-*pttS-nukS*	*E. coli* Rosetta 2(DE3) harboring pRSF-*pttS-nukS*	This study
E. coli pET21-*pbgS*/pET28-*nukS*	*E. coli* Rosetta 2(DE3) harboring pET-*pbgS* and pET-*nukS*	This study
E. coli pET21-*pbgS*/pRSF-*pttS*	*E. coli* Rosetta 2(DE3) harboring pET-*pbgS* and pRSF-*pttS*	This study
E. coli pET21-*pbgS*/pRSF-*pttS-nukS*	*E. coli* Rosetta 2(DE3) harboring pET-*pbgS* and pRSF-*pttS-nukS*	This study
E. coli pET28-*bglK*	*E. coli* Rosetta2(DE3) harboring pET-*bglK*	This study
Lc. lactis NZ9000	Derivative of *Lc. lactis* subsp. *cremoris* MG1363, *pepN*::*nisRK*	MobiTec Co., Ltd.
Lc. lactis pNZ7021	*Lc. lactis* harboring pNZ7021	This study
Lc. lacits pNZ7021-*nukS*	*Lc. lactis* harboring pNZ7021-*nukS*	This study
Lc. lacits pNZ7021-*pbgS*	*Lc. lactis* harboring pNZ7021-*pbgS*	This study
Lc. lactis pNZ7021-*pttS*	*Lc. lactis* harboring pNZ7021-*pttS*	This study
Lc. lacits pNZ7021-*pttS-pbgS-nukS*	*Lc. lactis* harboring pNZ7021-*pttS-pbgS-nukS*	This study

Table S2 Plasmids used in this study

Plasmid	Description	Source
pET-28a(+)	Kan^{K}, T7 promoter, pBR322ori, expression vector	Novagen
pET-21b(+)	Amp^{K}, T7 promoter, pBR322ori, expression vector	Novagen
pRSFDuet-1	Kan^{K}, T7 promoter, RSFori, co-expression vector	Novagen
pET28-*nukS*	Derivative of pET-28a(+) in which *nukS* gene was cloned in SalI and NotI sites	This study
pET28-*pbgS*	Derivative of pET-28a(+) in which *pbgS* gene was cloned in SalI and NotI sites	This study
pET28-*pttS*	Derivative of pET-28a(+) in which *pttS* gene was cloned in SalI and NotI sites	This study
pET28-*bglK*	Derivative of pET-28a(+) in which *bglK* gene encoding *β*-glucoside kinase (AAK58463.1) was cloned in SalI and NotI sites	This study
pET21-*pbgS*	Derivative of pET-21b(+) in which *pbgS* gene was cloned in SalI and NotI sites	This study
pRSF-*pttS*	Derivative of pRSFDuet-1 in which *pttS* gene was cloned in SalI and NotI sites	This study
pRSF-*pttS*-*nukS*	Derivative of pRSF-*pttS* in which *nukS* gene was cloned in BglII and XhoI sites	This study

Table S2 Plasmids used in this study (continued)

Plasmid	Description	Source
pNZ7021	Cm^{K}, P_{pepN} promoter (constitutive promoter), *repC*, *repA*, expression vector for LAB	MobiTec Co., Ltd.
pNZ7021-*nukS*	Derivaive of pNZ7021 in which *nukS* gene was cloned in SpeI and HindIII sites	This study
pNZ7021-*pbgS*	Derivative of pNZ7021 in which *pbgS* gene was cloned in SpeI and HindIII sites	This study
pNZ7021-*pttS*	Derivative of pNZ7021 in which *pttS* gene was cloned in SpeI and HindIII sites	This study
pNZ7021 -*pttS*-*pbgS*-*nukS*	Derivative of pNZ7021 in which *pttS*, *pbgS*, and *nukS* genes were tandemly cloned in SpeI and HindIII sites	This study

Table S3 Oligonucleotides used in this chapter

Oligonucleotide	Sequence (5' to 3')
27F	AGAGTTTGATCCTGGCTCAG
1525R	AAGGAGGTGATCCAGCC
516F	TGCCAGCAGCCGCGGTA
1087F	GGTTAAGTCCCGCAACGA
531R	TACCGCGGCTGCTGGCA
1104R	TCGTTGCGGGACTTAACC
518R	GTATTACCGCGGCTGCTGG
pheS-21F	CCGCAGCCAA
pheS-22R	AGGTGACCGT
oET-*nukS*-Fw	CCGGTCGACATGAGTAATATAACATTAGTTAACAGTGAA
oET-*nukS*-Rv	CCGAGATCTATGAGTAATATAACATTAGTT
oET-*pbgS*-Fw	CCGGTCGACATGAAATTTCCAAAGAACTTTTTATGGGGC
oET-*pbgS*-Rv	TTCGCGGCCGCTCATTTTACATATGCTCCTTGCAATTCAT T
oET-*pttS*-Fw	CCGGTCGACATGAGTAAAAATCAGCTCGCAAAATTAATT
oET-*pttS*-Rv	TTCGCGGCCGCTCAGGCAATGTTCAATAATGAATCGCCA AC
oRSF-*nukS*-Fw	TTCGCGGCCGCTCAATCACGTTCAACATCTCCGTAACGG CC
oRSF-*nukS*-Rv	TTCCTCGAGTCAATCACGTTCAACATCTCC
oNZ-*nukS*-Fw	CCGACTAGTGGACGTGGAACTGGAAATAG
oNZ-*nukS*-Rv	TTCAAGCTTTCAATCACGTTCAACATCTC
oNZ-*pbgS*-Fw	CCGACTAGTAGTCACAAATAGTAATGAT
oNZ-*pbgS*-Rv	CCGACTAGTAGTCACAAATAGTAATGAT
oNZ-*pttS*-Fw	CCGACTAGTTGAGATGTTGCTGCAACAC
oNZ-*pttS*-Rv	TTCAAGCTTTCAGGCAATGTTCAATAATG

The underlined sequence represents restriction sites.

Table S3 Oligonucleotides used in this chapter (continued)

Oligonucleotide	Sequence (5' to 3')
T7-promoter	TAATACGACTCACTATAGGG
T7-terminator	ATGCTAGTTATTGCTCAGCGG
ACYCDuetUP-1	GGATCTCGACGCTCTCCCT
pNZ7021-Fw	AGATCTGTCGACCTGCAGTA
pNZ7021-Rv	TCAACTGCTGCTTTTTGGCT

Table S4 Chemical reagents and metals added to the cell-free extracts reaction mixtures of *Lb. farciminis* KB1089.

LiCl	$MnSO_4$	ATP + $MgCl_2$	Hydrazine-HCl
NaCl	$FeCl_3$	ADP	Nitlirotriacetic acid
KCl	$AlCl_3$	NADH	Guanizine-HCl
CsCl	$CrCl_3$	NAD·	GEDTA
RbCl	$[Co(NH_3)_6]Cl_3$	NADPH	Iodoacetamide
$AgNO_3$	$Ce(SO_4)_2$	NADP·	2-Mercapt ethanol
$CaCl_2$	H_3BO_4	FAD	*N*-Ethylmaleimide (NEM)
BaCl2	$NiCl_2$	Aluminon	*N*-Bromosuccin imide
$MnCl_2$	NaF	α,α'-Bipyridyl	*p*-Choloromercuribenzoate (PCMB)
$BeSO_4$	NaN_3	8-Hydroxyquinoline	Phenylmethylsulfonyl fluoride (PMSF)
$CdCl_2$	Merthiolate·Na	2-Phenanthroline	L-Ascorbic acid
$MgCl_2$	$NaAsO_2$	Quinalizarin	Protease inhibitor cocktail (100 ×)
$CoCl_2$	KCN	EDTA · 2Na	
$HgCl_2$	NaSCN	Quinacrine	
$FeSO_4$	$NaIO_4$	Thiourea	
$ZnSO_4$	NH_4VO_3	Trypaflavine	
$CuSO_4$	Cacodylate·Na	Semicarbazide	
$SnCl_2$	H_2PtCl_6	Dinitrophend	
$(AcO)_2Hg$	$Ba(SCN)_2$	NH_2OH-HCl	
$PbCl_2$	NH_4Cl	2,4-Quinolinediol	
$Pb(NO_3)_2$	$Na_2S_2O_3$	Aminoguanizine Sulfate	
$SrCl_2$	Na_2SeO_4	3-Amino-1,2,4-triazole	
$Ce(SO_4)_2$	Na_2MoO_4	Fluoroacetate · Na	
$ZrCl_2O$	$NaWO_4$	2,3,5-Triphenyltetrazonium Chloride	

Concentrations of the reagents in the reaction mixtures were 1.0 mM for merthiolate·Na, H_2PsCl_6, and PCMB; 5.0 mM for quinalizarin, quinacrine, trypaflavine, 2-4-quinolinediol and 3-amino-1,2,4-triazole; 10 μL mL^{-1} for protease inhibitor cocktail (100 ×) (Nacalai tesque, Inc., Kyoto, Japan); 10 mM for the other mixtures, respectively.

Table S5 Protein stabilization reagents added to cell-free extracts reaction mixtures of *Lb. farciminis* KB1089.

0.50, 1.0, or 2.0 % (v/v)	glycerol
0.50, 1.0, or 2.0 % (v/v)	ethylenglycol
1.0 % (w/v)	glucose
1.0 % (w/v)	sucrose
1.0 % (w/v)	sorbitol
1.0 % (w/v)	trehalose
0.50 or 1.0 % (v/v)	ethanol
0.50 or 1.0 % (v/v)	acetone

Final concentrations of reagents used in reaction mixtures are described in this table.

Table S6 The accession numbers of draft genome sequence contigs deposited in International Nucleotide Sequences Database Collaborators (INSDC)

Strain	Accession numbers	Contigs	INSDC
Lb. farciminis KB1089	BHYW01000001-BHYW01000067	67	DDBJ
Lb. farciminis LMG9189	BHYX01000001-BHYX01000067	67	DDBJ
Lb. farciminis NRIC0416	BHYY01000001-BHYY01000112	112	DDBJ
Lb. farciminis NRIC0417	BHYZ01000001-BHYZ01000166	166	DDBJ

Table S7 Proteins expected to be expressed in each transformed *E. coli* strain and sinigrin-degrading activity of each strain.

Strain	Protein expected to express			Activity
	*Lf*PttS	*Lf*PbgS	*Lf*NukS	
E. coli pET-28a(+)	-	-	-	n. d.
E. coli pET-21b(+)/pET-28a(+)	-	-	-	n. d.
E. coli pRSFDuet-1	-	-	-	n. d.
E. coli pET-21b(+)/pRSFDuet-1	-	-	-	n. d.
E. coli pET28-*nukS*	-	-	√	n. d.
E. coli pET28-*pbgS*	-	√	-	n. d.
E. coli pET28-*pttS*	√	-	-	n. d.
E. coli pET21-*pbgS*/pET28-*nukS*	-	√	√	n. d.
E. coli pRSF-*pttS-nukS*	√	-	√	n. d.
E. coli pET21-*pbgS*/pRSF-*pttS*	√	√	-	+
E. coli pET21-*pbgS* /pRSF-*pttS-nukS*	√	√	√	+

n. d., not etected.

SUMMARY

Cruciferous vegetables such as broccoli are known to be providers of ITCs. ITCs are bioactive phytochemicals and raised from non-bioactive thioglucosides, glucosinolate (GSLs) contained in these cruciferous vegetables via hydrolysis of the *S*-glycosidic linkage by bacteria present in human gut. However, the detail mechanisms of the conversion of GSLs by gut bacteria have been unknown. In this study, the author show a novel enzyme system involved in GSL-metabolism in lactic acid bacteria, a kind of gut bacteria. *Lb. farciminis* KB1089 exhibited a notable activity of sinigrin (non-bioactive) degradation and generated AITC (bioactive). The author's physiological observation revealed the induction mechanisms of the enzyme system under the specific condition. Then, the author performed comparative proteomics analysis between induced and non-induced cells, and found two enzymes (PTS sugar transporter and aryl-phospho-β-D-glucosidase) responsible for the sinigrin degrading activity. As a result, the author illustrates a GSL-metabolizing pathway involving PTS and phosphorylated GSL hydrolyzing enzyme in gut lactic acid bacteria. This new concept should aid in further understanding relationships between food factors and gut bacteria and open new application of probiotics development.

REFERENCES

1. **Ohtsuru, M., Hata, T.:** Studies on the activation mechanism of the myrosinase by L-ascorbic acid, Agric Biol Chem., **37**(8), 1971−1972 (1973).
2. **Tani, N., Ohtsuru, M., Hata, T.:** Isolation of myrosinase producing microorganisms, Agric. Biol. Chem., **38**(9), 1617−1622 (1974).
3. **Elfoul, L., Rabot, S., Khelifa, N., Quinsac, A., Duguay, A., Rimbault, A.:** Formation of allyl isothiocyanate from sinigrin in the digestive tract of rats monoassociated with a human colonic strain of *Bacteroides thetaiotaomicron*, FEMS Microbiol. Lett., **197**(1), 99−103 (2001).
4. **Cheng, D., Hashimoto, K., Uda, Y.:** In vitro digestion of sinigrin and glucotropaeolin by single strains of *Bifidobacterium* and identification of the digestive products, Food Chem. Toxicol., **42**(3), 351−357 (2004).
5. **Luciano, F. B., Belland, J., Holley, R. A.:** Microbial and chemical origins of the bactericidal activity of thermally treated yellow mustard powder toward *Escherichia coli* O157:H7 during dry sausage ripening, Int. J. Food Microbiol., **145**(1), 69−76 (2011).
6. **Mullaney, J. A., Kelly, W. J., McGhie, T. K., Ansell, J., Heyes, J. A.:** Lactic acid bacteria convert glucosinolates to nitriles efficiently yet differently from enterobacteriaceae, J. Agric. Food Chem., **61**(12), 3039−3046 (2013).
7. **Luang-In, V., Narbad, A., Nueno-Palop, C., Mithen, R., Bennett, M., Rossiter, J. T.:** The metabolism of methylsulfinylalkyl- and methylthioalkyl-glucosinolates by a selection of human gut bacteria, Mol. Nutr. Food Res., **58**(4), 875−883(2014).
8. **Scheirlinck, I., Van der Meulen, R., Van Schoor, A., Huys, G., Vandamme, P., De Vuyst, L., Vancanneyt, M.:** *Lactobacillus crustorum* sp. nov., isolated from two traditional Belgian wheat sourdoughs, Int. J. Syst. Evol. Microbiol., **57**, 1461-1467 (2007).
9. **Morisaka, H., Matsui, K., Tatsukami, Y., Kuroda, K., Miyake, H., Tamaru, Y., Ueda, M.:** Profile of native cellulosomal proteins of *Clostridium cellulovorans* adapted to various carbon sources, AMB Express, **2**(1), 37 (2012).
10. **Bernardeau, M., Gueguen, M., Smith, D. G., Corona-Barrera, E., Vernoux, J. P.:** In vitro antagonistic activities of *Lactobacillus* spp. against *Brachyspira hyodysenteriae* and *Brachyspira pilosicoli*, Vet. Microbiol., **138**(1−2), 184−190 (2009).
11. **Inoue, H., Nojima, H., Okayama, H.:** High efficiency transformation of *Escherichia coli* with plasmids, Gene, **96**(1), 23-28 (1990).

12. **Thompson, J., Lichtenthaler, F. W., Peters, S., Pikis, A.:** β-glucoside kinase (BglK) from *Klebsiella pneumoniae*. Purification, properties, and preparative synthesis of 6-phospho-β-D-glucosides, J. Biol. Chem., **277**(37), 34310−34321 (2002)
13. **Okuda, S., Watanabe, Y., Moriya, Y., Kawano, S., Yamamoto, T., Matsumoto, M., Takami, T., Kobayashi, D., Araki, N., Yoshizawa, A. C., Tabata, T., Sugiyama, N., Goto, S., Ishihama, Y.:** jPOSTrepo: an international standard data repository for proteomes, **Nucl. Acid Res.**, **45**(D1), D1107-D1111 (2017).
14. **Postma, P. W., Lengeler, J. W., Jacobson, G. R.:** Phosphoenolpyruvate:carbohydrate phosphotransferase systems of bacteria, Microbiol. Rev., **57**(3), 543−594 (1993).
15. **Henrissat, B., Davis, G.:** Structural and sequence-based classification of glycoside hydrolases, Curr. Opin. Struct. Biol., **7**(5), 637−644 (1997).
16. **Saraste, M., Sibbald, P. R., Wittinghofer, A.:** The P-loop − a common motif in ATP- and GTP-binding proteins, Trends Biochem. Sci., **15**(11), 430−434 (1990).
17. **Zhang, Y., Talalay, P., Cho, C. G., Posner, G. H.:** A major inducer of anticarcinogenic protective enzymes from broccoli: isolation and elucidation of structure, Proc. Natl. Acad. Sci. USA, **89**(6), 2399−2403 (1992).
18. **Higdon, J. V., Delage, B., Williams, D. E., Dashwood, R. H.:** Cruciferous vegetables and human cancer risk: epidemiologic evidence and mechanistic basis, Pharmacol. Res., **55**(3), 224−236 (2007).
19. **Gross-Steinmeyer, K., Stapleton, P. L., Tracy, J. H., Bammler, T. K., Strom, S. C., Eaton, D. L.:** Sulforaphane- and phenethyl isothiocyanate-induced inhibition of aflatoxin B1-mediated genotoxicity in human hepatocytes: Role of GSTM1 genotype and CYP3A4 gene expression, Toxicol. Sci., **116**(2), 422−432 (2010).
20. **Ahn, Y. H., Hwang, Y., Liu, H., Wang, X. J., Zhang, Y., Stephenson, K. K., Boronina, T. N., Cole, R. N., Dinkova-Kostova, A. T., Talalay, P., Cole, P. A.:** Electrophilic tuning of the chemoprotective natural product sulforaphane. Proc. Natl. Acad. Sci. USA, **107**(21), 9590-9595 (2010).
21. **Elbarbry. F., Elrody, N.:** Potential health benefits of sulforaphane: a review of the experimental, clinical and epidemiological evidences and underlying mechanisms, J. Med. Plants Res., **5**(4), 473−484 (2011).
22. **Bernardeau, M., Gueguen, M., Smith, D. G., Corona-Barrera, E., Vernoux, J. P.:** In vitro antagonistic activities of *Lactobacillus* spp. against *Brachyspira hyodysenteriae* and *Brachyspira pilosicoli*, Vet. Microbiol., **138**(1−2), 184−190 (2009).
23. **Bernardeau, M., Vernoux, J. P., Gueguen, M.:** Probiotic properties of two *Lactobacillus* strains

in vitro, Milchwissenschaft, **56**(12), 663−667 (2001).

24. **Tareb, R., Bernardeau, M., Gueguen, M., Vernoux, J. P.:** In vitro characterization of aggregation and adhesion properties of viable and heat-killed forms of two probiotic *Lactobacillus* strains and interaction with foodborne zoonotic bacteria, especially *Campylobacter jejuni*, J. Med. Microbiol., **62**(Pt 4), 637−649 (2013).
25. **Ait-belgnaoui, A., Eutamene, H., Houdeau, E., Bueno, L., Fioramonti, J., Theodorou, V.:** *Lactobacillus farciminis* treatment attenuates stress-induced overexpression of Fos protein in spinal and supraspinal sites after colorectal distension in rats, Neurogastroenterol, Motil., **21**(5), 567−573, e18−19 (2009).
26. **Ettlinger, M. G., Lundeen, A. J.:** The structures of sinigrin and sinalbin; an enzymatic rearrangement, J. Am. Chem. Soc., **78**(16), 4172−4173 (1956).
27. **Llanos-Palop, M., Smiths, J. P., Brink, B. T.:** Degradation of sinigrin by *Lactobacillus agilis* strain R16, Int. J. Food Microbiol., **26**(2), 219−229 (1995).
28. **Jones, A. M., Winge, P., Bones, A. M., Cole, R., Rossiter, J. T.:** Characterization and evolution of a myrosinase from the cabbage aphid Brevicoryne brassicae, Insect. Biochem. Mol. Biol., **32**(3):275−284 (2002).
29. **Cordeiro, R. P., Doria, J. H., Zhanel, G. G., Sparling, R., Holley, R. A.:** Role of glycoside hydrolase genes in sinigrin degradation by *E. coli* O157: H7, Int. J. Food Microbiol., **205**, 105−111 (2015).
30. **Albaser, A., Kazana, E., Bennett, M., Cebeci, F., Luang-In, V., Spanu, P., Rossiter, J.:** Discovery of a bacterial glycoside hydrolase family 3 (GH3) β-glucosidase with myrosinase activity from a *Citrobacter* strain isolated from soil, **64**(7), 1520-1527 (2016).
31. **NIH HMP Working Group, Peterson, J., Garges, S., Giovanni, M., McInnes, P., Wang, L., Schloss, J. A., Bonazzi, V., McEwen, J. E., Wetterstrand, K. A., Deal, C., Baker, C. C., DiFrancesco, V., Howcroft, T. K., Karp, R. W., Lunsford, R. D., Wellington, C. R., Belachew, T., Wright, M., Giblin, C., David, H., Mills, M., Salomon, R., Mullins, C., Akolkar, B., Begg, L., Davis, C., Grandison, L., Humble, M., Khalsa, J., Little, A. R., Peavy, H., Pontzer, C., Portnoy, M., Sayre, M. H., Starke-Reed, P., Zakhari, S., Read, J., Watson, B., Guyer, M.:** The NIH Human Microbiome Project, Genome Res., **19**(12), 2317-2323 (2009).

CONCLUSION

In this study, the author discussed on gut bacterial metabolisms of food-derived compounds, playing significant roles on producing bioactive phytochemicals useful for human health. To date, enzymes and detailed mechanisms of ellagic acid and GSLs metabolisms to bioactive urolithin and ITCs, respectively, by gut bacteria have been remained unknown.

In Chapter I, the author analyzed ellagic acid metabolism in *G. urolithinfaciens* DSM 27213 from the aspects of chemical conversion and protein expression. As a result, activity of ellagic acid transformation to urolithin M5, urolithin M6, and urolithin C was found to be induced by ellagic acid or urolithin M5. A comparative proteome analysis between induced and non-induced cells showed that a gene cluster which containing notable genes, namely, *uroA1*, *uroA2*, *uroA3*, *uroH*, *uroB1*, *uroB2*, and *uroB3*, upregulated specifically in the induced cells which were grown in ellagic acid-added medium. Further analysis let the author identify a novel enzyme UroH as an ellagic acid lactonase, catalyzing ellagic acid conversion to urolithin M5. Moreover, through enzyme purification, the author showed that UroA1,A2 and UroB1,B2 were probably involved in urolithin dehydroxylation.

In Chapter II, the author investigated sinigrin metabolism in *Lb. farciminis* KB1089 as a model GSLs metabolizer from the aspects of chemical conversion and protein expression. As a result, the author identified two proteins (PTS sugar transporter and aryl-phospho-β-D-glucosidase) for the sinigrin degrading activity and illustrated a novel GSL-metabolizing pathway involving PTS and phosphorylated GSL hydrolyzing enzyme in gut lactic acid bacteria.

In conclusion, the author identified novel enzyme systems involved in ellagic acid and urolithin metabolism in *G. urolithinfaciens* DSM 27213 and GSLs metabolism in *Lb. farciminis* KB1089.

AKNOWLEDGEMENTS

The present study is based on the studies carried out from 2015 to 2020 at the laboratory of Fermentation Physiology and Applied Microbiology, Division of Applied Life Sciences, Graduate School of Agriculture, Kyoto University.

The author wished to express her deepest gratitude to Professor Jun Ogawa of Kyoto University, for his continuous guidance, invaluable supports, and warm encouragement during the course of this study.

The author's sincere thank to Professor Kenji Kano and Professor Tatsuo Kurihara from Kyoto University, for their constructive suggestions and thoughtful guidance.

The author greatly appreciates to Associated Professor Shigenobu Kishino for his kindly instruction in experimental techniques and direction of this study, constructive comments, and continuous encouragements. Valuable discussions and his constructive criticisms in the manuscripts strongly encouraged the author in her studies.

The author wishes to express her deep thanks to Emeritus Professor Sakayu Shimizu, Emeritus Professor Satomi Takahashi, Professor Makoto Ueda, Associated Professor Makoto Hibi, Associated Professor Ryotaro Hara, Assistant Professor Akinori Ando, and Assistant Professor Michiki Takeuchi, for their warm supports, encouragements, and valuable advice during the course of this study.

The author also wishes to thank Dr. Hiroaki Yamamoto, Dr. Masatake Kudo, Mr. Shunsuke Ishiwa, Dr. Motoko Hayashi, and Dr. Takanori Nakajima, DAICEL Corporation, for their helpful suggestions and technical supports.

The author is thankful to Assistant Professor Wataru Aoki and Dr. ShunsukeAburaya, Laboratory of Biomacromolecular Chemistry, Division of Applied Life Sciences, Graduate School of Agriculture, Kyoto University.

The author also wishes to thank Mr. Yudai Aoki and Dr. Hiroyuki Suganuma, Innovation Division, KAGOME CO., Ltd. for their helpful suggestions and technical supports.

The author is also grateful to Dr. Si-Bum Park, Dr. Hideaki Nagano, Dr. Yoshimi Shimada, Dr. Natsumi Okada, Dr. Nirdnoy Warawadee, Mr. Yuta Sugiyama, Dr. Akiko Hirata, Dr. Tomoyu Okuda, Ms. Nahoko Kitamura, and Ms. Atsuko Kitamura for their kind instruction in experimental techniques, helpful advice, constructive suggestion, constant encouragement, unquestionable helps and hearty personalities throughout this work.

The author greatly appreciated to Ms. Miho Tani, Mr. Kosuke Fujii, Mr. Kengo Osada, Mr. Ryota Nakatsuji, Ms. Azusa Saika, Mr. Riku Usami, Mr. Yuki Shimura, Ms. Chihiro Kenchu, Mr.

Kazuki Saito, Mr. Tasuku Kitamoto, Ms. Airi Nagai, Ms, Chisato Matsuoka, Mr. Masami Kugo, Mr. Daichi Toyama, Mr. Masafumi Horiki, Mr. Sui Yu-An, Mr. Wataru Shimada, Mr. Takuma Morikawa, Mr. Satoshi Maruyama, Mr. Brian Kim-Him Mo, Mr. Kensuke Ochi, Mr. Kei Munesato, Ms. Kanako Kumazawa, Mr. Tomohiro Akita, Mr. Taiki Shiraishi, Mr. Hiroyuki Jomen, Mr. Hironobu Kojima, Mr. Taku Mizutani, Ms. Maho Tanaka, Mr. Yuta Nishina, Mr. Hotaka Yatsu, Mr. Kazuaki Ota, Mr. Kenta Nishitani, and all members of Laboratory of Fermentation Physiology and Applied Microbiology, Division of Applied Life Sciences, Graduate School of Agriculture, Kyoto University.

Finally, the author sincerely appreciates to her parents and her family members who understand and support her during the past time.

PUBLICATIONS

1) Hiroko Watanabe, Shigenobu Kishino, Masatake Kudoh, Hiroaki Yamamoto, and Jun Ogawa. Evaluation of electron-transferring cofactor mediating enzyme systems involved in urolithin dehydroxylation in *Gordonibacter urolithinfaciens* DSM 27213. *J Biosci. Biotechnol.*, Accepted.

2) Hiroko Watanabe, Shigenobu Kishino, Masatake Kudoh, Hiroaki Yamamoto, and Jun Ogawa. Identification and functional analysis of the proteins involved in ellagic acid metabolism in *Gordonibacter urolithinfaciens* DSM 27213. in preparation.

3) Hiroko Watanabe, Riku Usami, Shigenobu Kishino, Kengo Osada, Yudai Aoki, Hironobu Morisaka, Yoshihiro Izumi, Takeshi Bamba, Wataru Aoki, Hiroyuki Suganuma, Jun Ogawa. Enzyme system involved in glucosinolate metabolism in lactic acid bacteria. Submitted.